

Department of Chemical Engineering

**Influence of molecular structure on the adsorption of
surfactants at water/air interface**

Ngoc Thu Le

This thesis is presented for the Degree of

Doctor of Philosophy

of

Curtin University

June 2012

DECLARATION

To the best of my knowledge and belief this thesis contains no material previously published by any other person except where due acknowledgment has been made.

This thesis contains no material which has been accepted for the award of any other degree or diploma in any university.

Signature:

Date: June 15th, 2012

ABSTRACT

Surfactants are widely use in our daily activities such as in mineral separation, water purification, petroleum refining/processing, etc. Surfactants behaviour at the gas/liquid interface is one of the interesting research fields for both fundamental and practical applications. This thesis focused on fundamental studies of the influence of surfactant molecular structure on its adsorption behaviour as single or mixture form.

A systematical study of equilibrium adsorption of alcohols and alkyltrimethylammonium bromide with different chain length and branching structure was conducted by Wilhelmy plate method. Theoretical models were applied for analyzing their adsorption activities and be utilized as the quantitative tools for evaluating the influence of molecular structure on their interfacial activities. The results showed that the longer chain length of molecule would have a higher surface activity. Moreover, the branching structure of the molecule has a lower capacity than its straight chain isomer in arranging at the interface.

When mixing branching molecule alcohol methyl isobutyl carbinol with Cetyl trimethylammonium bromide or 1-octanol, a positive synergism was observed, this finding has not been reported before. However, the equilibrium adsorption of mixture of straight chain isomer alcohol (1-hexanol) with $C_{16}TAB$ was described well by the two general models in the literature. The observation of the positive synergism is an initial evidence for the influence of bulky structure of molecule on the equilibrium adsorption of surfactant mixture.

A simple equation replaced the currently applied isotherm was integrated with dynamic models for analyzing the dynamic adsorption of surfactants. This new fitting approach in studying dynamic adsorption provided more reliable fitting results and better in prediction. The dynamic adsorption of bulky nonanol series and different chain length of alkyltrimethyl ammonium bromides were tested by pendant bubble and maximum bubble method, respectively. The experimental data were analyzed by this new fitting approach. The longer the chain length, the higher imbalance in the chain tail of molecule, the longer time is required for the surfactant reaching the interface.

In summary, the findings of this thesis are:

- (1) Provide a systematical fundamental picture of molecule structure (chain length, branching tail) to equilibrium adsorption;
- (2) Identify a special synergism which might be caused by bulky structure of methyl isobutyl carbinol in mixture with certain surfactants;
- (3) Develop a simple, efficient, reliable approach in analyzing and predicting dynamic adsorption of surfactants.

ACKNOWLEDGEMENTS

First, I gratefully acknowledge my supervisor, Prof. Ming Ang, for his unflinching encouragement and support in various ways. I am thankful to Prof. Ming for his precious times to read this thesis and other articles and gave his critical comments about them. Especially, I would like to record my gratitude to my co-supervisor, Dr. Chi Phan, for his supervision, advice, and guidance and critical contribution which is a backbone of this research. The joy and interest he has for the research gave me extraordinary experiences throughout the work, built up my knowledge in a completely new field starting from a blank background. I shall be forever indebted to him for all his supervision.

I would like to thank Curtin University and Department of Chemical Engineering for providing me providing me a scholarship during the course of my study.

I acknowledge Prof. Shin-ichi Yusa, University of Hyogo, Japan and his group for kindly providing the diffusion coefficient values measured by NMR. These data were essential for this study.

I would like to thank Prof. Anh Nguyen, University of Queensland, who read through our draft article and offered his precious suggestions.

It is desirable that I register my thank to Prof. Goen Ho, Dr. Martin Anda, Dr. Stewart Dallas, and other friends in Environmental Technology Center, Murdoch University, for their wonderful supporting and assistance during the early stage of my first arrival to Australia.

I would like to thank all the past and present staff of Chemical Engineering Laboratory, for their kindly supports during my working time in the laboratory.

I am thankful to all my friends at Curtin University for their amazing friendship which made my time in Curtin so unforgettable. Special thanks to our family friends who made our life more enjoyable.

Lastly, I would like to thank my family for all their love, encouragement. I am deeply grateful to our parents, Thanh Le & Huong Nguyen; An Tran & Mai Le, who gave all their boundless love, their joy, their untiring support to us. Especially, I am indebted to my husband Kha Tran and my daughter Chau Tran for their continuous supporting and motivating me to complete this work.

This thesis is dedicated to my family

LIST OF PUBLICATIONS

Journal Articles

1. Le, T. N., Phan, C. M., Nguyen, A. V. and Ang, H. M. (2012). **An unusual synergistic adsorption of MIBC and CTAB mixtures at the air-water interface.** *Minerals Engineering*, 39, 255-261
2. Phan, C.M., Le, T. N. and Yusa, S. (2012) . **A new and consistent model for dynamic adsorption of CATB at air/water interface.** *Colloids and Surfaces A: Physicochemical and Engineering Aspects*, 406, 24-30.
3. Phan, C.M., Nakahara, H., Shibata, O., Moroi, Y., Le, T.N., Ang, H.M. (2011). **Surface Potential of Methyl Isobutyl Carbinol Adsorption Layer at the Air/Water Interface.** *The Journal of Physical Chemistry B*, 116(3), 980-986.
4. Le, N.T., Phan, C. M., Ang, H.M. (2010). **Influence of molecular structure on the adsorption of surfactant on water/air interface.** *Asian-Pacific Journal of Chemical Engineering*. 7(2), 250-255. March/April 2012.

Conference Articles

1. Le, T. N., Phan, C. M., Ang, H. M., Gia, H. P. and Yusa, S. (2012). **Dynamic Adsorption of Tetradecyltrimethylammonium Bromide at Water/Air Interface. Chemeca 2012.** Wellington, New Zealand, Sep 2012.
2. Le, N.T., Phan, C.M., Ang, H.M. (2011). **Synergistic adsorption of MIBC/1-heptanol and MIBC/1-octanol mixtures at air/water interface.** Chemeca2011. Sydney, Australia, 27-29 September.
3. Le, N.T., Phan, C.M., Ang, H.M. (2009). **Influence of molecular structure on the adsorption of surfactant on water/air interface.** Chemeca 2009, Perth, Australia, Sep 2009

Table of contents

Chapter	Title	Page
	Table of contents	viii
	List of figures	xi
	List of tables	xiv
	List of abbreviations	xvi
CHAPTER 1	INTRODUCTION	18
1.1	BACKGROUND	18
1.2	OBJECTIVES OF THE THESIS	20
1.3	THESIS ORGANIZATION	20
CHAPTER 2	LITERATURE REVIEW	22
2.1	ADSORPTION PHENOMENON OF SURFACTANTS AT WATER/AIR INTERFACE	22
2.2	EQUILIBRIUM SURFACE TENSION	23
2.2.1	Theoretical models for individual surfactant	23
2.2.2	Molecular structure of surfactants and surface tension	25
2.2.3	Adsorption of mixture of surfactants	28
2.3	DYNAMIC SURFACE TENSION	31
2.3.1	Theoretical models for surfactant	32
2.3.2	Current fitting procedures of dynamic adsorption	36
2.3.3	Diffusion coefficient	37
2.3.4	Dynamic adsorption of different structure of surfactants	39
2.4	OTHER INTERFACIAL PROPERTIES	39
2.4.1	Surface elasticity	39
2.4.2	Surface potential	41

2.5 Other approaches to study interfacial properties	41
CHAPTER 3 METHODOLOGY	42
3.1 CHEMICALS	42
3.1.1 Non-ionic surfactants: alcohols	42
3.1.2 Cationic surfactants	43
3.2 APPARATUS	47
CHAPTER 4 INFLUENCE OF HYDROPHOBIC PART OF SURFACTANTS MOLECULE TO EQUILIBRIUM SURFACE TENSION	55
4.1 INTRODUCTION	55
4.2 ALCOHOLS	56
4.2.1 Results	57
4.2.2 Summary	63
4.3 CATIONIC SURFACTANTS	64
4.3.1 Results	64
4.3.2 Summary	69
4.4 CHAPTER CONCLUSION	70
CHAPTER 5 DETERMINATION OF DIFFUSION COEFFICIENT	71
5.1 INTRODUCTION	71
5.2 THEORETICAL DIFFUSION COEFFICIENT	71
5.3 ¹ H NMR SPECTRUM METHOD RESULTS	72
5.3.1 TTAB	72
5.3.2 CTAB	74
5.3.3 Nonanol	77
5.4 CHAPTER CONCLUSION	78
CHAPTER 6 DYNAMIC ADSORPTION OF INDIVIDUAL SURFACTANTS AT WATER/AIR INTERFACE	79
6.1 INTRODUCTION	79

6.2 THEORETICAL DEVELOPMENT	79
6.3 MODELLING RESULTS	83
6.3.1 Cationic surfactants CnTAB	83
6.3.2 Alcohol : branching nonanol.	90
6.4 CHAPTER CONCLUSION	96
CHAPTER 7 INFLUENCE OF MOLECULAR STRUCTURES TO EQUILIBRIUM ADSORPTION OF MIXTURE OF SURFACTANTS	98
7.1 INTRODUCTION	98
7.2 MIXTURE OF NON-IONIC SURFACTANTS: ALCOHOLS	99
7.2.1 Adsorption of single surfactant systems	100
7.2.2 MIBC/1-heptanol	102
7.2.3 MIBC/1-octanol	102
7.2.4 Discussion	103
7.2.5 Summary	104
7.3 MIXTURE OF CATIONIC/NONIONIC SURFACTANTS	105
7.3.1 Adsorption of single surfactants systems	106
7.3.2 MIBC/CTAB	107
7.3.3 1-hexanol/CTAB	114
7.4 CHAPTER CONCLUSION	116
CHAPTER 8 CONCLUSIONS AND FUTURE RESEARCH DIRECTIONS	117
8.1 THESIS SUMMARY	117
8.2 FUTURE RESEARCH DIRECTIONS	118
8.3 CONCLUSION REMARKS	119
REFERENCES	120
APPENDICES	131

List of figures

Figure	Title	Page
Figure 1-1	Adsorption activity of surfactant at water/air interface.....	19
Figure 2-1	Fundamental process of dynamic adsorption cationic surfactants at air/water interface.....	33
Figure 2-2	Mutual diffusion example	38
Figure 3-1	Procedure for choosing the solvent used in recrystallization	45
Figure 3-2	Recrystallization procedure	46
Figure 3-3	Wilhelmy plate method	48
Figure 3-4	Tensiometer KSV Sigma 700/701.....	48
Figure 3-5	PAT1	51
Figure 3-6	Maximum bubble method	52
Figure 3-7	MPT2.....	53
Figure 4-1	Results of three surface tension measurement runs of 1-hexanol	57
Figure 4-2	Surface tension as function of bulk concentrations for alcohols.....	58
Figure 4-3	Predictions of 1-hexanol surface tension from parameters in Table 4-1..	61
Figure 4-4	Relationship between equilibrium surface excess and bulk concentration.	62
Figure 4-5	Possible arrangement of surfactants at interface	63
Figure 4-6	Relationship between Surface tension and concentration of C_n TAB.....	66
Figure 4-7	Surface excess vs. concentration of C_n TAB.....	67
Figure 4-8	Comparison of CTAB experimental data and reference (Miller, Fainerman et al. 2002).....	68
Figure 4-9	TTAB experiment and reference data (Miller, Fainerman et al. 2002)...	68
Figure 4-10	Gibbs elasticity vs. concentration of C_n TAB	69

Figure 5-1. (a) ^1H NMR spectrum with solvent suppression of TTAB in H_2O . (b) Fitted diffusion curve estimated from ^1H NMR DOSY using WATERGATE pulse sequence for 1.5 mM TTAB in H_2O	73
Figure 5-2 (a) ^1H NMR spectrum with solvent suppression of CTAB in H_2O . (b) Fitted diffusion curve estimated from ^1H NMR DOSY using WATERGATE pulse sequence for 0.4 mM CTAB in H_2O	75
Figure 5-3. (a) ^1H NMR with WATERGATE of saturated C18TAB in H_2O solution at 21 °C. (b) The fitted diffusion curve for DOSY with WATERGATE spectrum of saturated C18TAB in H_2O solution	76
Figure 5-4 (a) ^1H NMR with WATERGATE spectrum of 1.0 mM 2-nonanol in H_2O at 22.1 °C (b) Fitted diffusion curve for ^1H NMR DOSY with WATERGATE spectrum of 1.0 mM 2-nonanol in H_2O at 22.1 °C.....	77
Figure 6-1 Modeling equilibrium surface tension of CTAB (the modeled predictions were almost identical).	82
Figure 6-2 Diffusion adsorption of CTAB with two different sets of K and Γ_m	83
Figure 6-3 Dynamic surface tension of OTAB: lines are best-fitted curves with $K = 68577$ L/mol and $\Gamma_m = 2.638 \times 10^{-5}$ mol/m ²	87
Figure 6-4 Dynamic surface tension of CTAB: lines are best-fitted curves with $K = 2017$ L/mol and $\Gamma_m = 6.32 \times 10^{-6}$ mol/m ²	88
Figure 6-5 Dynamic surface tension of TTAB: lines are best-fitted curves with $K = 1716$ L/mol and $\Gamma_m = 3.76 \times 10^{-6}$ mol/m ²	89
Figure 6-6 Dynamic surface tension of 2-nonanol: lines are best-fitted curves with $K = 2017$ L/mol and $\Gamma_m = 6.34 \times 10^{-6}$ mol/m ²	92
Figure 6-7: Dynamic surface tension of 3-nonanol: lines are best-fitted curves with $K = 1000$ L/mol and $\Gamma_m = 6.00 \times 10^{-6}$ mol/m ²	93
Figure 6-8 Dynamic surface tension of 5-nonanol: lines are best-fitted curves with $K = 990$ L/mol and $\Gamma_m = 5.6 \times 10^{-6}$ mol/m ²	94
Figure 7-1 Surface tension as function of bulk concentrations for MIBC, 1-heptanol and 1-octanol (points: experimental data, lines: best-fitted curves)	101

Figure 7-2: Surface tension of MIBC/1-heptanol mixture: fitted by Fainerman's model, ($A_{12} = -0.516$, $\delta_y = 0.85$ mN/m)	102
Figure 7-3: Surface tension of MIBC/1-octanol mixture: fitted by Fainerman's model ($A_{12} = 1.477$, $\delta_y = 1.36$ mN/m).....	103
Figure 7-4 Adsorption isotherm of individual surfactants: CTAB, MIBC, 1-hexanol	107
Figure 7-5 Fainerman model, best fitted value of $A_{12} = -0.96$, $\delta_y = 1.77$ mN/m	108
Figure 7-6 Siddiqui model, best fitted value of $\beta = 0.51$, $\delta_y = 2.2$ mN/m.....	109
Figure 7-7 Best-fitted surface created by the empirical polynomial.....	111
Figure 7-8 The synergistic points of MIBC/CTAB (c_1 and Γ_1 are MIBC bulk and surface concentration, c_2 and Γ_2 are CTAB bulk and surface concentration, respectively).....	112
Figure 7-9 Surface tension versus percentage of CTAB at constant total concentration of mixture	113
Figure 7-10 Fainerman's models, best fitted value of $A_{12} = 0.34$, $\delta_y = 0.77$ mN/m....	115

List of tables

Table	Title	Page
Table 3-1	Alcohols used for this study	42
Table 3-2	Alkyltrimethylammonium Bromide used	44
Table 3-3	List of the advantages and disadvantages of Wilhelmy plate method.....	47
Table 4-1	Adsorption isotherm constants	59
Table 4-2	Adsorption isotherm parameters of C _n TAB	65
Table 5-1	Diffusion coefficient (<i>D</i>) of TTAB at various concentrations in H ₂ O at 20 °C measured using DOSY with WATERGATE method.....	72
Table 5-2	Diffusion coefficient (<i>D</i>) of CTAB at various concentrations in H ₂ O at 20 °C measured using DOSY with WATERGATE method.....	74
Table 5-3	Comparison the theoretical and experimental value of OTAB's diffusion coefficient.....	76
Table 5-4	Diffusion coefficient (<i>D</i>) of 2-nonanol.....	78
Table 6-1:	Fitting parameters for CTAB equilibrium surface tension ($\gamma_0= 71.21$ mN/m).	81
Table 6-2	Fitting parameters for C _n TAB equilibrium surface tension.....	84
Table 6-3	Dynamic fitting parameters of C _n TAB	85
Table 6-4	Fitting parameters of TTAB and CTAB dynamic adsorption with two different fitting concentrations	85
Table 6-5	Reported maximum surface excess of C _n TAB in literature.....	86
Table 6-6	Fitting parameters for equilibrium surface tension of nonanol series.	90
Table 6-7	Fitting parameters of new models for nonanol series.....	91
Table 6-8	Diffusion time scale (ms) of n-nonanol	95
Table 7-1:	Interaction parameter between molecules of different mixture of surfactants.	100

Table 7-2 Adsorption isotherm parameter of MIBC, 1-heptanol, 1-octanol.....	101
Table 7-3. Fitting parameters for single surfactant: CTAB, 1-hexanol, MIBC	106
Table 7-4 Coefficient values of polynomial function fitted for mixture.....	110

List of abbreviations

$^1\text{H NMR}$	Proton Nuclear magnetic resonance
$^1\text{HDOSY}$	Diffusion Ordered Spectroscopy
2D DOSY	Two-dimensional diffusion ordered spectroscopy
A	constant characterizing the lateral interaction among adsorbed surfactant molecules
A_{12}	Parameter accounting for cross-interaction between adsorbed molecules of the two surfactants
B	fitting parameter in the modified Langmuir-Hinshelwood kinetics
c_b	surfactant bulk concentration (M)
c_s	surfactant bulk concentration in the subsurface layer (M)
D	surfactant diffusion coefficient (m^2/s)
g	gradient strength
K	adsorption constant (M^{-1})
k^d	desorption rate (s^{-1})
k^a	adsorption rate (m/s)
K_L	Langmuir equilibrium adsorption constants (M^{-1})
K_F	Frumkin equilibrium adsorption constants (M^{-1})
R	universal gas constant (J/Kmol)
t	time (s)
T	absolute temperature ($^{\circ}\text{K}$)
V	Molar volume of surfactant at its boiling temperature, cm^3/mol
χ	new adsorption constant (M^{-1})
Γ	equilibrium surface excesses (mol/m^2)
$\Gamma(t)$	dynamic surface excesses (mol/m^2)
Γ_m	saturated surface excesses (mol/m^2)

δ	length of the gradient pulse (nm)
δ_γ	standard deviation in equilibrium surface tension models (mN/m)
τ	integration variable
γ_{eq}	equilibrium surface tension (mN/m)
γ_0	surface tension of pure water (mN/m)
$\gamma(t)$	dynamic surface tension (mN/m)
τ_D	diffusion time scale (ms)
θ	monolayer coverage
ω	Mean molar area
ξ	Activity coefficient calculated from the Gibbs free energy of mixing in monolayer
β	Parameter accounting for the non-ideal interface molecular interaction
η	Viscosity of water, cP
ϕ	Association factor of water

CHAPTER 1

INTRODUCTION

1.1 BACKGROUND

We are living in a complicated world which involves interaction of different phases: solid, liquids, gas, etc; among that air and water are two most commonly encountered elements. It is obvious that interfacial phenomenon between these two essential phases appear in many aspects of our daily activities. Physically quantifying the interfacial activities is via the values of surface tension. Surface tension is evident all around us, everywhere and at all the times, affecting our daily life in many ways.

Many industrial processes involve interfacial activities at the gas/liquid interface, for instance: mineral and coal extraction, separation by flotation (Crozier and Klimpel 1989); dissolved air flotation in wastewater treatment, water purification, storm water runoff treatment, toxic substance removal, algae separation, odor substance stripping, bacteria separation, groundwater purification, industrial waste treatment, municipal primary and secondary clarification, tertiary clarification, deinking operation (summarized by Wang and coauthors (Wang, Fahey et al. 2005); petroleum refining/processing (Schramm 2000); spreaders for agriculture chemicals, antifogging agent for greenhouse, window glass, foaming (with application in enhanced or recovery, or fire extinguisher) (Scamehorn 1986). These processes are based on the modification of the interfacial properties of water by using surfactants.

Surfactants are chemical compounds containing both hydrophilic (refer to the head which is water soluble) and hydrophobic (refer to the tail which is water repelling) part in the same molecule. When surfactants are dissolved in water they orientate at the surface so that the hydrophobic regions are removed from the aqueous environment, as shown in Figure 1-1. The reason for the reduction in the surface tension when surfactant molecules adsorb at the water surface is that the surfactant molecules replace some of the water molecules in the surface and the forces of attraction between surfactant and water molecules are less than those between two water molecules, hence the contraction force is reduced. The driving force is the hydrophobic effect as in this way the hydrophobic tails segregate from contact with water. This phenomenon, according to which a molecule comes from the bulk of a solution to place itself at the interface (with some specific orientation) is called

adsorption. This orientation of the surfactants reduces the free energy of the surface thus lowering the surface tension. The diffusion of surfactant molecules to the surface continue until equilibrium is established and the time- involved process associated with the movement of surfactant to surface is called dynamic adsorption.

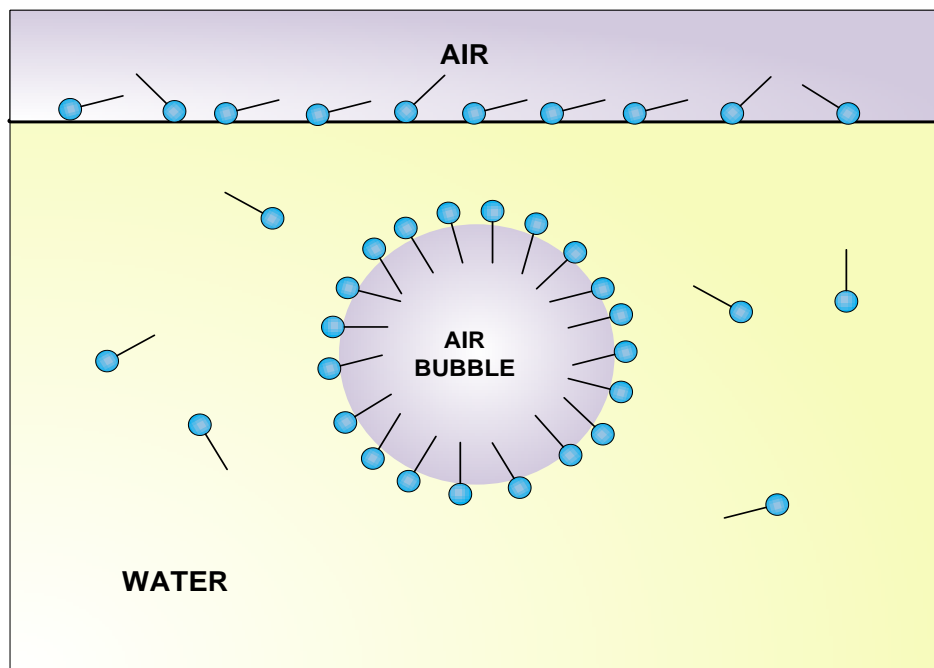


Figure 1-1 Adsorption activity of surfactant at water/air interface

The arrangement of surfactants at the interface, the movement process of surfactant from the bulk to the surface is strongly influenced by the chemical molecule structures, bulk solution physical characteristics such as temperature, pressure. In practice, a higher surface tension capacity means lower amount of surfactant is needed. To optimize the choice of surfactant for a specific application, the fundamental information about equilibrium and dynamic adsorption activity has to be identified by qualitative models which can mathematically analyze the experimental data obtained.

For decades, several experimental techniques have been developed such as the scattering and reflection of X-rays and neutron, electron microscopy, probe microscopy, imaging techniques, so as to set a better understanding about interfacial activity of surfactants. The Wilhelmy plate is one of the most popular methods for identifying equilibrium adsorption while maximum bubble method and pendant bubble method are mainly applied for dynamic adsorption studies.

The correlation of molecular structure and interfacial properties is one of the most researched fields both in theoretical and practical aspects (Thomas 2004)) as the knowledge of the molecular structure of surfactants can lead to huge differences in biodegradation characteristics, surface reduction capacity, solubility, foaming, etc. For instance, branched-chain alkyl benzene sulfonates which are used as detergents could not be broken down by microorganisms which lead to persistent foams, resulting in ecological damage to many rivers and lakes. They were replaced by straight-chain alkyl benzene sulfonates, such as sodium dodecylbenzenesulfonate and sodium xylenesulfonate. Methyl isobutyl carbinol (MIBC) is less surface active than the straight chain hexanol, but it is widely used due to its higher solubility and lower cost. The interesting relationship between structure and interfacial properties is also observed from the commercially available surfactants, with branched hydrocarbon tails. Using mixtures of several commercial surfactants instead of pure surfactant or replacing a branching isomer with straight chain surfactants might be more practical to adjust interfacial properties of one certain system.

A full understanding of the adsorption of surfactants with different molecular structures at the interface is highly desirable.

1.2 OBJECTIVES OF THE THESIS

The main objective of this study is to investigate the influence of molecular structure (chain length, branching structure) on interfacial activity. The surface tension reduction will be used as the main key for comparing surface activity. The adsorption progress and the arrangement of surfactants with concentrations lower than the critical micelle concentration (CMC) from the bulk to the interface will be the foci of this study.

1.3 THESIS ORGANIZATION

The layout of the thesis is listed below:

Chapter 1: Generally introduces surfactant properties and its relevance applications in human activities and provides the rationality for research on surfactant structures and their interfacial properties.

Chapter 2: Reviews theoretical models used for qualitative assessment of the surface tension reduction capacity of individual and mixture of surfactants and their dynamic adsorption behaviours. The gap of knowledge in comparative study in relationship of

structure-surface tension reduction will be highlighted throughout the literature review.

Chapter 3: Describes the apparatus for measuring the equilibrium and dynamic surface tension; the procedure for purifying chemicals; the conditions of the experiments; principal, advantages and disadvantages of measurement methods.

Chapter 4: Provides a systematical understanding of the influence of molecular structure (chain length and branching structure) on surface tension reduction by two sets of chemicals: alcohols (non-ionic surfactants), Alkyltrimethylammonium bromide (C_n TAB, cationic surfactants).

Chapter 5: Determinates diffusion coefficient of certain chemicals directly by diffusion –ordered NMR spectroscopy method. This parameter is essential in dynamic adsorption analyses.

Chapter 6: Introduces a new simple equation incorporating many other current models to analyze dynamic adsorption. This new approach in calculating dynamic adsorption has two main advantages: (1) high efficiency in predicting the dynamic activities at others concentration (2) can be used for comparative study purposes in terms of structure- interface properties. Two sets of chemicals (nonanol, C_n TAB) were analyzed using this new fitting approach for comparative studies.

Chapter 7: Describes surface tension of different mixtures: nonionic/nonionic, nonionic/cationic. The effect of branching structure on interfacial behaviour was the main target of this chapter. Two popular and generalize models were applied to quantify the interfacial properties.

Chapter 8: presents the conclusions, the recommendations for extending this research and the contributions of this study to the field.

CHAPTER 2

LITERATURE REVIEW

Understanding the surface properties of surfactants in solution is very important for many industrial processes which are involved large interface areas such as foam, emulsion and dispersion (Schramm, Stasiukb et al. 2003). Two major aspects of physical by quantifying surfactant adsorption are equilibrium and dynamic surface tension. This chapter first presents an overview of theoretical models for evaluating equilibrium adsorption of individual surfactants as well as for mixture of surfactants. This is followed by models for dynamic adsorption, which are important in areas such as photography, where the dynamic surface tension is monitored to prevent film deformation and irregularities, in crop protection products where wettability rate is vital for pesticide spreading on leaves, biological processes, and in paper and textile production (Schramm, Stasiukb et al. 2003). In addition, the review on studies about influence of molecular structure to adsorption activity is conducted. This chapter concludes by highlighting the gap of knowledge in existing study about the structure-surface tension properties which will be the framework for this thesis.

2.1 ADSORPTION PHENOMENON OF SURFACTANTS AT WATER/AIR INTERFACE

Due to the special hydrophobic tail and hydrophilic head present in any surfactant molecule, these molecules move forward to the interface to establish the interfacial conditions after some time. This phenomenon, called adsorption characteristic (surface activity), which is lowering the surface tension. The surfactant molecules like to have as great a surface area as possible, then minimizing the effect of the pure liquid resulting in a lower surface tension than that of pure water. With the time, more and more surfactant molecules will try to migrate from the bulk aqueous liquid and accumulate at the surface and the surface tension will decrease over the time as a consequence of adsorption process at the newly formed surface. That movement with time is called dynamic surface tension. In a stationary liquid surface, the concentration of surfactant will eventually reach equilibrium, when the surface tension remains unchanged. The value of surface tension at that point is referred to as static or equilibrium surface tension.

The reduction of surface tension is related to number of surfactant molecules arranged on the surface and replacing the solvent molecules. Other than using an advanced technique like neutron reflection, which used recently can provide a clearer picture of surfactant structure at the interface (Simister, Thomas et al. 1992; Eastoe, Dalton et al. 1997); the measurement of surfactant molecules at the interface is very difficult. The most common method to calculate the concentration of surfactants at the interface is based on the Gibbs equation (described in detail in the next section) which gives the relationship between surface tension γ and concentration surfactants in the bulk (c_b). This information can easily be obtained by many available methods (Chang and Franses 1995; Dukhin, G.; et al. 1995).

2.2 EQUILIBRIUM SURFACE TENSION

The equilibrium surface tension is one of the most evaluated parameters used in theoretical and practical situations to describe the characteristics of any surfactant. The equilibrium surface tension can be obtained by many techniques such as ring method, Wilhelmy plate method, sessile drop, which are all described in detail by (A.W. Adamson and Gast 1997)

The next part will summarize the mathematical models which are widely used for describing the equilibrium surface activity.

2.2.1 Theoretical models for individual surfactant

Surfactants tend to always concentrate on the surface in preference to the bulk liquid. The decrease of the surface tension depends on the number of adsorbed molecules per unit area, called the surface excess. The surface excess (Γ) is named after Gibbs who developed the model for describing the interfacial region between it and the bulk phase (Chang and Franses 1995; Eastoe and Dalton 2000). The relationship (Gibbs' model) among surface excess (Γ), surface tension (γ) and bulk concentration (C_b) is given by the following equation:

$$-nRT\Gamma = \left(\frac{\delta\gamma}{\delta\ln C} \right)_{\tau} \quad (2-1)$$

$$\text{or} \quad \Gamma = -\frac{1}{nRT} \cdot \frac{d\gamma}{d\ln C}$$

where $n=1$ for non-ionic surfactants, neutral molecules or ionic surfactants with the presence of excess electrolyte; $n=2$ for ionic surfactants; R: gas constant, T is the Kelvin temperature.

If we assume that the free energy of adsorption is constant, this relationship is described by Langmuir isotherm. The Langmuir adsorption isotherm has been widely applied to many adsorption processes. It has produced good agreement with a wide variety of experimental data for adsorption of a solute from a liquid solution. A basic assumption of the Langmuir theory is that the sorption takes place at specific homogeneous sites in the adsorbent. Moreover, when a site is occupied by a solute, no further adsorption can take place at that site.

$$c_b = \frac{1}{K_L} \frac{\Gamma}{\Gamma_m - \Gamma} \quad (2-2)$$

where c_b is the bulk concentration (mol/L); Γ and Γ_m are the equilibrium and maximum surface concentrations (mol/m²), respectively; K_L is the Langmuir equilibrium adsorption constant (L/mol).

However, there are some cases in which the Langmuir isotherm could not provide good agreement especially if there is strong attraction among the adsorbed molecules with long hydrocarbon chains (Karakashev, Nguyen et al. 2008). Frumkin isotherm (Eastoe and Dalton 2000) would be applied to improve by accounting for the interactions between the adsorbed molecules.

$$c_b = \frac{1}{K_F} \frac{\Gamma}{\Gamma_m - \Gamma} \exp\left(-A \frac{\Gamma}{\Gamma_m}\right) \quad (2-3)$$

K_F is the Frumkin equilibrium adsorption constant and A is a dimensionless constant accounting for the non-ideality of the mixing at the interface layer.

The surface concentration is related to the surface tension through the Szyszkowski equation (Eastoe and Dalton 2000):

$$\gamma(c_b) = \gamma_0 + nRT\Gamma_m \ln\left(1 - \frac{\Gamma(c_b)}{\Gamma_m}\right) + \frac{1}{2}nRTA\Gamma_m \left(\frac{\Gamma(c_b)}{\Gamma_m}\right)^2 \quad (2-4)$$

where γ, γ_0 are the solution and pure solvent surface tensions, respectively (mN/m), R is the gas constant and T is the temperature.

In this thesis, the numerical solution for the surface tension of surfactant solutions can be predicted as a function of the bulk concentration using Eqs. (2-2) and (2-4). Three adsorption constants (K_F , Γ_m and A) for each surfactant can be found by fitting the predicted values against experimental measurements. The fitting procedure was

done by Solver (in Microsoft Excel) in combination with a program coded in Visual Basic based on the least square method.

2.2.2 Molecular structure of surfactants and surface tension

There have been several researches on the relation between equilibrium adsorption properties of surfactants and its structures (Rosen 1972; Kwan and Rosen 1980 ; Rosen 1989). Rosen and coauthors (Rosen 1972; Rosen 1974; Rosen 1976; Kwan and Rosen 1980 ; Rosen, Cohen et al. 1982; Rosen, Dahanayake et al. 1982; Rosen, Zhu et al. 1992) conducted a series of investigation on the relationship of structure to surfactant properties in terms of comparing structure-properties by two measures: surfactant efficiency (the concentration of surfactant required to produce a given surface tension reduction) and surfactant effectiveness (the maximum reduction in surface tension that can be obtained, regardless of the concentration of surfactant present, CMC or solubility limit). Gibbs isotherm of these studies was mostly gained by Wilhelmy plate method. In this thesis, we focus on the adsorption behaviour of surfactants in range lower than CMC so that the efficiency in reducing the surface tension is more evident than effectiveness.

A summary on the influence of head-group structure to surface activity was thoroughly investigated and described by Aratono and Ikeda (Esumi K. and M. 1997). By comparing the equilibrium isotherm curve of five different types of nonionic surfactants $C_8H_{17}X$ with $X = OH, (OC_2H_4)_4OH, (CH_3)SO, (C_2H_4OH)SO, (CH_3)_2PO$, they found that the surface activity of these chemicals decrease respectively. The primary, secondary and tertiary function groups of cationic surfactants $RNH_y(CH_3)_{3-y}X^-$ ($y=3,2,1$) were also investigated and led to the conclusion that the surface excess increase in the order primary>secondary>tertiary>quaternary.

There was a huge number of comparative-work on the influence of chain length to surface activity. Rosen (Rosen 1972) concluded that the increase in length of the hydrophobic group (tail) will lead to an increase in efficiency of surfactant (surface activity) while the effectiveness decreases. Several works have been done to study the relationship between structure and surface activity to prove the accuracy of Rosen founding (Rosen 1972):

(1) $C_{12}H_{25}(OC_2H_4)_xOH$ with different number of ethenoxyethanol (Rosen, Cohen et al. 1982)

(2) C_nTHPSO_4N (Sodium 3-Alkyltetrahydropyranyl 4-Sulfates) with different n (Rosen and Kwan 1979)

(4) Octaethylene glycol-n-alkyl ethers (C_nE_8 ; n = 9 to 15) (Ueno M., Takasawa Y. et al. 1981).

(5) Sulphonate solutions of with different chain length C12, C14, C18 were investigated by Beneventi and others (Beneventi, Carre et al. 2001)

(6) short chain alcohols (methanol, ethanol, propanol, butanol) (Glinski, Chavepeyer et al. 1998)

Though the branched surfactants would create a different interfacial properties from their linear counterparts (Rosen 1972; Varadaraj, Bock et al. 1991), studies about the relationship of branched structure of surfactants to fundamental interfacial activity are limited (Wormuth and Zushma 1991) and can be summarized as follows:

(1) Combley and coauthors (Comley, Harris et al. 2002) used maximum bubble method to gain the equilibrium surface tension of n-alcohol (from propanol to octanol) homologous series. They found that the surface activity is increased with the increase of chain length. The influence of branch chain to surface tension also was mentioned by comparing MIBC and 1-hexanol. The branched structure of MIBC led to lower surface excess arranged in the interface which means lower surface activity than 1-hexanol.

(2) Varadaraj and others (Varadaraj, Bock et al. 1991) conducted studies on the fundamental interfacial behaviour of four alcohols: C16 linear alcohol, C16 and C12 linear Guerbet alcohols, C16 branched Guerbet alcohol (branched at the second or β -carbon). The interfacial tension was measured by Wilhelmy plate method. The Guerbet branching structure increases significantly the efficiency of surface tension reduction. The lower maximum surface excess

was observed for Guerbet branching structure compared with linear one. Further branching of the site chain length and reduction in the total number of carbons of the number of EO groups in Guerbet ethoxy sulfate also result in increase of effectiveness.

- (3) Another work of Varadaraj and co-authors (Varadaraj, Bock et al. 1991) conducted comparative work on the interfacial activity of Ethoxylated alcohol (C12E5, C13E5, C12E6, C13E6) with linear and branched structure by Wilhemy plate method. The branched structures produced lower efficiencies in surface tension reduction than the corresponding linear one with the same carbon chain.
- (4) The interfacial properties of six surfactants having the same polar head group (diethanolamine derivative of succinic anhydride) of which three of them have aliphatic alkyl chains (dodecyl, tetradecyl, hexadecyl) and the other three have branched hydrocarbon chains (polysobutylene) of average backbone carbon number 14, 22, 34 were conducted by ellipsometric (Ghaicha, Leblanc et al. 1992). They observed that branching of hydrocarbon chains caused a greater expansion of monolayer films compared to straight chain surfactants.
- (5) In one of Rosen group's work, Kwan and Rosen (Kwan and Rosen 1980) found that bulky isobutyl group ($R = \text{iso-C}_4\text{H}_9$) of $\text{ROC}_{10}\text{H}_6\text{SO}_3\text{Na}$ had greater surface tension reducing efficiency than n-butyl isomer. This finding is contrary to other observations (Rosen 1978).

Almost all of the branched surfactants examined in previous literature have complicated structure, but the methyl or ethyl-branched hydrocarbon chain of small molecule surfactants are still not systematically investigated. These following conclusions were gained from most of literature work:

- *An increase in the length of the hydrocarbon chain (hydrophobic) increases the surface activity. Most of branched molecules have lower capacity in lowering the surface tension compared to the straight chain ones.*
- *The importance of the influence of branching structure of surfactant to equilibrium adsorption has only been partially elucidated.*

2.2.3 Adsorption of mixture of surfactants

Mixture of surfactants are widely used in many commercial formulations: (1) frothers (Harris and Jia 2005; Ozmak 2006) to maximize the total range of mineral particle sizes recovery (Klimpel 1991); (2) different mixture of anionic/alcohols in flotation to improve the froth formation, to reduce collector consumption; (Rybinski and Schwuger 1986; Crozier and Klimpel 1989); (3) in enhanced oil recovery, mixture of surfactants are used to permit flooding of high salinity or hardness reservoirs while avoiding precipitation of surfactants; (3) in heavy duty detergents, mixture of anionic and nonionic surfactants are used to permit washing in hard water (Scamehorn 1986); powerful medium in synthetic of nanostructured or mesostructured materials (Antonietti 2001),etc.

The wide use of mixture surfactants is due to some of the following reasons (i) cheaper than producing, purifying isomerically pure surfactants (Holland and Rubingh 1992) (Scamehorn 1986); (ii) often having superior properties than a single surfactant for example for quick adsorption at an interface and not desorbed during external perturbations (Szymczyk and Jańczuk 2007; Fainerman, Aksenenko et al. 2010), (iii) improve the solubility of surfactants in water (Pugh 2000), (iv) environmental and health concerns information are more available than the use of a totally new surfactant ((Mulqueen and Blankschtein 1999).

The focus of the present study is based on the surface tension of mixtures in the dilute region. The adsorption of binary mixtures of surfactants at air/water interface has been investigated intensively both theoretically and experimentally (Nikas 1992; Mulqueen and Blankschtein 1999; Fainerman and Miller 2001; Fainerman, Miller et al. 2002; Kralchevsky, Danov et al. 2003). Most of the proposed models are based on the known characteristics of individual compounds and one additional parameter is

added to account for the interactions between molecules of combinations at the surface (Rosen 1989).

There are two theoretical models which were successfully applied to the adsorption behaviour of most of mixtures at interface. Firstly, the model is a general model developed by Fainerman and co-authors (Fainerman and Miller 2001; Fainerman, Miller et al. 2002), which could be used to predict the adsorption of surfactant mixtures in both "ideal" and "non-ideal" surface behaviour. This model also considered the different adsorption states of adsorbed molecules. Secondly, the model was proposed by Siddiqui and Franses (Siddiqui and Franses 1996), which is limited to Langmuir-type surfactants.

Fainerman's binary model

The adsorption isotherm for binary mixture is given by a system of two equations (Fainerman and Miller 2001; Fainerman, Miller et al. 2002):

$$K_1 c_1 = \frac{\theta_1}{(1-\theta_1-\theta_2)^{r_1}} \exp(-2A_2\theta_1 - 2A_{12}\theta_2) \exp[(1-r_1)(A_1\theta_1^2 + A_2\theta_2^2 + 2A_{12}\theta_1\theta_2)] \quad (2-5)$$

$$K_2 c_2 = \frac{\theta_2}{(1-\theta_1-\theta_2)^{r_2}} \exp(-2A_2\theta_2 - 2A_{12}\theta_1) \exp[(1-r_2)(A_1\theta_1^2 + A_2\theta_2^2 + 2A_{12}\theta_1\theta_2)] \quad (2-6)$$

Where

c_i and Γ_i are the bulk and the interface concentration of surfactant ($i=1,2$), respectively;

θ_i is the monolayer coverage, $\theta_i = \frac{\Gamma_i}{\Gamma_{m,i}}$

$\Gamma_{m,i}$, K_i and A_i are adsorption constant of surfactants, which are predetermined individually;

A_{12} is a parameter accounting for cross-interaction between adsorbed molecules of the two surfactants.

r_i is the surface area fraction, $r_i = \frac{1}{\Gamma_{m,i}\omega}$

The mean molar area, ω , is defined as:

$$\bar{\omega} = \frac{\frac{\Gamma_1}{\Gamma_{m,1}} + \frac{\Gamma_2}{\Gamma_{m,2}}}{\Gamma_1 + \Gamma_2} \quad (2-7)$$

The equation of state of the mixtures is given:

$$\gamma_0 - \gamma = \frac{RT}{\omega} \ln[(1 - \theta_1 - \theta_2)] + A_1\theta_1^2 + A_2\theta_2^2 + 2A_{12}\theta_1\theta_2 \quad (2-8)$$

The numerical solution is as follows: **Eq.2-7** can be substituted into r and then **Eq.2-5** and **Eq.2-6**. The system of these 2 equations can be solved simultaneously for two unknowns, Γ_1 and Γ_2 , at any given values of c_1 and c_2 . Consequently, Γ_1 and Γ_2 can be used to calculate θ_1 , θ_2 and substituted into Eq. 2-8 to find the surface tension.

Siddiqui's binary model

Assuming the applicability of the Langmuir isotherm for both components of the mixture, Siddiqui and Frances (Siddiqui and Frances 1996) derived the maximum monolayer density and the adsorption equilibrium constant.

$$\left(1 + K_{L,1} \frac{c_1}{\xi_1 x_1}\right)^{\Gamma_{m,1}} = \left(1 + K_{L,2} \frac{c_2}{\xi_2 x_2}\right)^{\Gamma_{m,2}} \quad (2-9)$$

and

$$\frac{x_1(\xi_1 x_1 + K_{L,1} c_1)}{\Gamma_{m,1} K_{L,1} c_1} + \frac{x_2(\xi_2 x_2 + K_{L,2} c_2)}{\Gamma_{m,2} K_{L,2} c_2} = \frac{1}{\Gamma_1 + \Gamma_2} \quad (2-10)$$

The activity coefficient ξ_i is calculated from the excess Gibbs free energy of mixing in the monolayer ($i=1,2$):

$$\xi_i = \exp[\beta (1 - x_i)^2] \quad (2-11)$$

β is a dimensionless parameter accounting for the non-ideal interface molecular interaction. x_i is defined as follows:

$$x_i = \frac{\Gamma_i}{\Gamma_1 + \Gamma_2}, \quad (2-12)$$

The surface tension of the mixture can be calculated as either:

$$\gamma = \gamma_0 + \Gamma_{m,1} RT \ln \left(1 + K_{L,1} \frac{c_1}{\xi_1 x_1}\right) \quad (2-13)$$

or

$$\gamma = \gamma_0 + \Gamma_{m,1} RT \ln \left(1 + K_{L,1} \frac{c_1}{\xi_1 x_1}\right) \quad (2-14)$$

As in Fainerman's model, the system of 2 equations **Eq. 2-9** and **Eq. 2-10** can be solved simultaneously to determine Γ_1 and Γ_2 . Subsequently, surface tension can be found from equation either **Eq. 2-13** or **Eq. 2-14**. In comparison with Fainerman's model, this second model is limited to Langmuir-type surfactants only, i.e. the individual adsorption is described by **Eq. 2-3**.

With some satisfaction, these models have been applied to binary mixtures containing alcohols, such as: 1-heptanol/1-octanol and 1-octanol/1-hexanol (Fainerman 1983); sodium dodecyl sulfate (SDS) and n-alkanols (Zdziennicka and Jan'czuk 2010); SDS and propanol, SDS and ethanol (Kovtun, Khilko et al. 2010); SDS and C₁₂E₈; C₁₂E₅ and Triton X-100 (Siddiqui and Franses 1996), CTAB and propanol (Zdziennicka and Janczuk 2008) .

Though structural changes in the tail group affect surface activities of mixtures (Rosen 1989; Penfold, Staples et al. 2003), only a few studies on the correlation of chain structure to the capacity of reducing surface tension were made. Most of the reported work on mixture were focused on chain length effect such as that of Rosen and coauthors (Rosen and Zhou 2001). They were conducted on a series of studies on structure–property relationship: polyethylene glycol n-alkyl ethers (C_nEO_m, with n =12, 14, m= 4,6,7, 8) were mixed with C₁₂SO₃Na at 25°C. They found that the strength of the interactions between two components in the mixture was reported to be less negative (which means that the molecular interactions in mixture are less attractive than the interactions in either of the individual surfactants) as the value of m is reduced. Surface tension of polyoxyethylene (10) alkyl ether C_nE₁₀ (n= 12,16) and *N*-decanoyl-*N*-methylglucamine (MEGA-10) mixtures were measured by ring method (Sulthana, Rao et al. 2000). They found that an increase in hydrocarbon chain did not strongly affect the surface activity of mixtures. However, as the chain length exceeds 16 (n > 16), there was a strong effect of the tail length to surface activity of mixtures (Rosen 1989).

So far, no work on the influence of branching structure of the tail to adsorption behaviour of mixture has been conducted.

2.3 DYNAMIC SURFACE TENSION

Although surfactant adsorption can be characterized by the equilibrium surface tension, dynamic adsorption is more relevant to natural and industrial processes with

the dynamic step lasting from a few milliseconds to a few days. During flotation, emulsification and foaming processes, new interfaces (bubbles and droplets) are formed continuously. In these instances, the adsorption rarely reaches equilibrium. In wetting and coating processes, where the interface expands continuously, the dynamic wetting rate is shown to correlate with the dynamic surface tension rather than the corresponding equilibrium value (Rosen and Xi 1990).

The techniques to perform dynamic adsorption measurements can be hydrostatic e.g. the pendant bubble technique or the Wilhelmy plate technique, or, they can have leading order flow e.g. the maximum bubble pressure technique; the drop weight method; the oscillating jet method, etc.

2.3.1 Theoretical models for surfactant

Dynamic adsorption can be described in terms of surface concentration and surface tension changing with time. Dynamic adsorption includes three elementary processes Figure 2-1: (i) diffusion from the bulk to the sub-surface layer; (ii) adsorption from the sub-surface layer to the interface; (iii) possible rearrangement of the surfactant molecules at the surface. (Chang and Franses 1995; Chang and Franses 1995; Dukhin, G.; et al. 1995; Eastoe and Dalton 2000).

In early studies, the dynamic surface tension was modelled using the adsorption isotherm and diffusion equation only (Ward and Tordai 1946; Mysels 1982). In diffusion controlled model, the transport of the surfactant molecules in bulk solution is governed by the Fickian diffusion and the subsurface and the surface reach equilibrium instantaneously.

However, the diffusion coefficient obtained from this model was unrealistically low for most surfactants. Consequently, an “adsorption barrier” was proposed (Tsonopoulos, Newman et al. 1971; Miller and Kretzschmar 1980; Borwankar and Wasan 1983) to account for the delay in adsorption step. In this approach, the subsurface and surface concentrations are not always in equilibrium and the overall adsorption at the interface is controlled by both diffusion and adsorption kinetics. Hence, the model is preferred to as either “diffusion-kinetic-mixed” model (Miller 1981), or “barrier-limited” model (Tsonopoulos, Newman et al. 1971). The model solves diffusion and kinetics equations simultaneously to find the subsurface and surface concentrations.

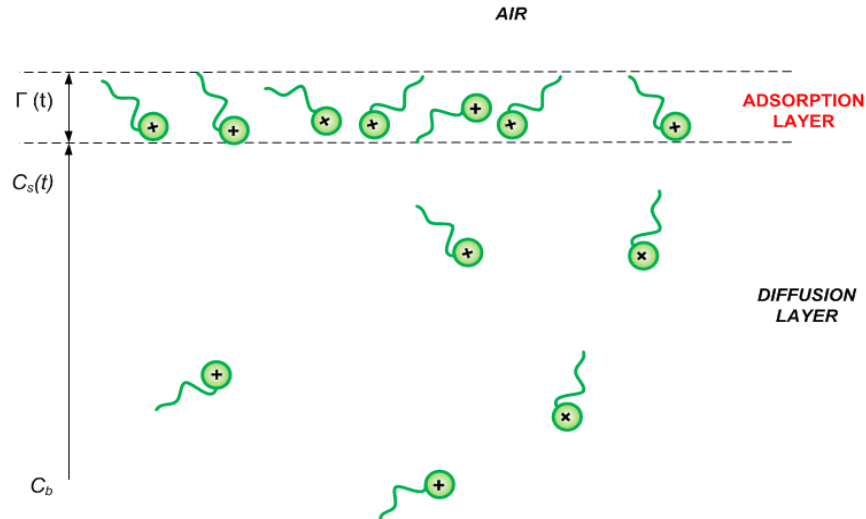


Figure 2-1 Fundamental process of dynamic adsorption cationic surfactants at air/water interface.

Equilibrium isotherm. The surface excess, $\Gamma(t)$, is assumed to be in equilibrium with sub-surface concentration, and can be determined by an adsorption isotherms such as Langmuir isotherm (Eastoe and Dalton 2000):

$$c_s(t) = \frac{1}{K} \left(\frac{\Gamma(t)}{\Gamma_m - \Gamma(t)} \right) \quad (2-15)$$

where $\Gamma(t)$ and Γ_m are transient and saturated surface excess of absorbed surfactant in the interface respectively; $c_s(t)$ is concentration in sub-surface layer and K is adsorption constant.

As equilibrium, the sub-surface concentration equals to bulk concentration, i.e. $c_s(\infty) = c_b$, Eq. 2.15 becomes:

$$c_b = \frac{1}{K} \left(\frac{\Gamma_{eq}}{\Gamma_m - \Gamma_{eq}} \right) \quad (2-16)$$

where c_b is the bulk concentration and Γ_{eq} is the corresponding equilibrium surface excess.

Diffusion equation.

For a one-dimension system, diffusion process is given by the Ward and Tordai equation (Ward and Tordai 1946; Mysels 1982):

$$\Gamma(t) = 2c_b \sqrt{\frac{Dt}{\pi}} - 2\sqrt{\frac{D}{\pi}} \int_0^{\sqrt{t}} c_s(t) d(\sqrt{t-\tau}) \quad (2-17)$$

where D is the diffusion coefficient and τ is a dummy variable of integration.

With the assumption that diffusion is the only mechanism in establishing adsorption equilibrium, the dynamic surface tension was modeled using the adsorption isotherm (Eq. 2-15) and diffusion equation (Eq. 2-17) only (Chang and Franses 1995).

As mentioned above, this model provides the diffusion coefficient with unrealistically low value for most surfactants. In these cases, another proposed model, “diffusion-kinetic-mixed” or “barrier-limited” model, was applied. With this model, diffusion and kinetics equations are solved simultaneously to find the subsurface and surface concentrations as reviewed by Phan and coauthors (Phan, Nguyen et al. 2005).

Kinetics equation. For this model, Langmuir isotherm is replaced by kinetics equation, which accounts for the delay in adsorption/desorption step. It is often assumed that the dynamic adsorption rate is linearly dependent on the sub-surface ($c_s(t)$) and surface concentrations ($\Gamma(t)$); while the desorption rate is dependent on $\Gamma(t)$ only (Miller and Kretzschmar 1980; Borwankar and Wasan 1983). The general equation for the adsorption kinetics is:

$$\frac{d\Gamma}{dt} = k^a G[\Gamma] c_s(t) - k^d F[\Gamma] \quad (2-18)$$

where k^a and k^d are the rate constants for adsorption and desorption movements, respectively; and G and F are a functions of $\Gamma(t)$.

Since the kinetic equation reduces to an adsorption isotherm at equilibrium, expression for G and F can be obtained using the adsorption isotherm. A kinetic equation, consistent with the Langmuir isotherm, is given as (Chang and Franses 1995):

$$\frac{d\Gamma}{dt} = k^a c_s(t) \left[1 - \frac{\Gamma(t)}{\Gamma_m} \right] - k^d \Gamma(t) \quad (2-19)$$

where $k^d = \frac{k^a}{K\Gamma_m}$

Alternatively, the kinetics equation can be simplified as:

$$\frac{d\Gamma}{dt} = k^a \left\{ c_s(t) \left[1 - \frac{\Gamma(t)}{\Gamma_m} \right] - \frac{\Gamma(t)}{K\Gamma_m} \right\} \quad (2-20)$$

Numerical modelling.

Although the above models can determine the dynamic surface concentrations, experimental measurements of $\Gamma(t)$ and $c_s(t)$ are not practical. Consequently, the adsorption is often quantified in term of surface tension. To relate the transient surface excess to dynamic surface tension, an additional equation is required. In the literature, the Gibbs equation is used to link surface tension to adsorption concentration (Chang and Franses 1995; Chang and Franses 1995; Eastoe and Dalton 2000) :

$$\Gamma = -\frac{1}{nR_g T} \frac{d\gamma}{d \ln c} \quad (2-21)$$

where γ is the surface tension, n accounts for the ionic state of the surfactant ($n = 2$ for ionic surfactants and $n = 1$ for non-ionic surfactants), T is absolute temperature and R_g is the gas constant.

Using Eq. 2-15, Eq. 2-21 integrating will result in:

$$\gamma_0 - \gamma(t) = -nR_g T \Gamma_m \ln(1 + Kc_s(t)) \quad (2-22)$$

where γ_0 and $\gamma(t)$ are surfactant-free (pure solvent) and dynamic surface tension, respectively.

At equilibrium, Eq. 2-22 reduces to the Szyszkowski equation(Chang and Franses 1995):

$$\gamma_0 - \gamma_{eq} = -nR_g T \Gamma_m \ln(1 + Kc_b) \quad (2-23)$$

2.3.2 Current fitting procedures of dynamic adsorption

The dynamic models can only fit experimental data at different concentrations separately. However, the best-fitted values of adjustable parameters are not consistent as bulk concentration changes.

The dynamic modelling typically consists of 3 steps (Chang and Franses 1995):

1. Equilibrium surface tension is fitted against Eq. 2-22 to determine K and Γ_m .
2. Diffusion model is applied to dynamic data to find best-fitted value of D .
3. If best-fitted D is smaller than theoretical value, “diffusion-kinetic-mixed” model is applied to find kinetics constant.

There are a number of shortcomings of the current fitting procedure especially for the first and third steps.

- In the first step, the accuracy of fitting Eq. 2-22 to equilibrium data can be questionable since there would be different combinations of K and Γ_m to fit data well (Prosser and Frances 2001). Moreover, different combinations of K and Γ_m can give good fitting for dynamic adsorption (Lee, Lin et al. 2001). It should be noted that the above number of fitting parameters are applicable for Langmuir isotherm only. With Frumkin isotherm or other complicated isotherms (Lin, Wang et al. 1997; Stubenrauch, Fainerman et al. 2005), additional parameters are required. With more parameters, there could be numerous combinations for good fitting.
- In the third step, the best-fitted values of k^a were not consistent (Bleys and Joos 1985; Bleys and Joos 1985; Lin, Wang et al. 1997). To improve the consistency of dynamic model, more complicated kinetics models were proposed, such as the modified Frumkin kinetics (Borwankar and Wasan 1983) and the modified Langmuir-Hinshelwood kinetics (Chang and Franses 1992). However, these kinetic equations are difficult to verify since the physical nature of kinetics step is not established yet. Mathematically, these modified kinetics equations did not improve the consistency of kinetics constant. For instance, the best-fitted values of B , an additional kinetics

parameter, also varied with 1-octanol concentration (Chang and Franses 1992).

Another fitting approach was proposed using K , Γ_m and k^a as adjustable parameters (Phan, Nguyen et al. 2005; Phan 2010; Phan 2010). Although this approach does not require equilibrium surface tension data (step 1), at least 3 parameters are adjustable during fitting process. Such multivariate fittings are computer-intensive and often result in local instead of global optimum. More importantly, the best-fitted value of k^a was also not consistent. For example, the best-fitted value of k^a for 1-octanol varied from 2×10^{-3} to 37×10^{-3} m/s as c_b changes from 0.6 to 1 mM (Phan 2010)

In summary, the kinetics constants from the current fitting procedures varied with the bulk concentration, which is directly contradictory to the assumption in Eq 2.19, i.e. k^a is independent of c_b . The inconsistency in dynamic model may arise from different inconsistencies of fitting equilibrium modeling (step 1). The kinetics constants from the current fitting procedures varied with the bulk concentration, which is directly contradictory to the assumption in Eq. 2-17.

As mentioned in the shortcomings of current fitting procedures, with the variety of k^a value with different surfactant concentrations, it is inconvenient to use fitting parameters with these current fitting approaches for comparison and prediction purposes.

2.3.3 Diffusion coefficient

It is obvious that the adsorption rate of surfactant molecules depends on its diffusion coefficient and concentration (Eq.2-16). The diffusion coefficient is normally denoted by D . In fact, there were two types of diffusion coefficients: intradiffusion and mutual diffusion.

- Intradiffusion relates to the diffusion of a labelled component within a homogeneous mixture, an example would be the intradiffusion of sucrose when a 1.00 mol dm^{-3} aqueous sucrose solution is brought into contact with another 1.00 mol dm^{-3} aqueous sucrose solution in which a portion of the sucrose molecules are tagged with ^{14}C (Leaist and Hao 1994).
- Mutual diffusion is the diffusion of one constituent in a binary system, for example, sucrose and water move in opposite directions (Leaist and Hao

1994). Figure 2-2 shows the diffusivity of sucrose and water component in solution.

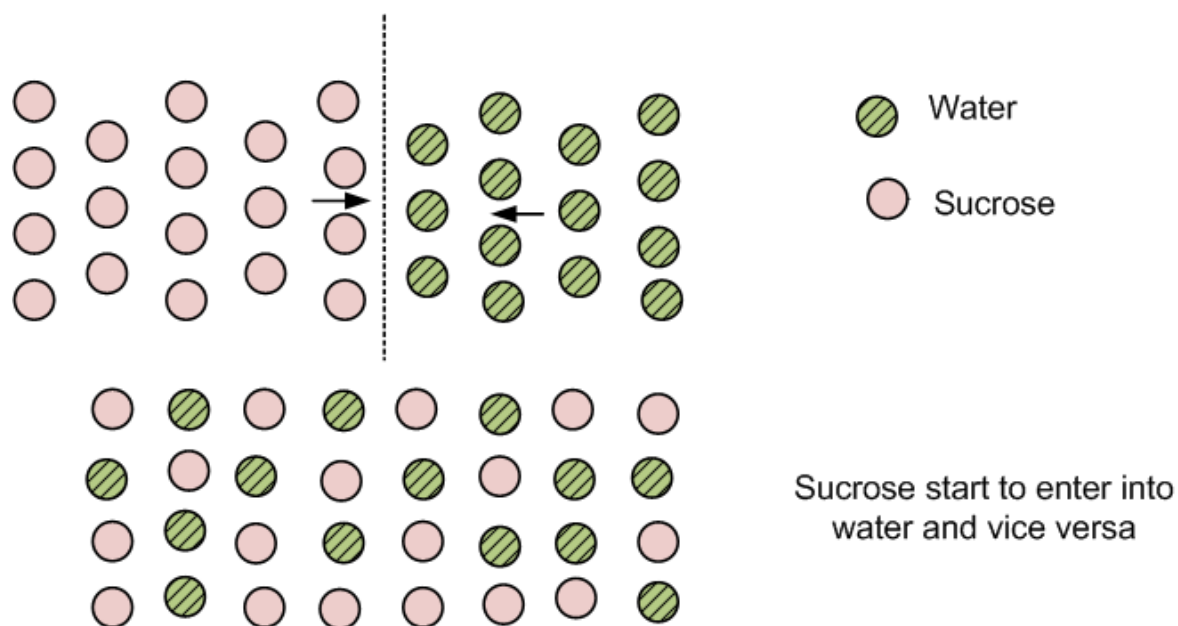


Figure 2-2 Mutual diffusion example

Whereas mutual diffusion is important in a wide range of practical mass transport processes, intradiffusion coefficients provide fundamental information about the structure and dynamics of solutions (Leaist and Hao 1994). Generally, the mutual diffusion coefficient is used for studying the dynamic adsorption of surfactant in solution.

Diffusion coefficient is measured by several methods: Nuclear magnetic resonance (NMR) (D'Errico, Ortona et al. 2001) or radioactive isotopes (Leaist 2002) or Taylor dispersion (Hao and Leaist 1996; D'Errico, Ortona et al. 2001; Leaist 2002), conductimetric cell (Ribeiro, Lobo et al. 2004), etc.

Diffusion coefficients depends on concentration of surfactants in solution, thus the average value of diffusion coefficient will be used for analyzing the kinetic adsorption.

In case of no available experimental data of diffusion coefficient, several estimation methods were proposed. These estimation methods are independent with concentration and based on molecular structures. The difference between experimental data and predicted value are acceptable (Poling, Prausnitz et al. 2001).

2.3.4 Dynamic adsorption of different structure of surfactants

There were several researches on the chain length to dynamic adsorption (Lin, McKeigue et al. 1991; Geeraerts, Joos et al. 1993; Fainerman and Miller 1996; Aksenenko, Makievski et al. 1998), such as Joos and Serrien (Joos and Serrien 1989) who measured dynamic surface tension of alcohol (n-propanol to n-heptanol) by oscillating jet technique in the range of a few milliseconds up to 20 ms. Using the first modeling approach as described above with one fitting parameter k^a (adsorption rate constant), they could compare the dynamic activities of alcohols as the chain length increased. They concluded that the adsorption rate constant depended on chain length while the desorption rate is constant. Propanol, butanol and pentanol had adsorption kinetics (controlled by the transfer from the subsurface to the surface). On the other hand, hexanol and heptanol followed mixed adsorption kinetics (both diffusion from the bulk to the subsurface and the transfer from subsurface to the surface were important); octanol was diffusion controlled.

Though some research work on effect of chain length on dynamic adsorption were done as mentioned above, only a few studies focused on branching chain structure to dynamic adsorption. Chi Phan (Phan 2010) conducted dynamic adsorption study of octanols by using pendant drop method. Applying the second approach in fitting dynamic adsorption mentioned above with three fitting parameters K , Γ_m and k^a , he compared dynamic adsorption activity of different surfactants at certain concentrations. Phan found that as the OH group moved inside the chain length, higher rate of adsorption resulted. The correlation between fitting parameters and structure change was not very clear.

It can be seen that the relationship between surfactant structure and dynamic surface tension properties is an almost unexplored area especially for important role of hydrocarbon branching (Varadaraj, Bock et al. 1991).

2.4 OTHER INTERFACIAL PROPERTIES

2.4.1 Surface elasticity

Surface elasticity: Gibbs-Marangoni elasticity has been recognized as an important parameter for a better understanding of foam stability (Wang and Yoon 2008), (Malysa and Lunkenheimer 2008) (Wantke, Malysa et al. 1994). The Gibbs-

Marangoni elasticity stabilizes foam because it is a force to pull back the foam film if it has been stretched (Tadros 2005).

$$E = \frac{2d\gamma}{d\ln A} \quad (2-24)$$

Where γ is the surface tension, A is the geometric area of the surface. The Gibbs elasticity (E) is applied to cases in which insufficient surfactants in film to restore the equilibrium surface concentration after deformation (thin film). This parameter can be determined by equilibrium adsorption isotherm (Christenson and Yaminsky 1995; Danov, Kolev et al. 2000; Kolev, Danov et al. 2002; Wang and Yoon 2008).

Langmuir isotherm:

$$E_G = kT\Gamma \frac{\Gamma_m}{\Gamma_m - \Gamma} \quad (2-25)$$

Frumkin isotherm:

$$E_G = kT\Gamma \left(\frac{\Gamma_m}{\Gamma_m - \Gamma} - \frac{2A\Gamma}{kT} \right) \quad (2-26)$$

While the Marangoni elasticity (E_M) is a temporary restoring force to prevent dangerous thin film which is linked to the diffusion rate of surfactant from the solution (Tadros 2005); E_M is more significant than E on its effect on foam stability (Schramm and Green 1995; Wang and Yoon 2008). E_M can be determined by measuring dynamic surface tension with known surface area changes such as maximum bubble method (Schramm and Green 1995; Tan, Fornasiero et al. 2006).

So the Marangoni elasticity is calculated by:

$$|E_M| = \left| 2 \frac{d\gamma}{d\ln A} \right| \quad (2-27)$$

The empirical modeling dynamic surface tension of Rosen was applied and is summarized by Eastoe and Dalton ((Eastoe and Dalton 2000) below:

$$\gamma(t) = \gamma_{eq} + \frac{\gamma_0 - \gamma_{eq}}{1 + \left(\frac{t}{t^*}\right)^n} \quad (2-28)$$

Where γ_0 and γ_{eq} are known for the surfactant solution, n and t^* are constants.

Marangoni surface elasticity can be calculated from the derivatives of Eq. 2-28:

$$|E_G| = \left| \frac{2n(\gamma_{eq} - \gamma_0) \left(\frac{t}{t^*}\right)^{n-1}}{\left[1 + \left(\frac{t}{t^*}\right)^n\right]^2} \right| \quad (2-29)$$

2.4.2 Surface potential

The surface potential, ΔV , an electrical property of interface, depends on the adsorption activities at the surface. It signifies the difference in potential at the air/liquid interface between the clean substrate and that covered either by a spread or adsorbed monolayer. The distribution of excess surfactant molecules at the surface form a monolayer similar to the one created by spreading certain insoluble substances at the interface (Posner, Anderson et al. 1952).

There were some cases where surface tension reduction could not clearly be counted by the relationship of molecular structure –surface activity, and surface potential could offer a better solution (Neys and Joos 1998).

Surface potential is complementary information which should be included in addition with surface tension information, especially with anionic/cationic surfactants or the presence of multivalent ions.

Measuring the surface potential is a rather delicate procedure and method-dependent. It can be measured by the dynamic capacitor method, the radioactive probe method, and the jet electrode method (Markin and Volkov 2002).

2.5 Other approaches to study interfacial properties

Neutron reflections

Currently, neutron reflection is considered as the most powerful technique in studying structure at the interface (Bradley J.E., Lee E.M. et al. 1988; J. and K. 1990). The reflection of neutrons (neutron reflectometry) at a surface is very similar to the better known phenomenon of the reflection of light. It determines the composition of the surface layer and gives low resolution structural information along the direction normal to the surface. It directly provides accurate information about surface excess at the interface while other methods could not.

CHAPTER 3

METHODOLOGY

Different surfactants (nonionic, cationic surfactants) were investigated for their adsorption behaviour at water/air interface through the measurement of the equilibrium and dynamic surface tension. Three main methods commercially available devices were used for this study

- Equilibrium adsorption data: Wilhelmy plate method
- Dynamic adsorption data: Pendant drop and maximum bubble methods

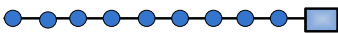
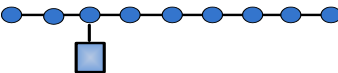
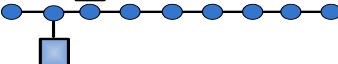
3.1 CHEMICALS

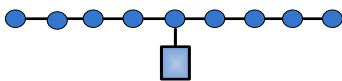
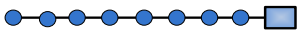
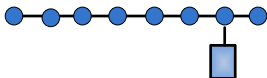
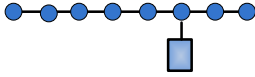
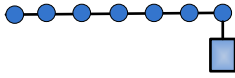

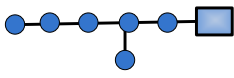
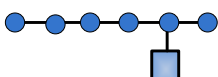
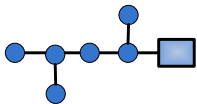
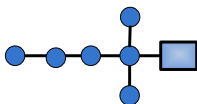
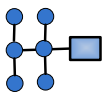
Though impurity of surfactants used in industry is the common issue but purity is one of the important factors in the accuracy of the surface tension measurement. In the theoretical study especially in investigation in molecular structure, chemical purity is essential. Almost of chemicals used was bought with highest purity from the supplier (analytical grade). For alkyltrimethyl ammonium bromide surfactants, all studied chemicals were further purified before use.

3.1.1 Non-ionic surfactants: alcohols

A full set of alcohols (C6 to C10) were investigated to find the relationship between the molecular structure and the adsorption behaviour at air/water interface. Table 3-1 shows the structure and suppliers of alcohols used.

Table 3-1 Alcohols used for this study

<i>Formula</i>	<i>Chemicals</i>	<i>Structure</i>	<i>Suppliers</i>	<i>Purity</i>
$C_{10}H_{22}O$	1-nonanol		Sigma Aldrich	98%
	2-nonanol		Sigma Aldrich	98%
	3-nonanol		Sigma Aldrich	99%

	<i>5-nonanol</i>		Sigma Aldrich	95%
$C_8H_{18}O$	<i>1-octanol</i>		Fluka	99%
	<i>2-octanol</i>		Sigma Aldrich	97%
	<i>3-octanol</i>		Sigma Aldrich	99%
$C_7H_{16}O$	<i>1-heptanol</i>			
$C_6H_{14}O$	<i>1-hexanol</i>		Fluka	99%
	<i>2-methyl 1-pentanol</i>		Sigma Aldrich	99%
	<i>2-hexanol</i>		Sigma Aldrich	99%
	<i>Methyl Isobutyl Carbinol (MIBC), 4-methyl-2-pentanol</i>		Rowe Scientific	98%
	<i>2-methyl 2-pentanol</i>		Sigma Aldrich	99%
	<i>2,3-dimethyl 2-butanol</i>		Sigma Aldrich	99%

3.1.2 Cationic surfactants

The alkyltrimethylammonium bromide (C_n TAB) cationic surfactants used in this study for $n = 12, 14, 16, 18$ were with structures and suppliers as listed in Table 3-2.

Table 3-2 Alkyltrimethylammonium Bromide used

<i>Formula</i>	<i>Chemicals name</i>	<i>Structure</i>	<i>Supplier</i>	<i>Purification solvent</i>
C₁₂TAB (DTAB)	Dodecyltrimethylammonium bromide	$\text{CH}_3(\text{CH}_2)_{11}\text{N}(\text{CH}_3)_3\text{Br}$	Sigma Aldrich	50:50% by weight acetone and ethanol
C₁₄TAB (TTAB)	Myristyltrimethylammonium bromide	$\text{CH}_3(\text{CH}_2)_{13}\text{N}(\text{Br})(\text{CH}_3)_3$	Sigma Aldrich	50:50% by weight acetone and ethanol
C₁₆TAB (CTAB)	Cetyltrimethylammonium bromide	$\text{CH}_3(\text{CH}_2)_{15}\text{N}(\text{Br})(\text{CH}_3)_3$	Sigma Aldrich	Methanol
C₁₈TAB (OTAB)	Octyltrimethylammonium bromide	$\text{CH}_3(\text{CH}_2)_{17}\text{N}(\text{CH}_3)_3(\text{Br})$	Sigma Aldrich	50:50% by weight acetone and ethanol

C_nTAB salts possessed the common trimethylammonium or other impurities: for example C₁₂TAB with dodecanol, C₁₄TAB with tetradecyl bromide (Simister, Thomas et al. 1992). The recrystallization was applied to remove the impurities in these chemicals.

With each C_nTAB, the suitable solvent was chosen by the following procedure:

- Adding 1-2 mL of solvent into a small amount of solid.
- If the surfactant dissolved in cold solvent, the solvent would not work, another solvent was further tested.
- If surfactant did not dissolve in the cold solvent, the mixture was heated on a hotplate. If surfactant dissolved, it was cooled, and then watched for crystals formation. If crystals appear, the solvent selected was appropriate.

The procedure of choosing a suitable solvent for recrystallization is shown in Figure 3-1

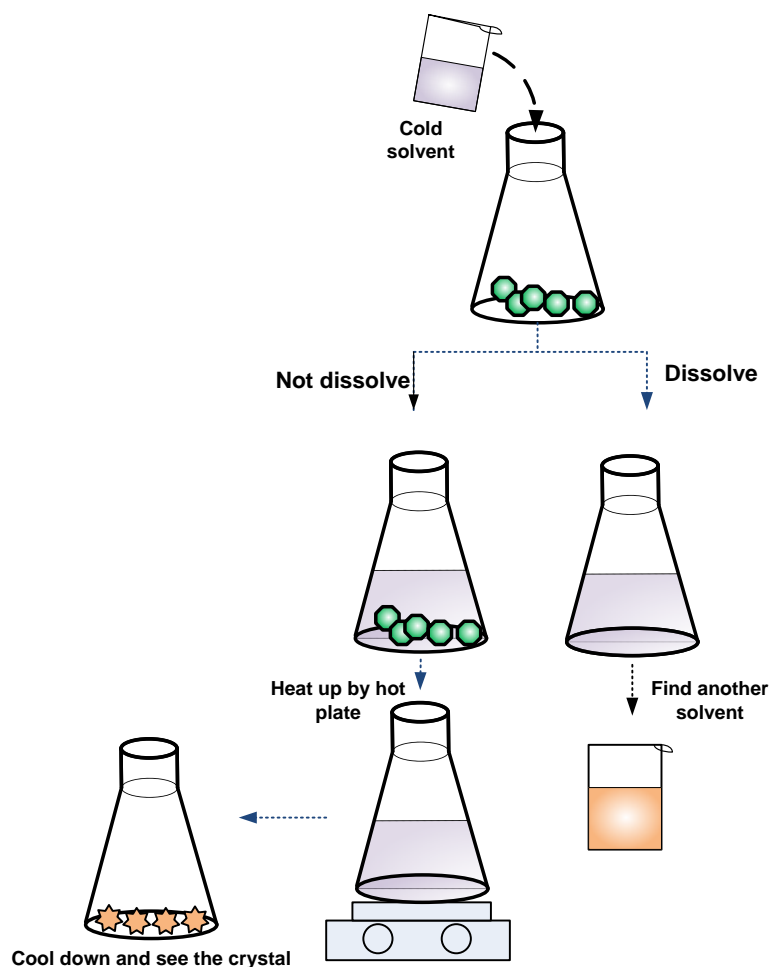


Figure 3-1 Procedure for choosing the solvent used in recrystallization

Crystallization process:

- Transfer the crude crystals of surfactant into an Erlenmeyer flask containing a small amount of solvent.
- Heat the mixture with a hot plate to boiling. More solvent is added to the mixture in small portions using a pipette until the solid just dissolves (saturated solution).
- Remove the flask from the heat source and allow it to cool to room temperature undisturbed. After about 10 minutes, further cool the flask in an ice bath. As the solution cools, the solubility of the solid decreases and the solid crystallizes.
- Wait until the crystals appeared and collected by vacuum filtration. Rinse the crystals with a small amount of a cold solvent.

- Save the filter paper and the material in it. Allow it to air dry overnight and put into desiccators.
- Repeat this procedure twice and test by measuring equilibrium surface tension curve of purified chemical solution with no minimum peak (Stubenrauch, Fainerman et al. 2005) and getting the repeatability.
- Figure 3-2 shows the crystallization procedure applied in this study.

Most of C_n TAB ($n=12,14,18$) were crystallized three times with 50:50 percentage of weight of acetone and ethanol. The exception was C_{16} TAB which was crystallized with methanol twice.

The adsorption study of C_{12} TAB to C_{14} TAB solutions was conducted at neutral pH. Except for OTAB, due to its limitation of solubility at room temperature, the NaOH was applied to increase pH to 11, which in turn increased the solubility of OTAB.

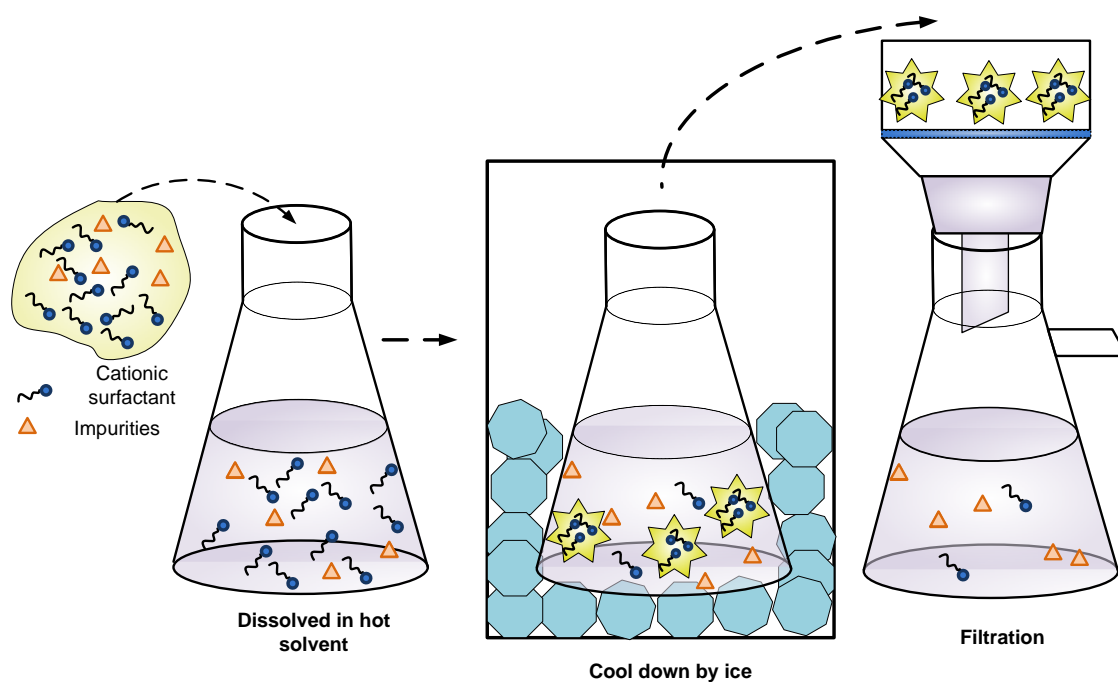


Figure 3-2 Recrystallization procedure

3.2 APPARATUS

3.2.1.1 Wilhemy plate method

This method is seemed to be the simplest one by dipping the roughened plate in to the interface of solution. The microbalance will record the force of lifting the plate detached from the interface (Figure 3-3).

$$F = W + \gamma p \quad (3-1)$$

where W is the weight of the plate, p is the contact length of the plate with liquid ($p = 2 \times (x + y)$). The increase by weight by the liquid layer touched the plate is calculated by

$$\Delta W = \gamma p \cos\theta \quad (3-2)$$

Where θ is the contact angle which is equal to zero as the plate is completely wetted by the liquid layer. Hence γ (surface tension) will be gained directly from the variation of weight.

The plate has to be vertical and clean to ensure the contact angle is 0.

Table 3-3 List of the advantages and disadvantages of Wilhelmy plate method

<i>Advantages</i>	<i>Disadvantages</i>
Fluid densities not required	Lineliness
Little interface distortion so can be used to measure the time-dependent changes in interfacial tension	
No correction factors needed	
Can be used for measuring dynamic surface tension	

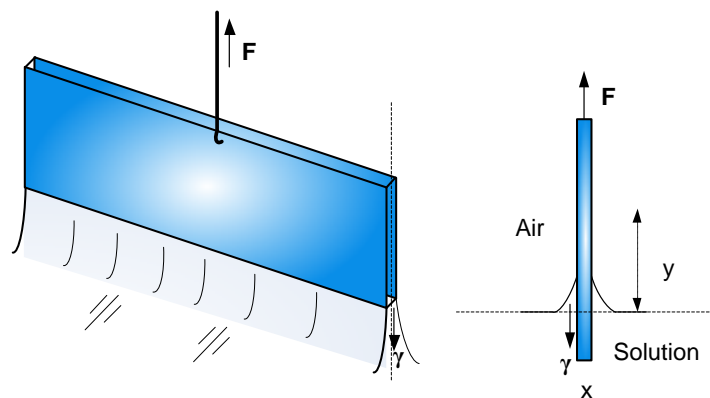


Figure 3-3 Wilhelmy plate method

The equilibrium surface tension in this study was applied by Wilhelmy plate method with the tensiometer KSV Sigma 700/701 (Figure 3-4).

The Sigma main unit was switched on at least 24 hours before measurement to stabilize the balance.

Before measurement, the plate has to be flushed with pure ethanol and water and then burned with a Bunsen burner for a few seconds to remove impurities.

The dispenser and container were cleaned with 6% by volume Deconex 15E solution (from Borer, Switzerland) several times and then rinsed with distilled water.

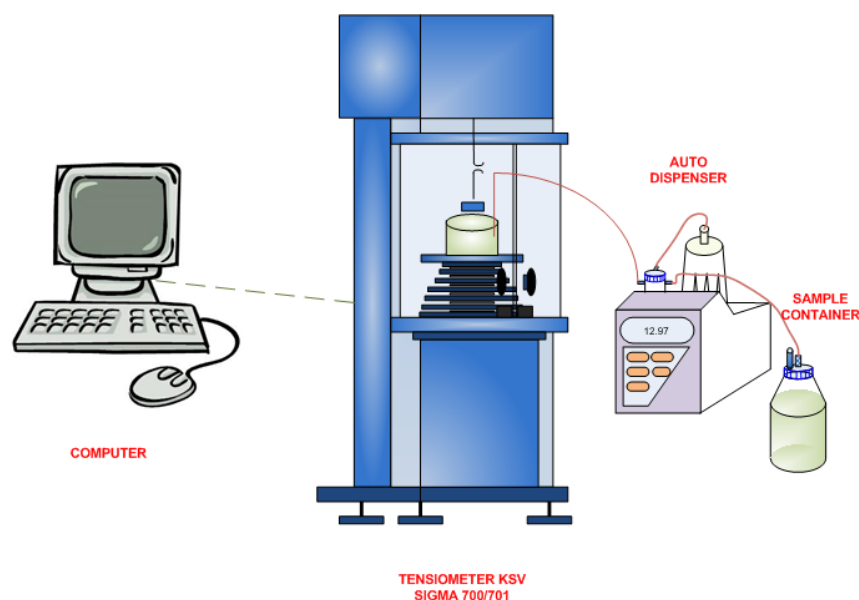


Figure 3-4 Tensiometer KSV Sigma 700/701

All samples were measured at certain temperature by means of a water bath.

Surfactant concentration was increased gradually by dispenser from a stock solution. The software automatically determined the surface tension as a function of bulk concentration.

The dynamic surface tension measurement for one small concentration of investigated chemical was conducted in advance to verify the time to reach equilibrium surface tension.

Error source:

The error of the data gained from this instrument can result from:

- An unclean container, plate or dispenser
- The vibration of the lab though the instrument was sitting on the anti-vibration table.
- Deformation of the plate which cannot ensure the contact angle is completely zero.

Advantage of tensiometer KSV Sigma 700/701 and auto dispenser: The concentration was prepared automatically which eliminate the error of the manual sample preparation

The dynamic adsorption of surfactant with the time was gained by using two different methods: pendant drop method (for those surfactants taking a long time to reach the equilibrium) and maximum bubble method for those reaching the equilibrium value in short time (millisecond range)

3.2.1.2 Pendant drop method

Drop shape analysis: pendant bubble method

The bubble created on the needle tip forms a pendant shape, not a sphere. The fundamental of the profile of bubble is described by the Young-Laplace equation. The shape of a bubble is determined by its radii of curvature, R1 and R2. The relationship between interfacial pressure (the pressure across the interface) and these radii of curvature are called the Young-Laplace equation:

$$\Delta P = \gamma \left(\frac{1}{R_1} + \frac{1}{R_2} \right) \quad (3-3)$$

where

ΔP = interfacial pressure difference

γ = interfacial tension

R_1, R_2 = surface's radii of curvature

Precise geometric definitions of these radii are described carefully by Adamson and coauthor (A.W. Adamson and Gast 1997).

In a column of fluid of density ρ and height h ,

$$\Delta P = \rho gh \quad (3-4)$$

with g is the acceleration due to gravity (9.8m/s^2).

Among other things, the Young-Laplace equation shows the pressure is quite high in a small drop (e.g., radius of 5 microns).

The volume (or, more correctly, the weight) of a pendant drop that can be supported on a round tip is described by Tate's Law:

$$W = 2 \pi r \gamma \quad (3-5)$$

where W is weight of drop, R is radius of wetted tip, γ is surface tension

The instrument was from PAT1 (from SInterface, Germany, Figure 3-5) which have been described in detail by (Phan 2010): a Perspex cell was filled with the surfactant solution and placed in the path of a parallel light beam. A bubble was formed on an inverted needle immersed in the solution. The light beam cast a bubble shape onto a CCD camera using an objective lens. The image was recorded and stored in a computer for further image analysis by computer. The bubble was rapidly formed using a gas-tight micro syringe, which was motorized and fully controlled by a computer. Distances on the video image were calibrated using a sphere of precisely known diameter of 1.5879 mm.

The surface tension corresponding to each bubble image was found. The system was calibrated using the outer diameter of the inverted needle. Checks on the calibration were performed at regular intervals by measuring the surface tension of purified Milli-Q water.

The experimental procedure:

Step1: determine the geometry: pendant bubble method

Step2: load the gas into the syringe and obtain a good video image, provide the internal diameter of the syringe for the software so the pump will be calibrated

Step3: magnification calibration: form a nicely shaped of the bubble, the image must be in precise focus.

Step 4: Set the program for capturing the image with the time, provide the solution density and start the automatic program.

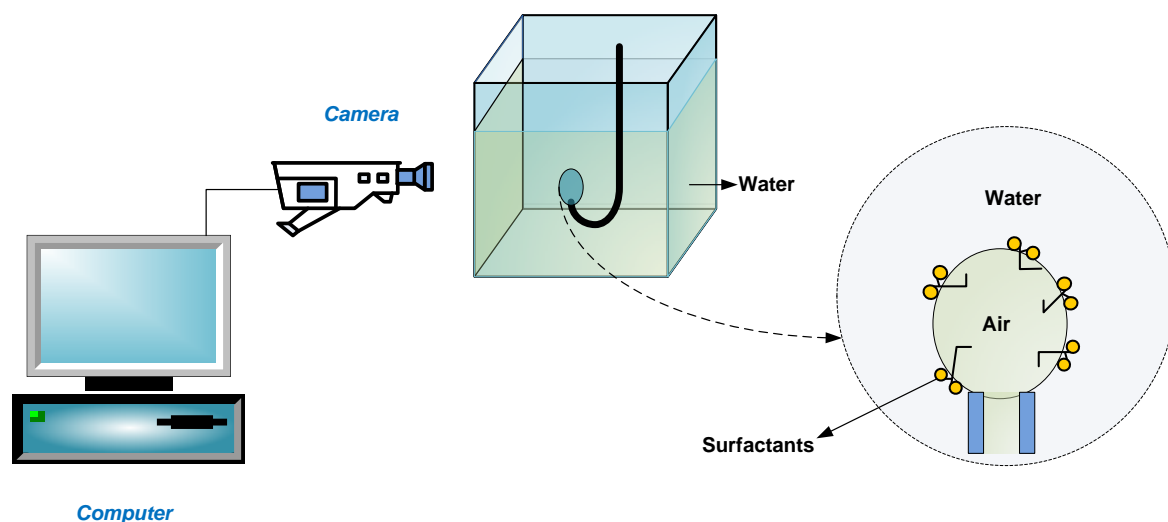


Figure 3-5 PAT1

Advantages: This technique allows the dynamic surface tension measured with minimal disruption to the interface (Ferri and Stebe 1999). This is a hydrostatic method so the dynamic artifacts associated with non-uniform surface tension (Marangoni effect) and convective effects in the surfactant mass transfer are avoided (Ferri and Stebe 1999). Calibration is straightforward in that only optical magnification is needed. This can be measured with high accuracy and is easy to trace to national standards (density must be known.) Solid surfaces of the apparatus involved need not have any special cleanliness because their wettability, does not affect the result.

3.2.1.3 Maximum bubble method

Maximum bubble pressure method (Figure 3-6) is based on the measurement of the maximum pressure in a bubble growing at the tip of a capillary immersed into the liquid knowing the density of the liquid and the size and depth of immersion of the capillary, the surface tension of the liquid can be calculated. As the gas is let into the capillary with an open end, the pressure is constantly monitored. First the curve

gas/liquid interface forms inside the tube and then driven down the tube by the gas flow. The pressure rises until the bubble forms a hemisphere is formed. After that the pressure decreases as the bubble size keeps increasing until the bubble will eventually drop off the tube. Another bubble will start to form and the process is repeated (Buzzacchi, Schmiedel et al. 2006).

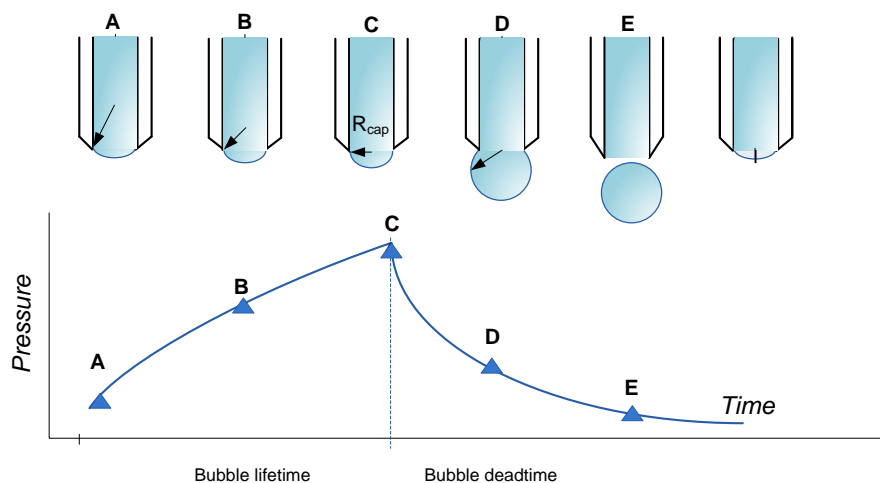
The dynamic surface tension at the time when the pressure gets to the maximum value is derived by Laplace's relation:

$$\gamma(t_{max}) = \frac{p_{max} - p_0}{2} R \quad (3-6)$$

With p_0 is the hydrostatic pressure at the tip of the capillary

R is the maximum bubble radius, p_{max} is the maximum value of the pressure

The method has advantage in that the influence of surface impurities is small and a wide variety of liquids and gases can be accommodated, ranging from simple hydrocarbon liquids to molten metals (Schramm and Green 1992).



Bubble formation

Figure 3-6 Maximum bubble method

The maximum bubble method was conducted by using MPT2 (Lauda, Germany, Figure 3-7). The apparatus, with capillary diameter of 100 microns, can measure dynamic surface tension from 10 ms to 1s.

The calibration process has to be done with certain submerge height. The instrument will auto calibrate with water and save the information. A volume of investigated

solution (same with volume of water used to calibrate) measured with the calibrated capillary to ensure unchanged submerged height.

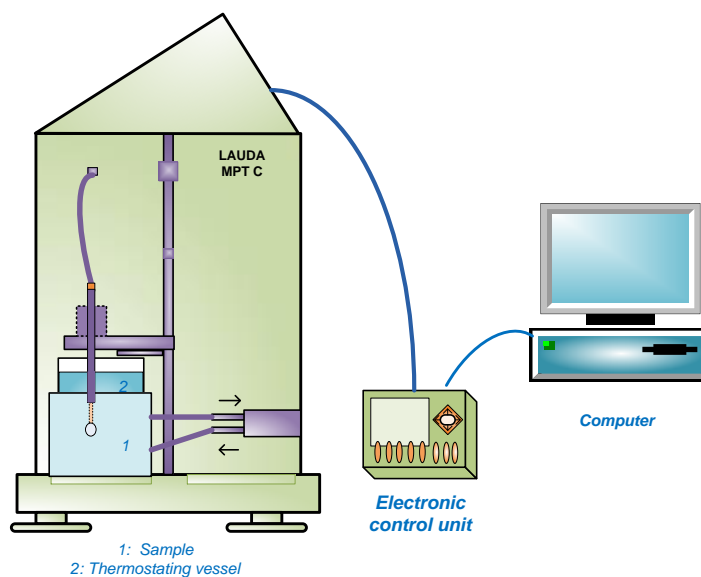


Figure 3-7 MPT2

All solutions were prepared using ultra-pure water with resistivity higher than 18 M Ω cm. This water was purified by a Milli-Q four-bowl system, which consists of a pre-filter, a carbon cartridge, two mixed-bed ion exchange cartridges and an ultra-filtration cartridge. All experiments were conducted at constant room temperature 22°C degree

3.2.1.4 Diffusion-ordered NMR spectroscopy (DOSY).

Proton NMR self-diffusion experiments were carried out using a Bruker DRX500 apparatus at 500.13 MHz to identify the diffusion coefficient of CTAB, TTAB and OTAB. This work was done in Japan through a collaborative project.

The C_nTAB solutions were prepared in a H₂O, which were transferred to the 5 mm NMR tube with D₂O containing sealed glass tube. A 2D sequence for diffusion measurements using stimulated echo and for water suppression using a pulse sequence with gradients was chosen (stebpgp1s19 pulse sequence). The variation of the intensity of one selected resonance peak in the ¹H NMR spectrum (*I*) is related to the strength of the gradient (*g*) by the following equation:

$$\frac{I}{I_0} = e^{[-(\gamma\delta g)^2 \times (\Delta - \frac{\delta}{3})D]} \quad (3-7)$$

where γ is gyromagnetic ratio of the proton, δ is length of the gradient pulse (small delta), g is gradient strength, Δ is delay between the midpoints of the gradients (big delta), and D is the self-diffusion coefficient. Prior to recording the 2D DOSY experiment, the δ and Δ values were optimized for each sample by using the 1D sequence for diffusion measurements (stebpgp1s191d, δ ($2 \times P30$) and Δ (d20), Bruker's software) (Söderman, Stilbs et al. 2004; Furó 2005).

^1H DOSY experiments, the standard pulse program, stebpgp1s19, employing stimulated echo, bipolar gradient pulses, and one spoil gradient with 3-9-19 pulse sequence (WATERGATE) solvent suppression to suppress the H_2O signal was used (Piotto, Saudek et al. 1992).

The 2D DOSY experiment was recorded with the optimized δ and Δ values. For all the experiments, $\delta = 3.0$ ms and $\Delta = 100$ ms were used. It was necessary to accumulate 256 scans per spectrum to increase the signal-to-noise (S/N) ratio concerning the peaks of the solutes. The data were analyzed with the Bruker's software, which provided directly D .

CHAPTER 4

INFLUENCE OF HYDROPHOBIC PART OF SURFACTANTS MOLECULE TO EQUILIBRIUM SURFACE TENSION

4.1 INTRODUCTION

Owing to the chemical structure of surfactants, they move to the surface, lower the surface tension and create stable foam, lower the stress needed to deform or break the droplet (emulsifying). The influence of chemical structures to equilibrium adsorption behaviour of surfactants and its application are the basic research for many authors (Fainerman, Miller et al. 2000; Beneventi, Carre et al. 2001; Comley, Harris et al. 2002; Goloub and Pugh 2005; Stubenrauch, Fainerman et al. 2005).

To compare the adsorption activity of surfactants with different molecular structures, most of the studies were based on qualitative model parameters especially surface excess (Rosen 1976; Kwan and Rosen 1980 ; Ueno M., Takasawa Y. et al. 1981; Rosen, Cohen et al. 1982; Sokolowski and Burczyk 1983). The surface excess gained from the equilibrium isotherm can be used directly for evaluating the surface activities or calculating others parameters such as efficiency, adsorption depth, diffusion scale (Ferri and Stebe 2000) which are essential for comparing purpose. This parameter was also applied for determining the Gibbs surface elasticity which is used for evaluating the stability of the foam. The equilibrium data are important for studying dynamic activity of surfactants or equilibrium adsorption of mixtures (Fainerman, Miller et al. 2002).

As highlighted in section 2.2.2, there was still lacking of a systematical study on branching structure- surface properties. To contribute filling this gap of research, in this chapter we conducted the investigation of two groups of surfactants: the alcohol frother groups and the C_nTAB groups. For alcohol group, the influence of chain length, branching structure to surface activity was identified. For cationic group, the correlation between chain length and surface behaviour was evaluated. The equilibrium data are also the basis for further parts of this thesis.

4.2 ALCOHOLS

For decades, substantially all commercial frothers were alcohols containing five to ten carbon atoms (Crozier and Klimpel 1989) due to their advantages in flotation practice than most members of the other frother groups (Klimpel 1991). Alcohol has amphiphilic characteristic which comprises of two components: hydrophilic group (-OH) and hydrophobic group (alkyl). The alkyl group determines the adsorption activity of alcohol, and is characterized by a functional connection between the number of adsorbed molecules at the interface and the relevant volume concentration of alcohol.

Although the effect of alcohols structure on surface tension of adsorbed monolayer has been reported in the literature (Addison 1945; Posner, Anderson et al. 1952; Jachimaska, Lunkenheimer et al. 1995; Comley, Harris et al. 2002), there were only a few systematic studies of the influence of hydrophobic to tension behaviour (Wade, Morgan et al. 1978). Besides, these studies focused mainly on n-alkanols (primary alcohols with straight alkyl tails). On the other hand, the effect of the location of hydrophilic group (-OH) and alkyl structure on surface tension remains not understood despite the application of many branched surfactants (Varadaraj, Bock et al. 1991; Rekvig, Kranenburg et al. 2003). It is also noteworthy that there were conflicting results in the literature on the reported values of adsorption constants due to measurement errors, impurities and incomplete experimental data (Prosser and Frances 2001)

We investigated static surface tension of isomeric $C_nH_{2n+2}OH$ with $n = 6-9$ at air/water interface by Wilhelmy plate method in combination with an automatic dispenser. The efficiency of a surfactant can be characterized by the equilibrium surface concentration, which can be quantified by applying common isotherms such as Langmuir or Frumkin isotherms. The experimental setup, in combination with theoretical analysis, was applied to determine the adsorption isotherm with high accuracy and reliability. The results were used to quantify the influence of hydrophobic tail on the adsorption behaviours of isomeric nonanols, octanols, heptanol and hexanols.

4.2.1 Results

The Langmuir and Frumkin isotherm described in chapter 2 were applied to analyze the relationship between surface tension and concentration gained by using Wilhelmy plate method as described in chapter 3. Each chemical has been run several times to ensure reproducibility.

4.2.1.1 Reproducibility

As aforementioned, the represented results of each chemical from several runs will be used for the analyses. Figure 4-1 shows an example of the reproducibility of 1-hexanol measurements.

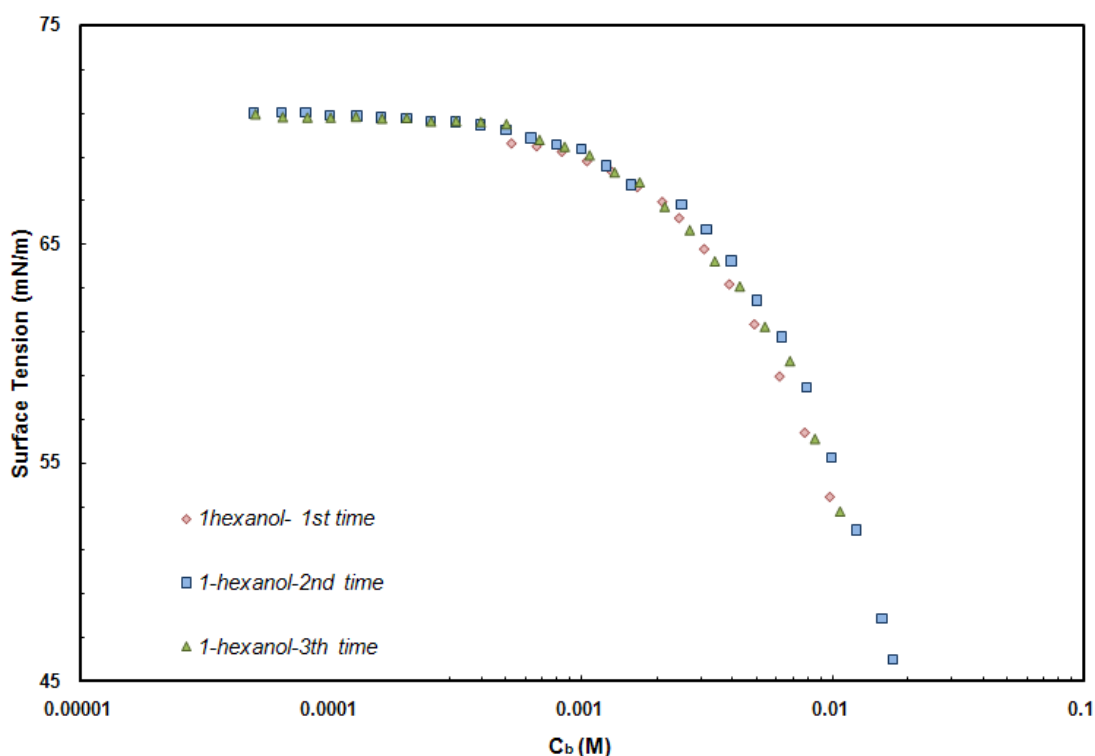


Figure 4-1 Results of three surface tension measurement runs of 1-hexanol

4.2.1.2 General observation

Each surfactant was measured at more than 15 concentrations. The concentrations were increased automatically by the dispenser. Isomers of alcohols were measured in range from 1×10^{-5} M to maximum solubility in the literature at 25°C (Yalkowsky and He 2003).

With low concentration ($\sim 10^{-4}$ M), the reduction in surface tension was not significant for most of investigated series except the n-nonanol. However, at higher

concentrations, there was significant difference for all alcohol series. Molecular weight plays an important role in the determination of the surface performance whereas the structural influence appeared less evident. The higher the molecular weight of the chemicals, the stronger adsorption capacity of the frothers: n-nonanol > n-octanol series > n-heptanol > n-hexanols.

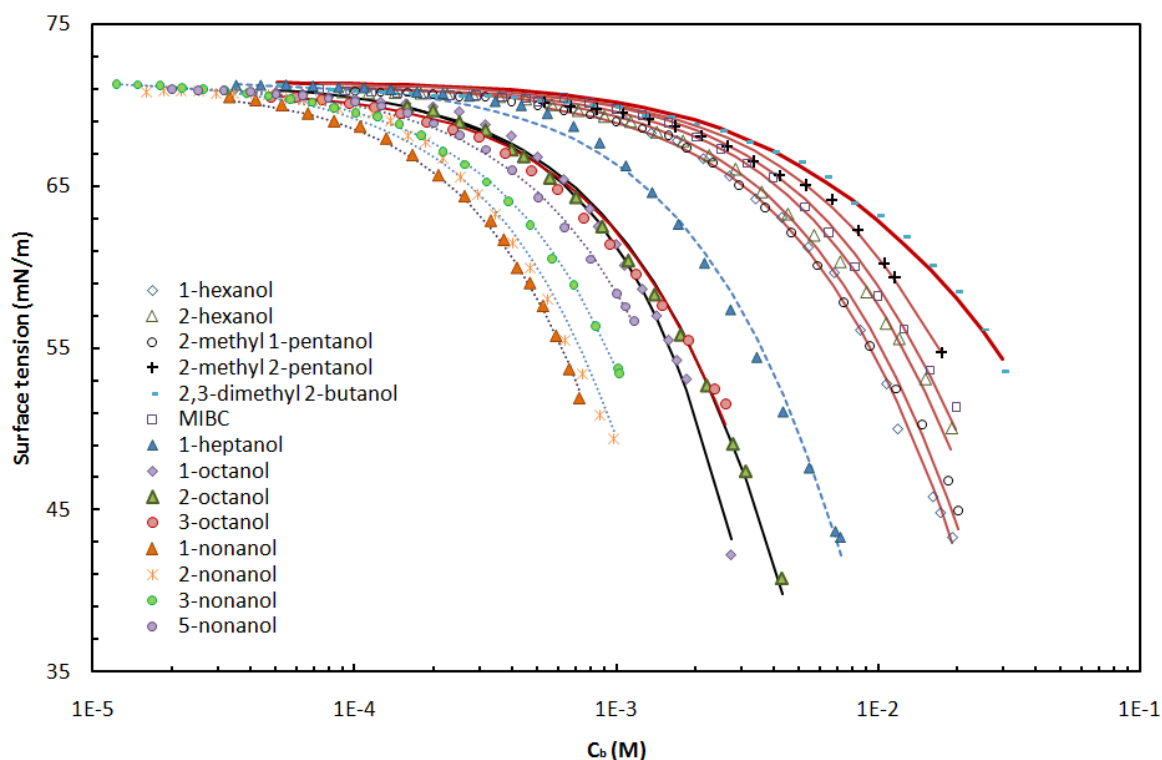


Figure 4-2 Surface tension as function of bulk concentrations for alcohols.

The relationship between surface tension and concentration of all investigated surfactants is shown in Figure 4-2. Due to the solubility limit of investigated alcohols, no CMC (critical micelle concentration) was observed. As the molecular weight increases, the solubility decreases, and consequently reduces the interfacial performance of these surface active chemicals.

4.2.1.3 Isotherm constants

Langmuir and Frumkin isotherms were used to fit with the raw experimental data as shown in Figure 4-2. The best-fitted values of adsorption parameters are tabulated in Table 4-1. The values of A are significant for most of primary surfactants.

The standard deviation in Table 4-1 was calculated for all modeled results using the following equation:

$$\delta_{\gamma} = \sqrt{\frac{\sum(\gamma_{exp} - \gamma_{modelled})^2}{n}} \quad (4-1)$$

when n is the number of measurement, which are greater than 15 for all surfactants used in this investigation.

The standard deviations for all surfactants are smaller than 1 mN/m, which indicate very reliable fitting (Prosser and Frances 2001) .

The best-fitted values of Γ_m from our data were different to the derived values from other studies (Lavi and Marmur 2000; Comley, Harris et al. 2002). It should be noted that neither these values were in agreement with the value provided by (Chang and Franes 1995). Moreover, Comley and co-authors as well as Chang and Franes derived the saturation surface excess from dynamic instead of equilibrium surface tension.

The reason for the discrepancy in fitting parameters could be the difference in measured temperature, impurities and the measurement method as well as the range of tested concentrations. This can be demonstrated in Figure 4-3, in which our prediction is compared with Lavi's prediction (Lavi and Marmur 2000) for 1-hexanol. It can be seen that the two predictions are very close and small error in measurement can significantly alter the best-fitted values of fitting parameters.

Table 4-1 Adsorption isotherm constants

Chemicals	$\Gamma_m (\times 10^6, \text{ mol/m}^2)$		$K_F (\text{L/mol})$		A	δ_{γ} (mN/m)
	This study	Literature	This study	Literature		
1-nonanol	50		220		0.5	0.25
2-nonanol	48		205		0	0.6
3-nonanol	32		200		0	0.36
5-nonanol	29		195		0	0.23

Chapter 4 Influence of hydrophobic part on equilibrium surface tension

C₈H₁₈O	1-octanol	23.5	9.2 ^a , 6.4 ^c	174		1.25	0.13
	2-octanol	23.0	5.8 ^c	172		4.4×10 ⁻³	0.53
	3-octanol	22.8	5.2 ^c	170		1.5×10 ⁻³	0.62
C₇H₁₆O	1-heptanol	22	8.3	98		0.019	0.51
		17	7.6 ^b	49	178 ^b	-8×10 ⁻⁵	0.29
C₆H₁₄O	1-hexanol		7.4 ^a				
			6 ^c				
	2-hexanol	14	4.8 ^b	48	300 ^b	1.3×10 ⁻²	0.49
	2-methyl 1-pentanol	15		50		0	0.6
	2-methyl 2-pentanol	11		48		0	0.25
	MIBC (methyl isobutyl carbinol, 4-methyl-2-pentanol)	13	5.0 ^a	49		3.0×10 ⁻³	0.41
2,3 dimethyl 2-butanol	11		47		1.16	0.39	

^a(Comley, Harris et al. 2002)

^b(Lavi and Marmur 2000)

^c(Chang and Franses 1995)

A: constant characterizing the lateral interaction among adsorbed surfactant molecules

4.2.1.4 Influence of molecular structure

Since the decrease in surface tension obtained is directly related to the surface excess adsorption of the surfactant by the Gibbs equation, a reduction in the amount of

material that can be adsorbed in a given surface area will reduce the ultimate surface tension lowering attained.

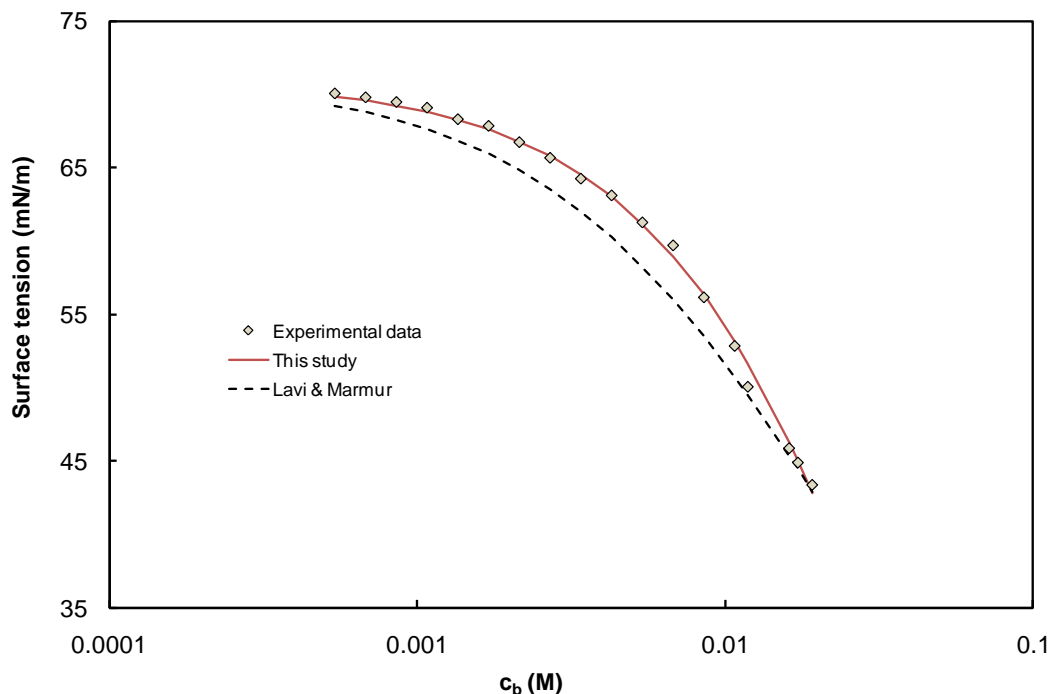


Figure 4-3 Predictions of 1-hexanol surface tension from parameters in Table 4-1.

The maximum surface concentration decreased significantly from nonanols to hexanols. Looking at the maximum surface concentration of straight chain alcohols, the Γ_m of 1-nonanol is the highest with the value of $50 \times 10^{-5} \text{ mol/ m}^2$. While the Γ_m of 1-hexanol is $17 \times 10^{-5} \text{ mol/ m}^2$.

Within the octanol series, the value of Γ_m decreases insignificantly as the hydroxyl group moves from the first carbon to the third carbon in the alkyl chain. For nonanol series, the maximum surface excess decreases as the OH group moves from the first to the fifth carbon (5×10^{-5} to $2.9 \times 10^{-5} \text{ mol/ m}^2$).

On the other hand, the variation was more significant for isomeric hexanols (from 1.7×10^{-5} to $1.1 \times 10^{-5} \text{ mol/ m}^2$). The value of Γ_m decreased with the increasing order of hydroxyl group (i.e. 1° alcohols $>$ 2° alcohols $>$ 3° alcohol). The only tertiary alcohol, 2-methyl 2-pentanol, was found to have the lowest value of Γ_m (1.1×10^{-5}

mol/m²). For the same order of hydroxyl group, Γ_m was smaller for bulkier isomers (i.e. 1-hexanol > 2-methyl 1-pentanol and 2-hexanol > MIBC).

The efficiency of MIBC (methyl isobutyl carbinol) was also found to be lower than 1-hexanol in the work reported by Comley (Comley, Harris et al. 2002). The straight chains of hydrophobic group showed strongest reduction of surface tension with highest Γ_m .

The results highlighted the decreasing trend of Γ_m with branching and increasing order of the hydroxyl group though Chang and co-authors (Chang and Franses 1995) summarized that this parameter is not significant trend for alcohols. The reduction of Γ_m with branching compounds have also been observed in butanol series: 5.74×10^{-6} mol/m² for 1-butanol, 4.65×10^{-6} for 2-butanol and 3.88×10^{-6} for *tert*-butanol (Jachimaska, Lunkenheimer et al. 1995).

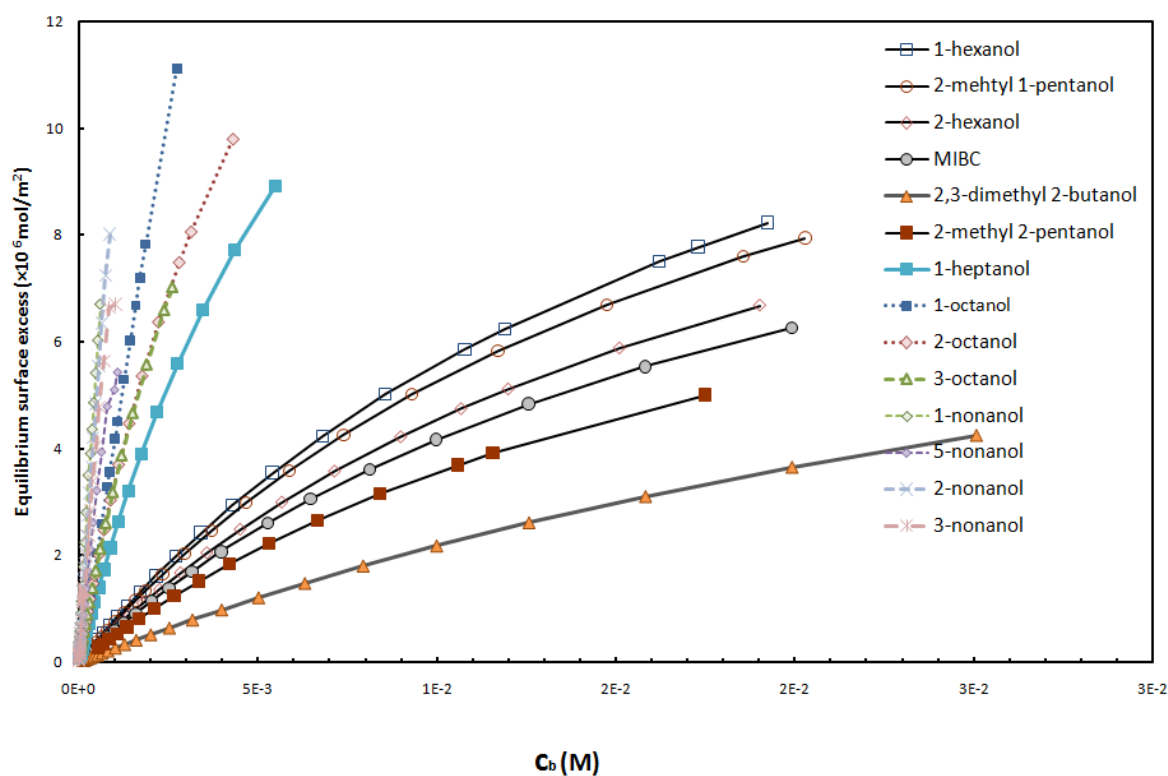


Figure 4-4 Relationship between equilibrium surface excess and bulk concentration.

Moreover, when the molecular weight is larger, the effect of OH position on maximum surface excess is higher.

The second parameter is equilibrium adsorption isotherm K_F . This value is varied slightly within each investigated series. For isomer of nonanol, we found that the

value of K_F are in range of 220-195 L/mol; while K_F values of octanol 169-172 L/mol and hexanol series are about 48-50 L/mol.

The influence of molecular structure on surface performance can be demonstrated by plotting the equilibrium surface excesses as a function of bulk concentration (Figure 4-4). The adsorbed concentrations were highest for the nonanol series. Two 2° octanols (3-octanol and 2-octanol) showed almost identical results. In contrast, the hexanol series demonstrated distinctly a decreasing order from the simplest to the most complex structure.

The tails of surfactants created by the movement of the hydrophilic group along a linear hydrocarbon chain (from 1-nonanol to 5-nonanol) show a relationship with fundamental interfacial properties: as the tails are made more equal in length (the head group are at the center of the chain), surfactants are less effective in reducing the surface tension. The branch tail structure of surfactant makes their density at the surface less than the related straight-chain alcohol with the same total carbon content (Figure 4-5). This possible arrangement leads to the less surface activity in branch structure than straight chain.

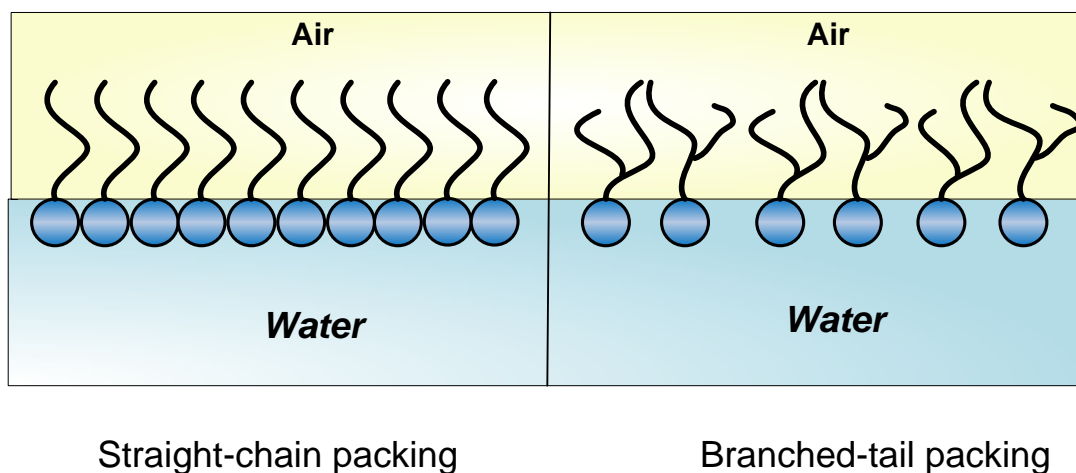


Figure 4-5 Possible arrangement of surfactants at interface

4.2.2 Summary

Langmuir isotherm proved to fit experimental data very well for branched surfactants while Frumkin was used for most of the primary alcohols (except for 1-hexanol). Due to the solubility of the investigated chemicals, no CMC was observed. Nevertheless, the performance of these surfactants was evaluated by the isotherm constants. With the same concentration, the straight chain alcohols were found to

reduce the interfacial tension stronger than the corresponding branching chain alcohols. The surface adsorption was strongly related to the position of hydroxyl groups, with primary alcohols showing strongest adsorption. The surface adsorption decreased with increasing complexity of alcohol structure.

4.3 CATIONIC SURFACTANTS

Alkylammonium bromide C_nTAB (n=12-18) were used widely in interfacial fundamental research for both equilibrium and dynamic adsorption (Stubenrauch, Fainerman et al. 2005), (Stubenrauch and Khristo 2005), (Bergeron 1997) (Monroy, Kahn et al. 1998) due to their high purity giving, less contamination problems than many other classical anionic surfactants (SDS) (Bergeron 1997), (Battal, Shearman et al. 2003). These chemicals also can be used in practical activity as precipitant, dispersant, absorbed on the particle surface, stabilized the particles and opposed further aggregation (Grieves, Bhattacharyya et al. 1976) in iron flotation or chemical for deinking process (with concentration higher than CMC value and pH higher than 11) (Chotipong, Scamehorn et al. 2007).

In this study the effect of chain length of C_nTAB on equilibrium adsorption activity was evaluated by equilibrium isotherm parameters. These parameters are also computed Gibbs elasticity E_G as well as later applied in calculating dynamic surface tension in chapter 5. The relationship of surface excess and concentration of these chemicals was gained by using Wilhelmy plate method.

4.3.1 Results

Langmuir equation gave good fitting for CTAB (C₁₆TAB) and OTAB (C₁₈TAB) adsorption isotherm while Frumkin equation was better for adsorption isotherms of DTAB (C₁₂TAB) and TTAB (C₁₄TAB) with low standard deviations. The isotherm parameters obtained in this study are quite close to those summarized by Miller (Miller, Fainerman et al. 2002) though they used Frumkin equation only for fitting. However, for CTAB adsorption fitting, both Langmuir and Frumkin isotherms fitted well with experimental data (Figure 4-8). For OTAB, due to the limitation of solubility, experiments were conducted with concentrations lower than CMC to ensure that completely solubility of OTAB in solution. The isotherm parameters for equilibrium adsorption of these chemicals are shown in Table 4.2.

Figure 4-6 shows the relationship of surfactants concentration and surface tension of C_nTAB surfactants. The maximum surface excess Γ_m increases as the length of these surfactants increases while literature data (Miller, Fainerman et al. 2002) shows that the surface excess is not correlated with carbon chain. C₁₈TAB which has the longest chain length shows the highest adsorption activity.

The adsorption constant K in this study also showed good correlation with the difference in the chemical structure. It increased significantly as the number of carbon chain increased. K values are from 263 L/mol of DTAB to 5878 L/mol of OTAB.

The CMC value increased as the chain length shortened. CMC of DTAB was about 15 mM, 3.6 mM of TTAB and 0.98 mM for CTAB. These values are quite accurate and compare well with results of other researchers (Monroy, Kahn et al. 1998; Chotipong, Scamehorn et al. 2007)

The relationship between bulk concentration and surface excess of Alkyltrimethylammonium bromide was demonstrated in Figure 4-7. The longer chain length resulted in stronger adsorption capacity of surfactant molecules.

Table 4-2 Adsorption isotherm parameters of C_nTAB

Chemicals	$\Gamma_m (\times 10^6, \text{ mol/m}^2)$		$K_F (\text{L/mol})$		A		δ_γ (mN/m)
	<i>This study</i>	<i>Literature¹</i>	<i>This study</i>	<i>Literature¹</i>	<i>This study</i>	<i>Literature¹</i>	
	C₁₂TAB (DTAB)	3.55	3.378	270	263	0.5	
C₁₄TAB (TTAB)	5	4.716	800	846	1	1.1	0.6
C₁₆TAB (CTAB)	5.3	3.22	2600	3050	0	1.3	0.17
C₁₈TAB	11.6		5878		0		1

(OTAB)

¹(Miller, Fainerman et al. 2002)

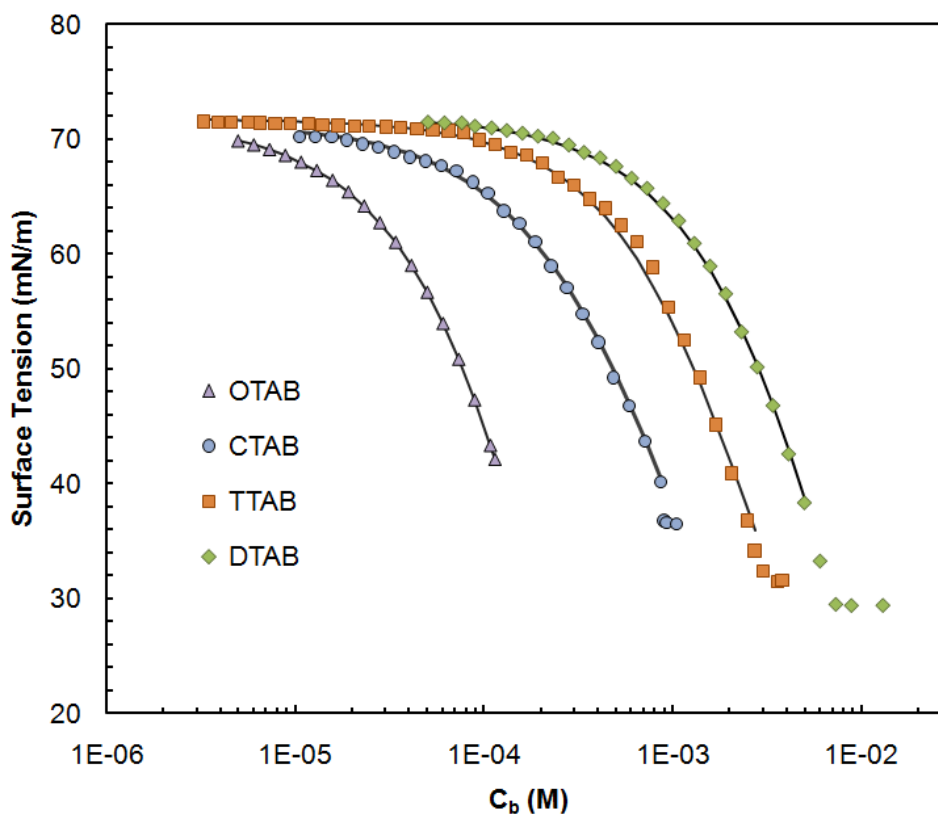


Figure 4-6 Relationship between Surface tension and concentration of C_nTAB.

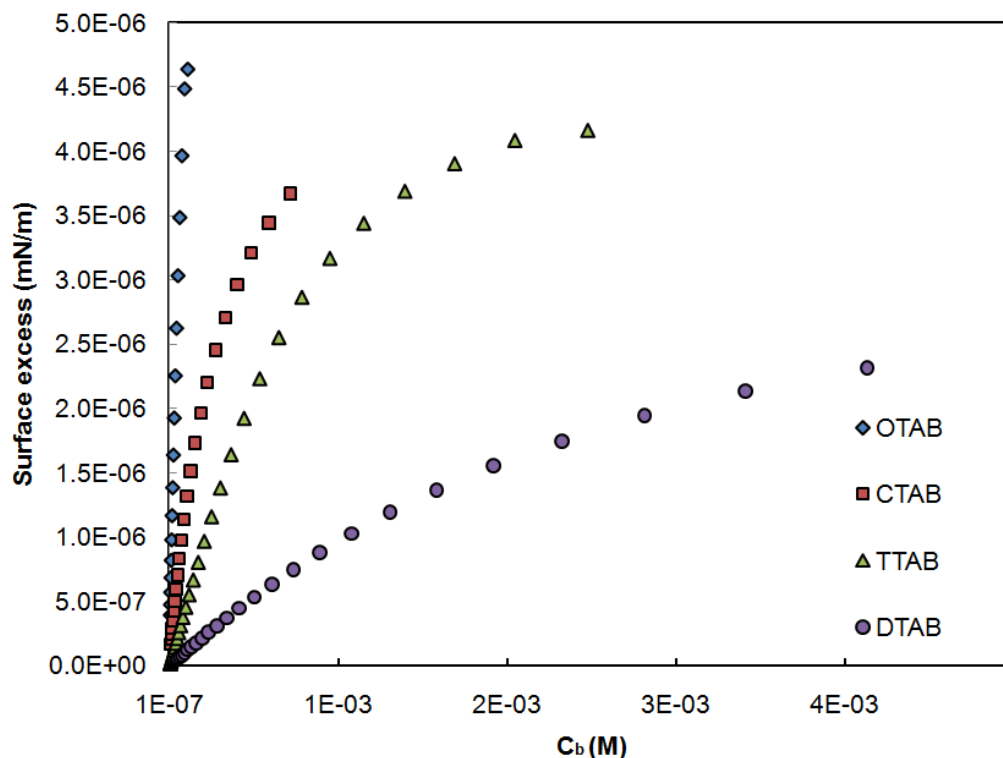


Figure 4-7 Surface excess vs. concentration of C_n TAB

The experimental results in this study were very close with predicted data of the reference (Miller, Fainerman et al. 2002). Figure 4-8, Figure 4-9 display the comparison of CTAB and TTAB experimental data with the one from the reference (Miller, Fainerman et al. 2002).

Equilibrium parameters are not only useful for comparing the surface active of different chemicals; they can also be used for calculating the Gibbs elasticity from equation when experiments are not available. The values of Gibbs elasticity were plotted against the log of surfactant concentration as shown in Figure 4-10..

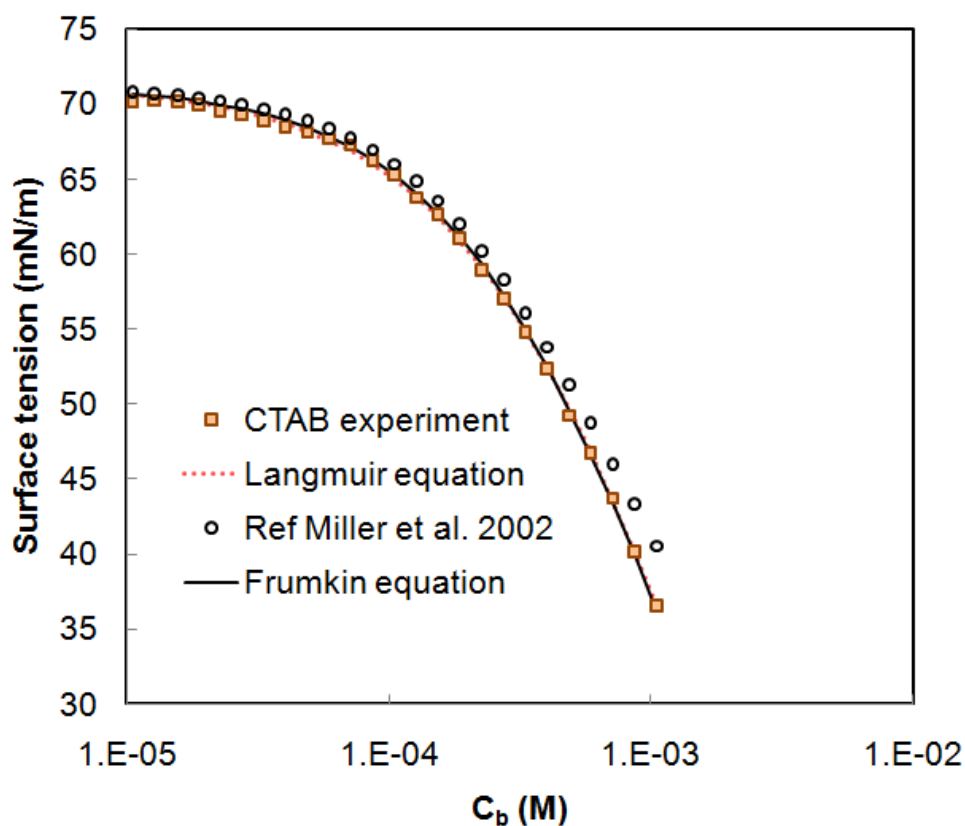


Figure 4-8 Comparison of CTAB experimental data and reference (Miller, Fainerman et al. 2002)

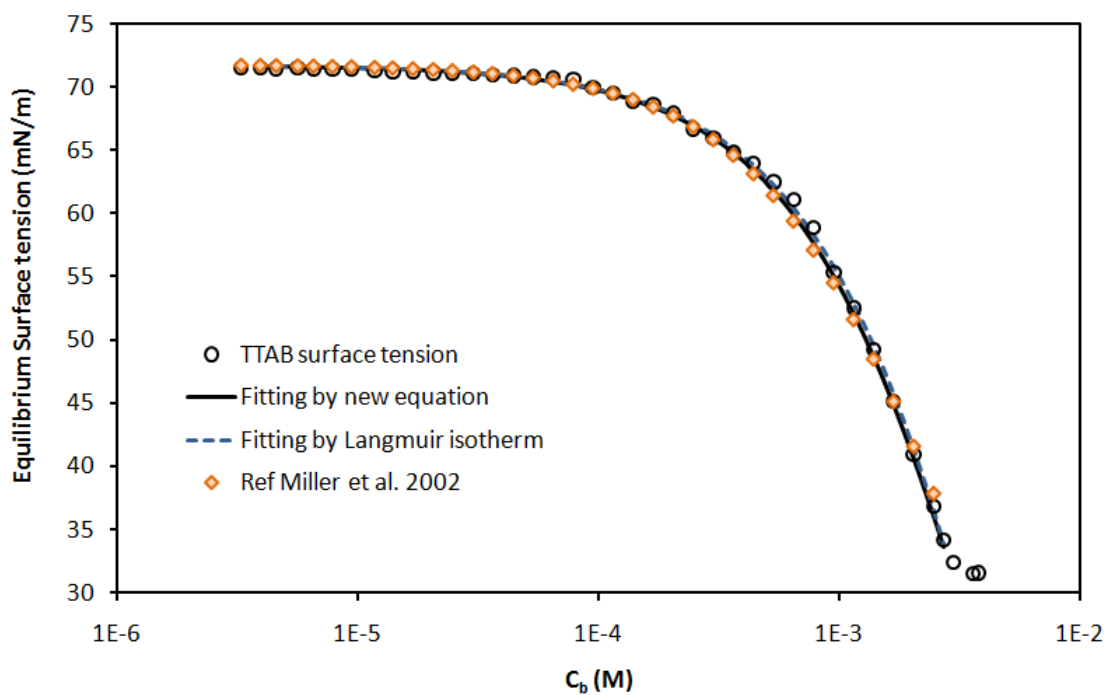


Figure 4-9: TTAB experiment and reference data (Miller, Fainerman et al. 2002)

The higher the number of carbon chain length in the molecule structure of C_n TAB, the higher is the surface elasticity (E_G). Normally, foams which are stabilized by surfactants with high elasticity are easy to form and are more stable (Stubenrauch and Khristo 2005; Georgieva, Cagna et al. 2009). Thus, it can be quickly concluded that the longer chain length of C_n TAB (higher number of n), the foam created will be more stable. Though the calculated value of Gibbs elasticity might be different with actual values and the stability of foam are dependent on other factors, the simple calculated E_G from equilibrium isotherm provides a initial evaluation of the foam behaviour of the C_n TAB (Georgieva, Cagna et al. 2009)

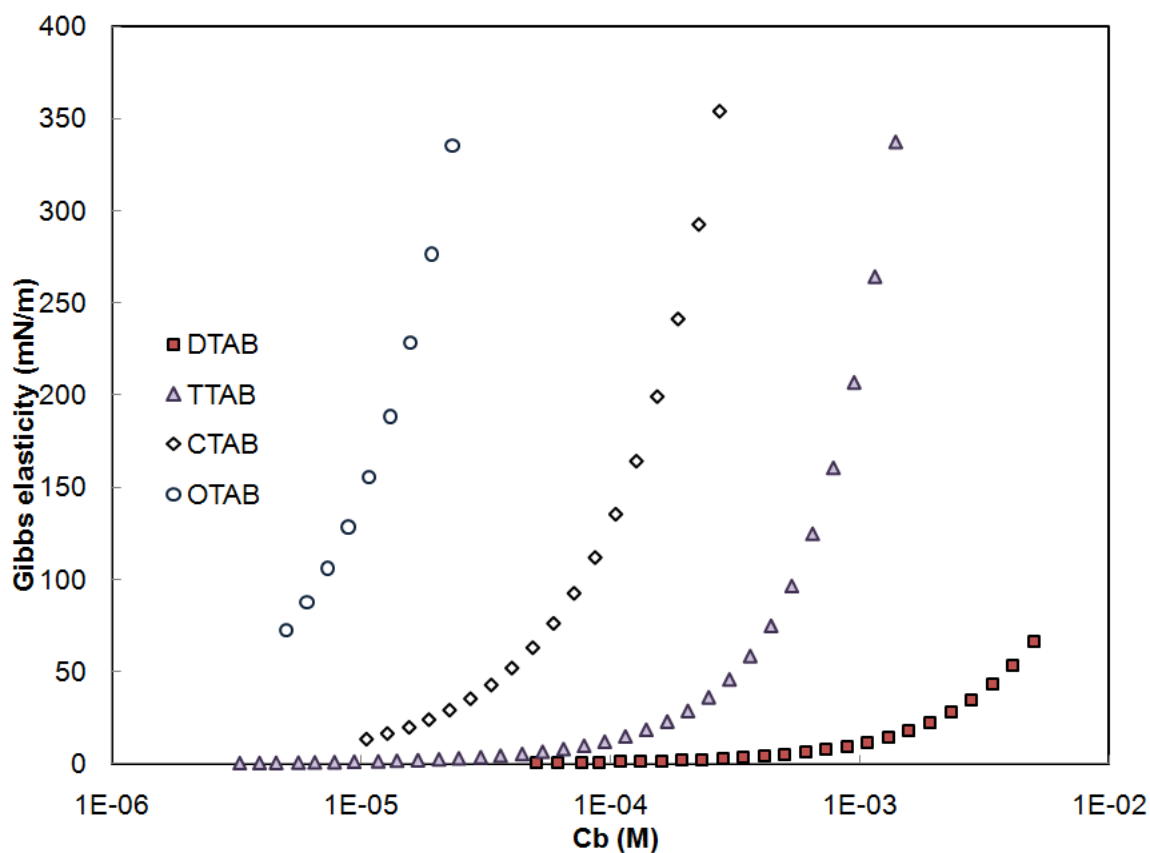


Figure 4-10 Gibbs elasticity vs. concentration of C_n TAB

4.3.2 Summary

For C_n TAB series, good agreement of experimental data was gained compared to the reference (Monroy, Kahn et al. 1998; Miller, Fainerman et al. 2002; Stubenrauch, Fainerman et al. 2005). Langmuir isotherm accounted for the adsorption activity of C_{12} TAB and C_{14} TAB while Frumkin was for C_{16} TAB and C_{18} TAB. The correlation between the surface excess and adsorption constant with the length of the carbon

chain is that: the longer the chain length of C_nTAB surfactants investigated, the higher values of isotherm parameters K and Γ_m .

4.4 CHAPTER CONCLUSION

Wilhelmy plate method was used to identify the equilibrium surface tension of isomeric alcohol series C_nH_{2n+2}OH (n = 9-6); and C_nTAB (n = 12-18) to evaluate the influence of molecular structure on the interfacial behaviour.

Different positions of hydroxyl group and branching alkyl structure of alcohols and the influence of chain length of C_nTAB to equilibrium adsorption were studied by comparing the Frumkin and Langmuir isotherm parameters. These equilibrium adsorption parameters of C_nTAB series can also be used to calculate the Gibbs elasticity which can be used in comparison to the temporary stability of foaming. They are very essential for later investigations of dynamic adsorption or equilibrium adsorption of mixtures.

A micro-dispenser was also used to prepare solutions automatically. The setup reduced errors caused by manual preparation and provided more data points in the curve of surface tension and concentration. Consequently, higher reliability of experimental data and high accuracy of modelling results obtained.

The study resulted in an overall influence of molecular structure on the equilibrium surface tension of two different types of surfactants (alcohols, the simplest non-ionic surfactant; and cationic surfactant C_nTAB). For mineral processing applications, the mixtures of surfactants as well as contaminants are more common. Consequently, the study should be extended to mixtures of similar or different type of surfactants to understand the interaction between these chemicals and the influence of surfactant structure on the efficiency of mixtures.

CHAPTER 5

DETERMINATION OF DIFFUSION COEFFICIENT

5.1 INTRODUCTION

As mentioned in section 2.3.3, diffusion coefficient is one of the two essential parameters that control the dynamic adsorption rate of surfactants. In this chapter, the diffusion coefficient values of investigated chemicals were derived from theoretical calculations and experimental results were derived from ^1H NMR spectrum method. The experimental data of diffusion coefficients were obtained by Prof. Shin-ichi Yusa from University of Hyogo, Japan.

5.2 THEORETICAL DIFFUSION COEFFICIENT

Using Wilke-Chang Estimation Method (Poling, Prausnitz et al. 2001) based on molecular structure, the diffusion coefficient of investigated chemicals can be calculated. The equation used in this method is described in Eq 5-1

$$D = \frac{7.4 \times 10^{-8} (\phi M_B)^{1/2} T}{\eta V^{0.6}} \quad (5-1)$$

where

D: diffusion coefficient, cm^2/s

M_B : molecular weight of water, g/mol

T: temperature, K

η : viscosity of water, cP

V: molar volume of surfactant at its normal boiling temperature, cm^3/mol

ϕ : association factor of water $\phi = 2.6$

The value of molar volume of surfactant was calculated by additive method of Schroeder summarized by Poling (Poling, Prausnitz et al. 2001) by Eq. 5-2

$$V = 7(N_C + N_H + N_O + N_N + N_{DB} + 2N_{TB}) + 31.5N_{Br} + 24.5N_{Cl} + 10.5N_F + 38.5N_I + 21N_S - 7N_{\text{ing}} \quad (5-2)$$

where: subscripts DB and TB stand for double and triple bonds and the last value N_{ing} is counted once if the compound has one or more rings, N is a number of atom/group.

These theoretical diffusion coefficient values of investigated chemicals were compared with the experimental values gained from ^1H NMR spectrum method.

5.3 ^1H NMR SPECTRUM METHOD RESULTS

The diffusion coefficient of surfactants is changing with their concentration. In this thesis, the average values of diffusion coefficient of different investigated concentrations.

5.3.1 TTAB

Figure 5-1a shows ^1H NMR spectrum for 1.5 mM TTAB in H_2O . The H_2O signal was suppressed using a WATERGATE pulse sequence. The resonance bands observed at 1.1-1.3, 1.6, and 3.2 ppm are attributed to the methylene protons. The resonance peak observed at 0.7 ppm is attributed to the terminal methyl protons in the alkyl chain. The singlet resonance peak at 2.9 ppm is assigned to methyl protons attached to a nitrogen atom. ^1H DOSY was measured for the peak at 1.1-1.3 ppm, because the resonance band is good S/N ratio. Therefore, Figure 5-1b shows the fitted diffusion curve estimated from the ^1H DOSY experiment at 1.1-1.3 ppm. The obtained data were fitted with Eq 3-7 to obtain diffusion coefficient (D). It has been found that $D = 4.313 \times 10^{-10} \text{ m}^2/\text{s}$. Values of D with different concentration, the comparison of the average value of experimental data and theoretical value were shown in Table 5-1.

Table 5-1 Diffusion coefficient (D) of TTAB at various concentrations in H_2O at 20 $^\circ\text{C}$ measured using DOSY with WATERGATE method

<i>Concentration</i> (mM)	<i>D</i> $\times 10^{-10}$ (m^2/s)	<i>Average D</i> $\times 10^{-10}$ (m^2/s)	<i>Theoretical D</i> $\times 10^{-10}$ (m^2/s)
1.5	4.313	4.34	4.470
1.1	4.329		
0.8	4.333		
0.6	4.360		
0.4	4.370		

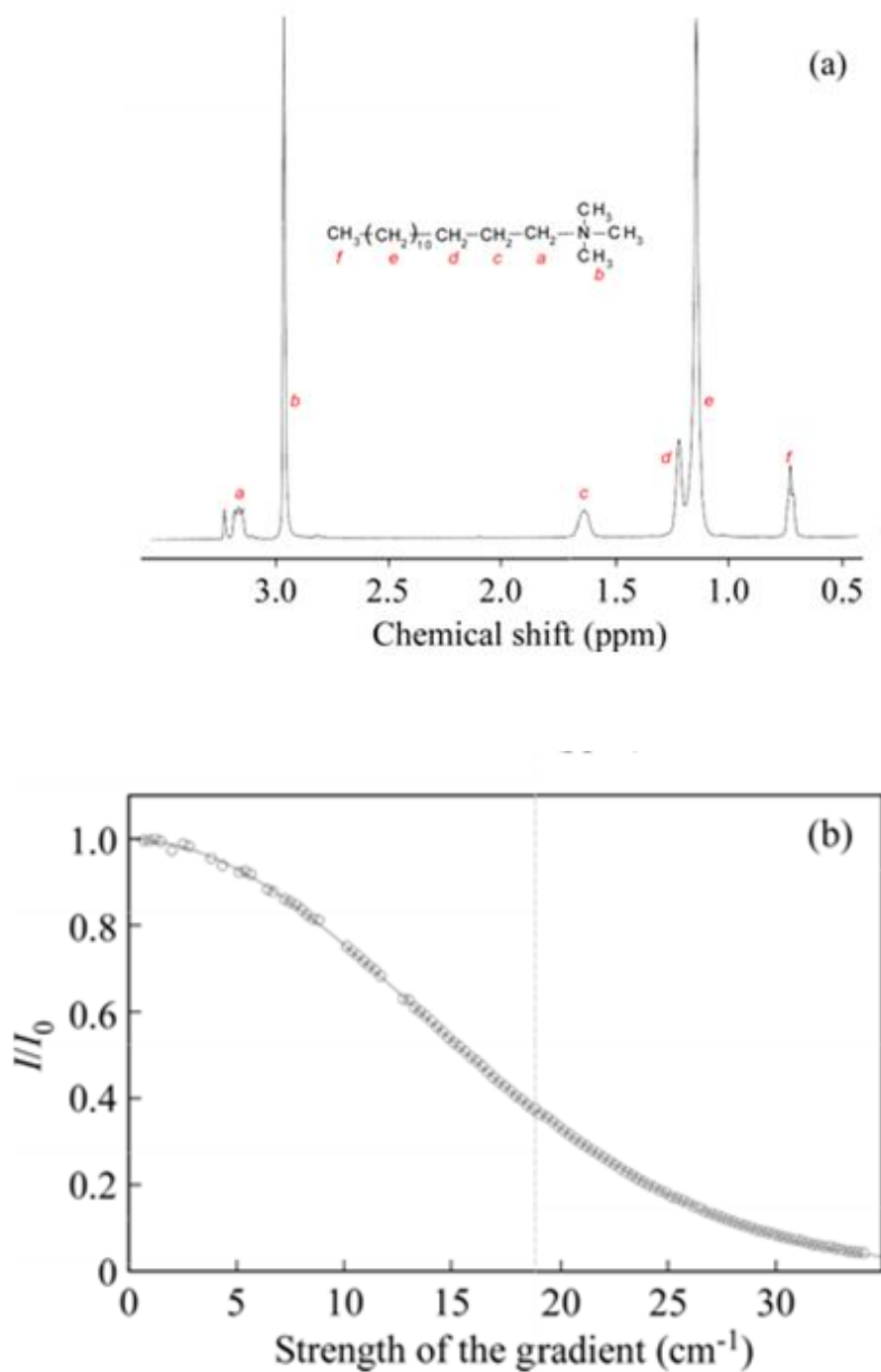


Figure 5-1. (a) ^1H NMR spectrum with solvent suppression of TTAB in H_2O . (b) Fitted diffusion curve estimated from ^1H NMR DOSY using WATERGATE pulse sequence for 1.5 mM TTAB in H_2O

5.3.2 CTAB

Figure 5-2a shows ^1H NMR spectrum for 0.4 mM CTAB in H_2O . The H_2O signal was suppressed using a WATERGATE pulse sequence. The resonance bands observed at 1.0-1.2, 1.6, and 3.2 ppm are attributed to the methylene protons. The resonance peak observed at 0.4 ppm is attributed to the terminal methyl protons in the alkyl chain. The singlet resonance peak at 2.9 ppm is assigned to methyl protons attached to a nitrogen atom, which is good S/N ratio and not overlapped any other peaks. Figure 5-2b shows the fitted diffusion curve estimated from the ^1H DOSY experiment at 0.4 mM. Therefore, ^1H DOSY measurements were performed for 2 curves estimated from the ^1H DOSY experiment at 2.9 ppm is data were fitted with Eq. 3-7 to determine diffusion coefficient $3.798 \times 10^{-10} \text{ m}^2/\text{s}$, which is consistent with reported diffusion coefficient (Lindman, Puyal et al. 1984).

The theoretical and experimental data of diffusion coefficient values of C16TAB are displayed in Table 5-2.

Table 5-2 Diffusion coefficient (D) of CTAB at various concentrations in H_2O at 20 $^\circ\text{C}$ measured using DOSY with WATERGATE method

<i>Concentration</i> (mM)	<i>D</i> $\times 10^{-10}$ (m^2/s)	<i>Average D</i> $\times 10^{-10}$ (m^2/s)	<i>Theoretical D</i> $\times 10^{-10}$ (m^2/s)
0.4	3.798	3.798	4.23
0.5	3.797		

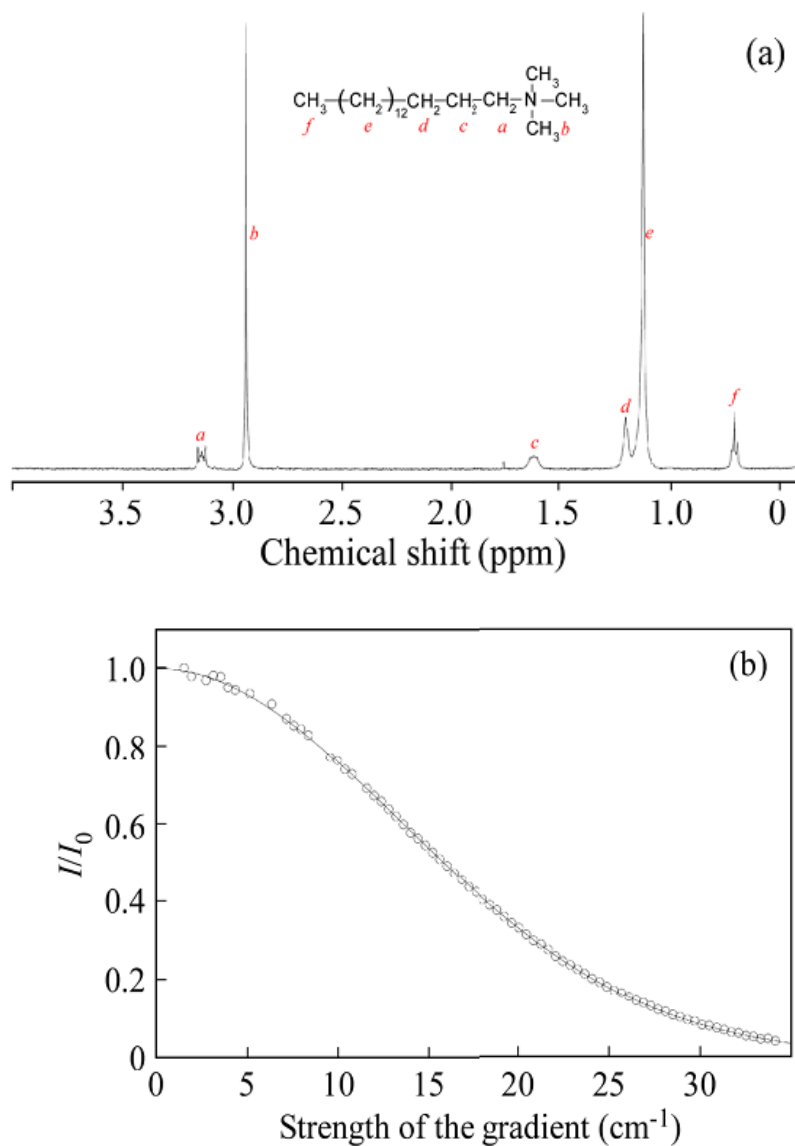


Figure 5-2 (a) ^1H NMR spectrum with solvent suppression of CTAB in H_2O . (b) Fitted diffusion curve estimated from ^1H NMR DOSY using WATERGATE pulse sequence for 0.4 mM CTAB in H_2O

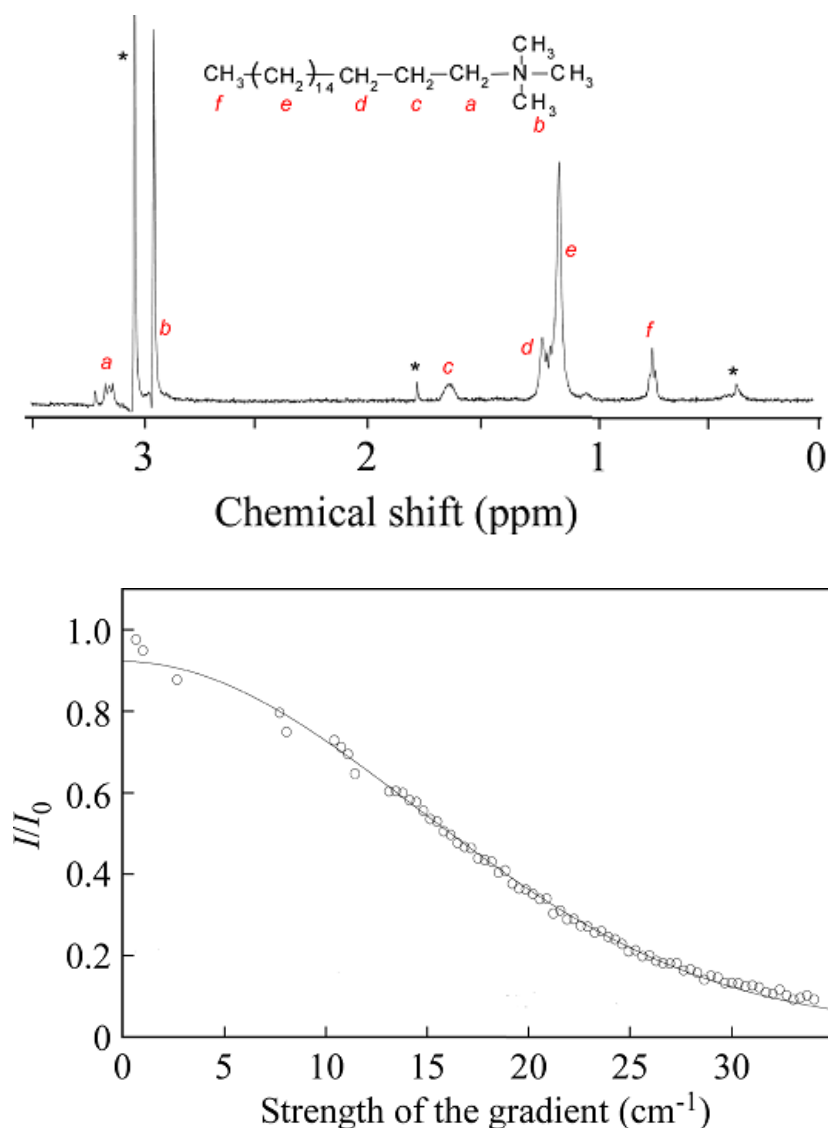


Figure 5-3. (a) ^1H NMR with WATERGATE of saturated C18TAB in H_2O solution at 21 °C. (b) The fitted diffusion curve for DOSY with WATERGATE spectrum of saturated C18TAB in H_2O solution

The peaks, $d + e$, can be attributed to methylene protons. The value of D of C18TAB is $3.422 \times 10^{-10} \text{ m}^2/\text{s}$. The theoretical and experimental data are displayed in Table 5-3.

Table 5-3 Comparison the theoretical and experimental value of OTAB's diffusion coefficient

Chemicals	Theoretical $D \times 10^{-10}$ (m^2/s)	Experimental $D \times 10^{-10}$ (m^2/s)
OTAB	4.017	3.422

5.3.3 Nonanol

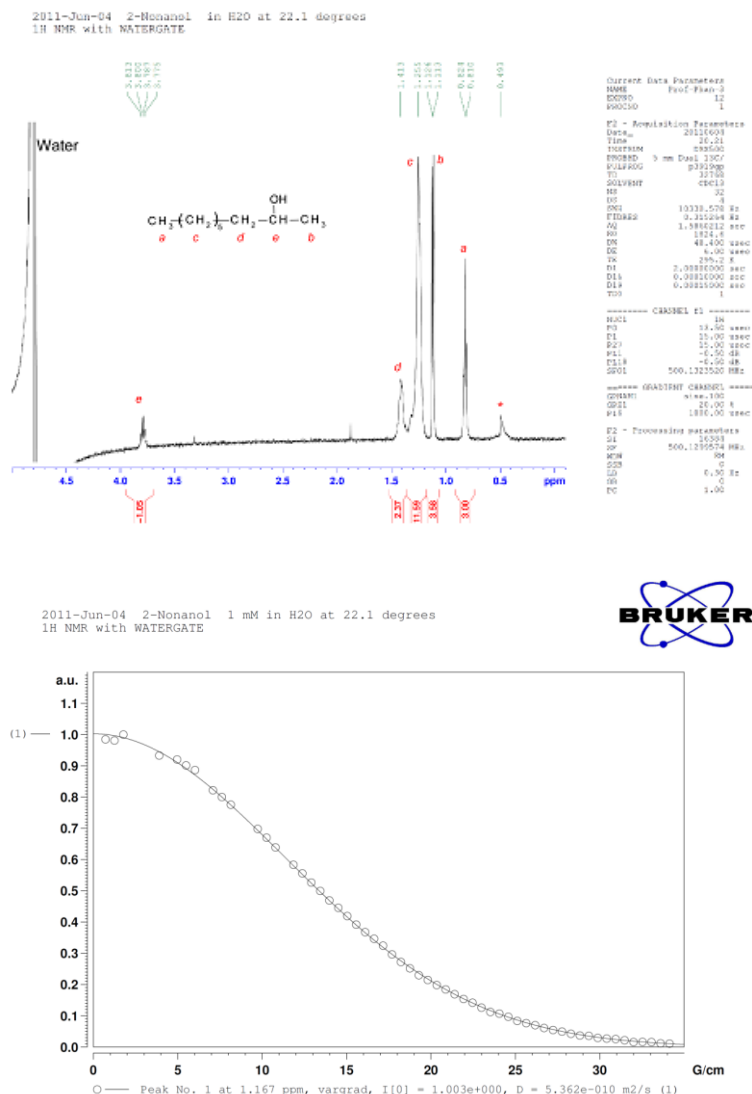


Figure 5-4 (a) ^1H NMR with WATERGATE spectrum of 1.0 mM 2-nonanol in H_2O at 22.1 $^\circ\text{C}$ (b) Fitted diffusion curve for ^1H NMR DOSY with WATERGATE spectrum of 1.0 mM 2-nonanol in H_2O at 22.1 $^\circ\text{C}$.

The peak *c* of Figure 5-4a can be attributed to 2-nonanol. The theoretical and experimental diffusion-coefficient values are displayed in Table 5-4.

We got the diffusion coefficient of 2-nonanol is $5.3885 \text{ m}^2/\text{s} \times 10^{-10}$. Since the diffusion coefficient of isometric alcohols varies slightly with molecular structure and bulk concentrations (Ferri and Stebe 1999; Phan 2010), this value was also used for 3-nonanol, 5-nonanol.

Table 5-4 Diffusion coefficient (D) of 2-nonanol

Concentration (mM)	$D \times 10^{-10}$ (m ² /s)	Average D $\times 10^{-10}$ (m ² /s)	Theoretical D $\times 10^{-10}$ (m ² /s)
1	5.362	5.388	5.226
0.8	5.402		
0.6	5.328		
0.4	5.462		

5.4 CHAPTER CONCLUSION

The differences between the theoretical diffusion coefficient values and experimental values of C_nTAB and nonanol are low (less than 3%). For C_nTAB, the diffusion coefficient decreased as the surfactant chain length increases. This result showed that the longer carbon chain need more time to unfolding/reorient, therefore dynamic step is longer. The experimental diffusion coefficients will be used for dynamic adsorption analyzing.

CHAPTER 6

**DYNAMIC ADSORPTION OF INDIVIDUAL
SURFACTANTS AT WATER/AIR INTERFACE****6.1 INTRODUCTION**

Dynamic surface tension is an important property of surfactant solution which control many applications in practice: foaming, emulsification, coating, and wetting (Chang and Franses 1995; Tan, Fornasiero et al. 2005; Tan, Pugh et al. 2005; Wang and Yoon 2008). As summarized in chapter 2, though the research in dynamic adsorption of surfactants have been conducted theoretically and experimentally in the last few decades, the dynamic models can only fit experimental data at different concentration range. The best-fitted values of adjustable parameters changed with bulk concentration, which is contradicting to the model assumptions. Consequently, the available models are inadequate for prediction and comparison purposes.

In this chapter, the dynamic surface tension of two sets of surfactants were measured: (i) alcohols: 2-nonanol, 3-nonanol, 5-nonanol and (ii) alkyltrimethyl ammonium bromide C_nTAB (n=14,16,18). The new fitting approach was applied with a recently proposed equation (Phan 2010) used for analyzing experimental data. This approach can overcome all the mentioned issues in dynamic adsorption data analysis. The effect of branching structure of alcohol to the dynamic adsorption activity as well as the relationship between chain lengths of C_nTAB to dynamic properties will be discussed based on quantitative parameters of this new fitting approach.

6.2 THEORETICAL DEVELOPMENT

From the experimental with equilibrium adsorption of surfactant at air/water interface, a new equation Eq. 6.1 (Phan 2010) was recently proposed to replace Eq.2.4

$$\gamma = \gamma_0 e^{-\chi c_b} \quad (6-1)$$

where χ is a new adsorption constant which has same unit as K (L/mol or M⁻¹).

During the dynamic adsorption, it can be assumed that the relationship remains valid for dynamic surface tension and transient value of bulk concentration of the sub-surface layer:

$$\gamma(t) = \gamma_0 e^{-\chi c_s(t)} \quad (6-2)$$

Hence, Eq.6-2 can replace Eq. 2-23 to predict the dynamic surface tension. Consequently, the equation can be combined with current theory, Eq. 2-15 to Eq. 2-20. By applying this new model eliminates the limitations of current fitting approaches by not using Gibbs isotherm Eq. 2-21, or the resulting equations, Eq. 2-22, Eq.2-23;

Fitting procedure.

A numerical scheme developed previously (Phan, Nguyen et al. 2005) was employed to solve Eq. 2-15 and 2-17 to find the transient sub-surface concentration, $c_s(t)$. Subsequently, $c_s(t)$ is substituted into Eq. 6-2 to find dynamic surface tension.

The diffusion model was applied first to analyze experimental data. The predicted surface tension was fitted against experimental data at 2 different concentrations for each investigated chemicals by adjusting K and Γ_m . That set of K and Γ_m was used to predict the dynamic surface tension of other concentration of that chemical and compare with the experimental data.

To highlight the uncertainty of Eq. 2-23, the least-squares method (using Excel Solver) was applied with different initial values to calculate the equilibrium of CTAB data. The initial and best-fitted values are tabulated in Table 6-1. For Eq. 2-15, the best-fitted value is independent of initial value used. For Eq. 6-1 however, the best-fitted results varied significantly with the initial values.

Table 6-1: Fitting parameters for CTAB equilibrium surface tension ($\gamma_0 = 71.21$ mN/m).

Models	Adjustable parameters	Initial value	Fitting		
			Best-fitted value	δ (mN/m)	
Eq. 6-1	χ (M^{-1})	500	747.06	0.673	
	χ (M^{-1})	1000	747.06		
Eq. 2-23	Case 1	K (M^{-1})	500	496.52	0.930
		Γ_m ($\times 10^5$ mol/m ²)	4.00	1.990	
	Case 2	K (M^{-1})	900	887.23	0.744
		Γ_m ($\times 10^5$ mol/m ²)	4	1.210	
	Case 3	K (M^{-1})	1500	1499.95	0.713
		Γ_m ($\times 10^5$ mol/m ²)	5	0.799	
	Case 4	K (M^{-1})	1800	1799.91	0.776
		Γ_m ($\times 10^5$ mol/m ²)	5	0.670	

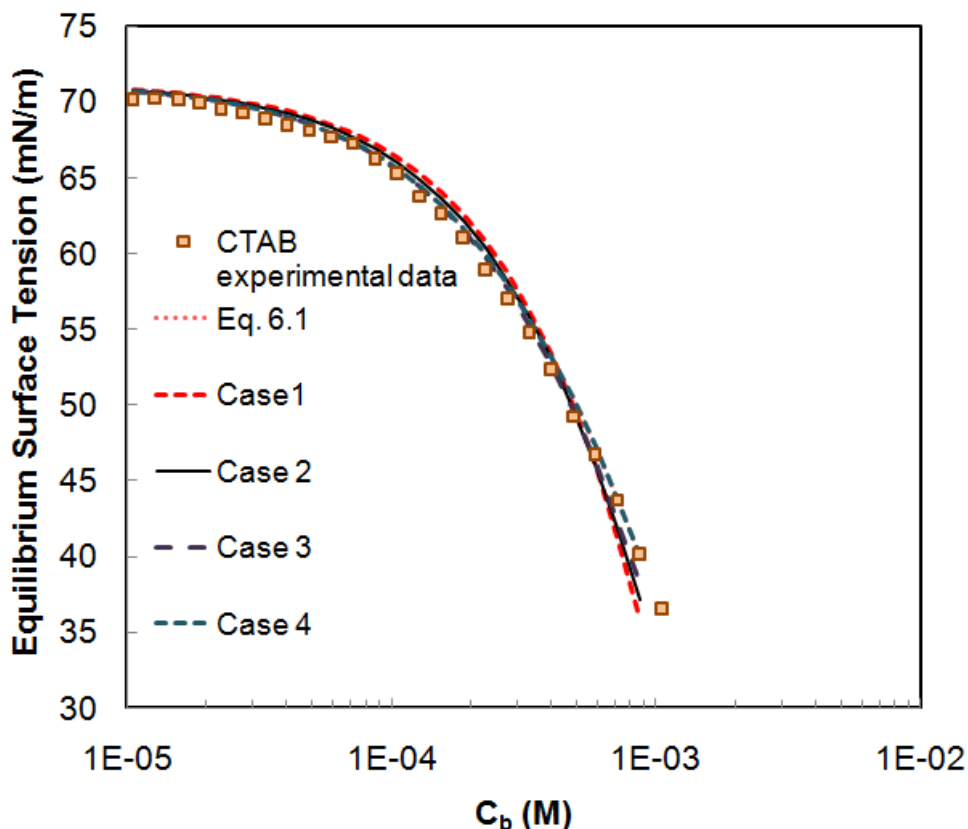


Figure 6-1 Modeling equilibrium surface tension of CTAB (the modeled predictions were almost identical).

From Figure 6-1, it can be seen that all models provided similar results. More importantly, all deviations were smaller than 1 mN/m, which is considered as acceptable limit for modelling equilibrium surface tension (Prosser and Frances 2001). The variation in Table 6-1 demonstrates the inadequacy of determining K and Γ_m by fitting Eq. 2-23 to equilibrium surface tension. For predicting equilibrium surface tension, any of these combinations can be adequate. With the measurement error of 0.5 mN/m, one cannot discard any of these combinations. However, these variations can significantly affect the dynamic modelling. Hence, Eq. 6-1 can effectively replace Eq. 2-23 in modelling the dynamic adsorption.

Conventional method

The fitting parameters obtained by Langmuir isotherm for the equilibrium of CTAB (case 1 and case 3 as shown in Table 6-1) were used as the initial input for CTAB dynamic adsorption analyzing. The results showed that the fitting data are far from the experimental data (Figure 6-2).

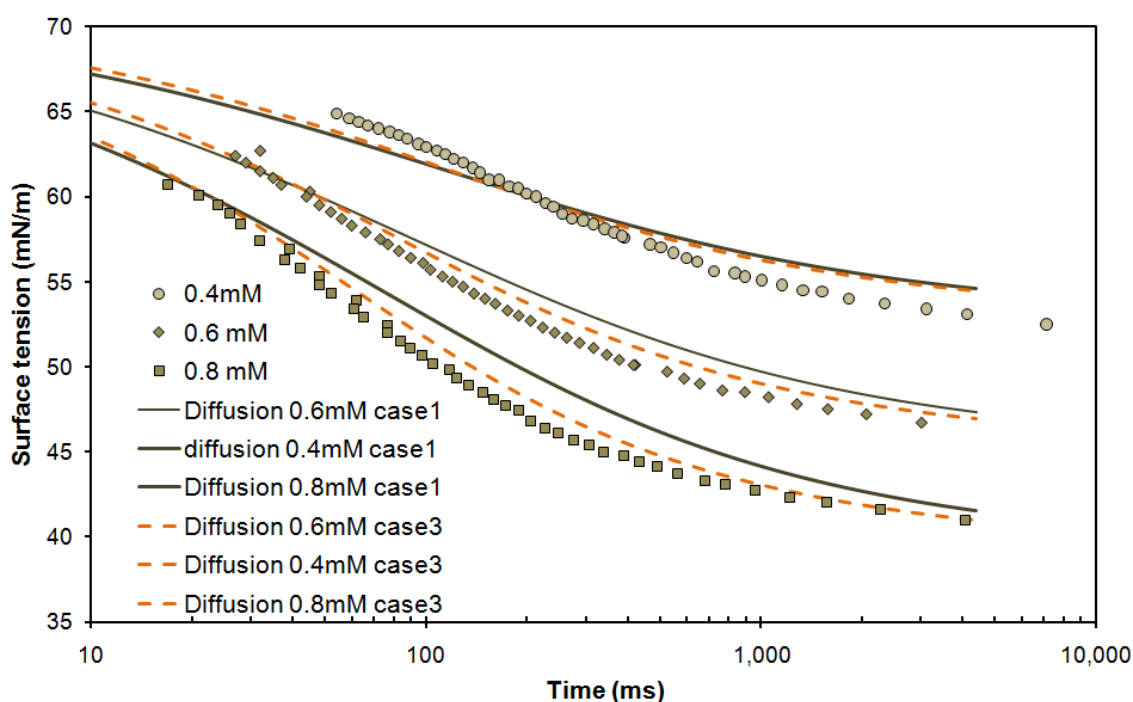


Figure 6-2 Diffusion adsorption of CTAB with two different sets of K and Γ_m

6.3 MODELLING RESULTS

The newly developed model will be applied with two series of chemicals: one with alcohols (2-nonanol, 3-nonanol, 5-nonanol) and another with CnTAB ($n=14,16,18$) to verify the quality of fitting and effectiveness of the new model as well as to compare the influence of the structure of chain group in surfactant molecules.

6.3.1 Cationic surfactants CnTAB

6.3.1.1 Dynamic adsorption analysis

Using Eq. 6-1 we can quantify the equilibrium adsorption of CnTAB with fitting parameters as shown in Table 6-2.

The value of χ (new adsorption constant) increased as number of CH_2 group in the chain increase.

Table 6-2 Fitting parameters for C_nTAB equilibrium surface tension

<i>C_nTAB</i>	<i>Adjustable parameters</i>	<i>Best-fitted value</i>	<i>95% Confidence interval</i>	<i>δ (mN/m)</i>
C₁₄TAB (TTAB)	χ (M ⁻¹)	269.962	272.89-267.034	0.175
	γ_0 (mN/m)	71.6954	71.5809-71.81	
C₁₆TAB (CTAB)	χ (M ⁻¹)	747.06	780.038 -730.713	0.67
	γ_0 (mN/m)	71.4315	71.0646 -71.7984	
C₁₈TAB (OTAB)	χ (M ⁻¹)	4638.55	4641.92-4635.17	0.07
	γ_0 (mN/m)	71.4971	71.4874-71.5068	

Dynamic adsorption of C_nTAB was measured by using maximum bubble method as described in section 3.2.1.3. The newly developed model was applied to analyze the dynamic adsorption of C_nTAB. The dynamic modeling parameters gained from fitting two concentrations for each chemical are shown in Table 6-3. All the standard deviations of these fitting were lower than 1 mN/m (excellent fitting). These results demonstrated that the dynamic adsorption of TTAB, CTAB, and OTAB are diffusion-controlled. Those results are contrasting with other results from other authors who analyzed dynamic model of C_nTAB by conventional approach. They argued that the adsorption of C_nTAB at water interface is governed by kinetic step (Stubenrauch, Fainerman et al. 2005; Stubenrauch and Khristo 2005). All the dynamic fitting parameters of C_nTAB (K and Γ_m) are within physically feasible range (Prosser and Frances 2001)

Table 6-3 Dynamic fitting parameters of C_nTAB

<i>Chemicals</i>	<i>K (L/mol)</i>	<i>Γ_m (mol/m²)</i>	<i>Standard deviation for two fitting curves δ (mN/m)</i>
TTAB	1716	3.76×10 ⁻⁶	0.34
CTAB	2017	6.323×10 ⁻⁶	0.72
OTAB	68577	2.638×10 ⁻⁵	0.42

As the number of carbon atoms in the tail of cationic surfactants increased, K increased, which means lower adsorption rates.

Using two different concentrations for this new fitting approach, a different set of fitting parameters was obtained for TTAB and CTAB and is shown in Table 6-4.

Table 6-4 Fitting parameters of TTAB and CTAB dynamic adsorption with two different fitting concentrations

Surfactants	Two fitting concentrations	K (L/mol)	Γ_m (mol/m²)	Standard deviation δ_γ
TTAB	0.4mM & 0.8mM	1716	3.671×10 ⁻⁶	0.341
	0.6mM & 1.1mM	1833	3.968×10 ⁻⁶	0.206
	0.8mM & 1.5mM	1716	3.29×10 ⁻⁶	0.381
CTAB	0.4mM & 0.8mM	1995	6.323×10 ⁻⁶	0.61
	0.5mM & 0.8mM	1937	6.323×10 ⁻⁶	0.445
	0.6mM & 0.8mM	2199	6.326×10 ⁻⁶	0.346

The difference between the maximum and minimum values of fitting parameters of TTAB was around 6% for K and 17% for Γ_m. The variation of K value of CTAB was around 12% and almost unchanged for Γ_m. All the standard deviations of those fitting were very low (<1mM) which mean these fittings were very good. The values of maximum surface excess Γ_m were in the range reported by other authors as shown in Table 6-5.

Table 6-5 Reported maximum surface excess of C_nTAB in literature

References	Fitting models	$\Gamma_m (\times 10^6 \text{ mol/m}^2)$	
		TTAB	CTAB
Stubenrunch et al. (Stubenrauch, Fainerman et al. 2005)	Frumkin model	3.62	3.424
	Compressibility of surfactant molecules	4.71	4.8
Bergeron (Bergeron 1997)	Frumkin model	4.71	3.105
Pradines et al. (Pradines, Fainerman et al. 2010)	Frumkin model	4.71	4.807
Gilányi et al. (Gilányi, Varga et al. 2008)	Gibbs equation + adsorption free energy change	3.5 - 4.0	3.5 - 4.0

6.3.1.2 Prediction efficiency of new model

The set of fitting parameters for dynamic activities of C_nTAB will be used to predict other concentrations C_nTAB.

(a) Dynamic adsorption of OTAB

The set of K and Γ_m gained from fitting two concentration of 0.06 mM and 0.1mM (Table 6-3) was applied to predict the dynamic behaviour of solution of 0.08 mM. The prediction was excellently fitted with experimental data. The standard deviation for this fitting was 0.4 mM/m. The standard deviation for each concentration of C₁₈TAB is shown in Appendix 1. The dynamic adsorption behaviour of OTAB (C₁₈TAB) is shown in Figure 6-3.

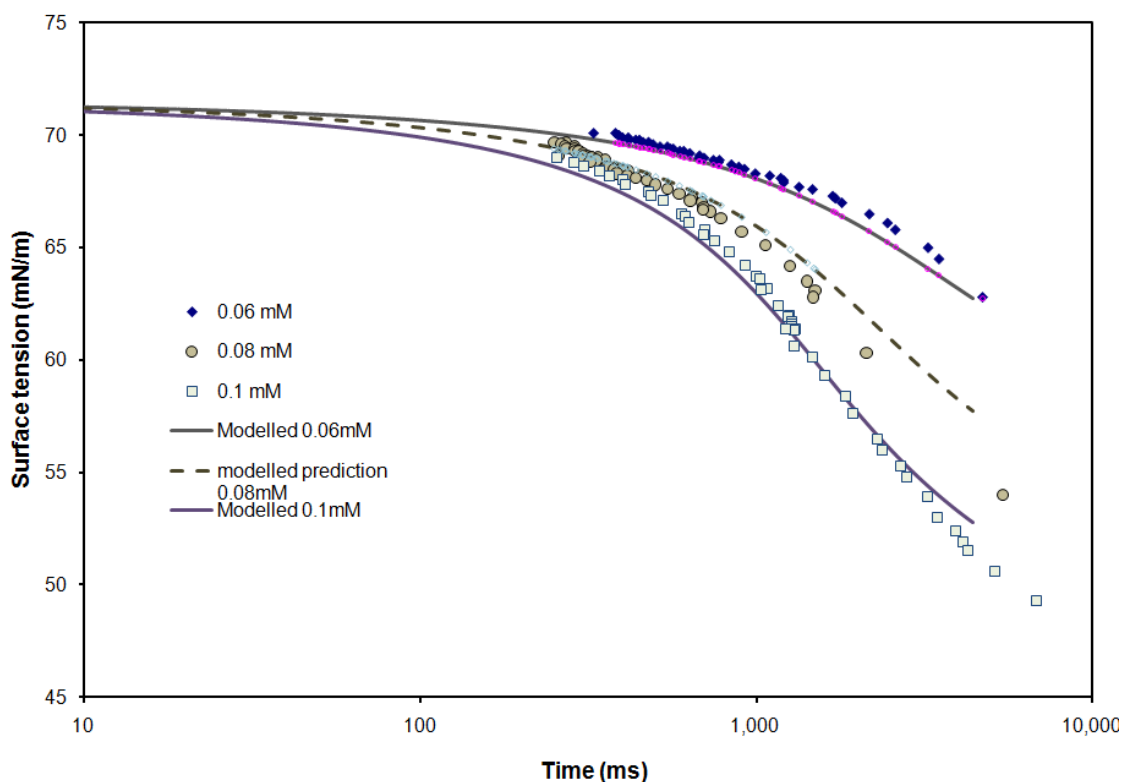


Figure 6-3 Dynamic surface tension of OTAB: lines are best-fitted curves with $K = 68577$ L/mol and $\Gamma_m = 2.638 \times 10^{-5}$ mol/m²

(b) Dynamic adsorption of CTAB

The dynamic adsorption data of CTAB at two concentrations: 0.6mM and 0.8mM were the input for the newly developed model to obtain the set of fitting parameter $K = 2199$ and $\Gamma_m = 6.323 \times 10^{-6}$ mol/m². Dynamic adsorption of other concentrations of 0.4 mM, 0.5mM and 0.7mM were predicted and shown in Figure 6-4. Standard deviations of fitting for each concentration were displayed in Appendix 2.

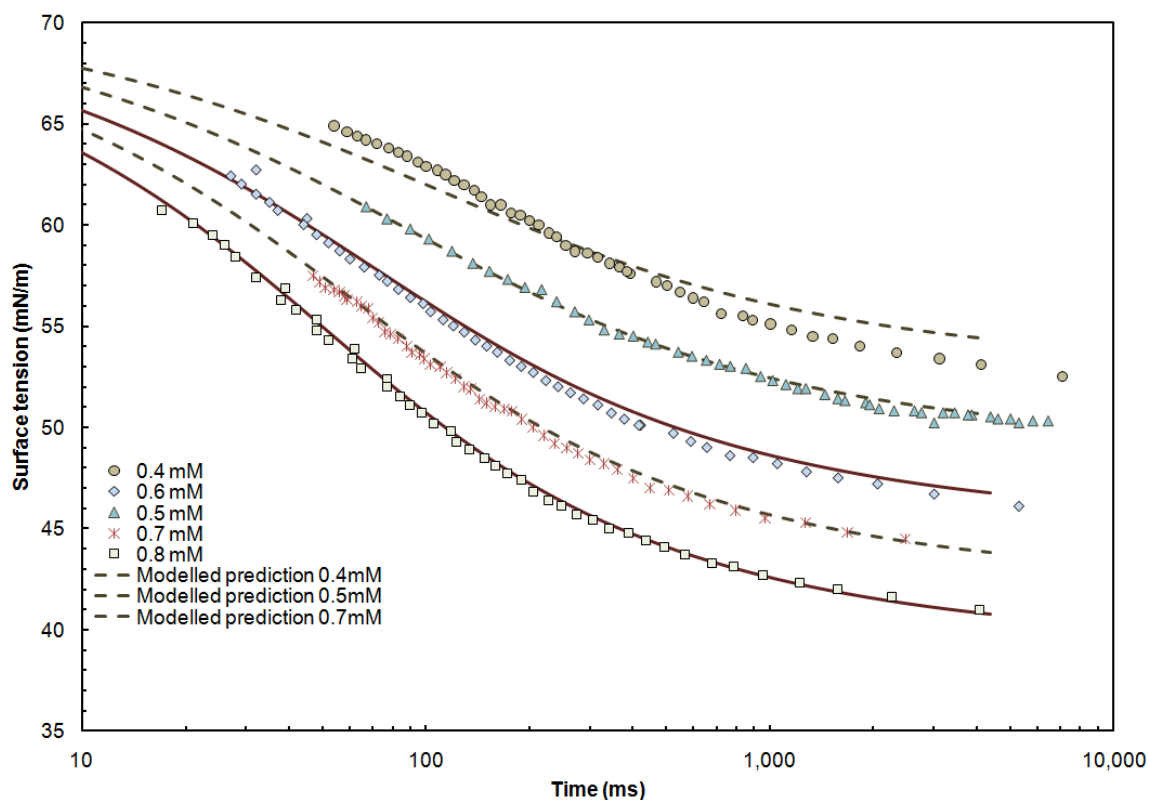


Figure 6-4 Dynamic surface tension of CTAB: lines are best-fitted curves with $K = 2017 \text{ L/mol}$ and $\Gamma_m = 6.32 \times 10^{-6} \text{ mol/m}^2$

(c) Dynamic adsorption of TTAB

Similar to prediction procedure applied for OTAB and CTAB, the set of K and Γ_m (Table 6-2) was applied to predict other concentrations of 0.6mM, 1mM, 1.1mM. All fittings were in good agreement with experimental data. The standard deviation of fitting for each concentration was described in Appendix 3.

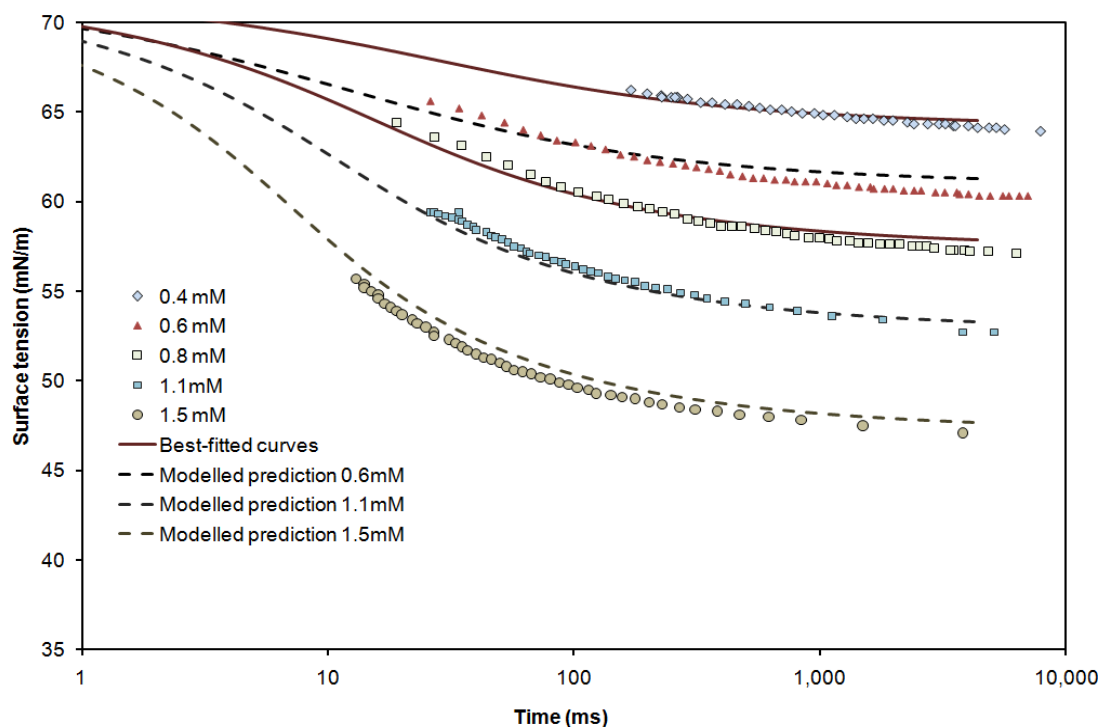


Figure 6-5 Dynamic surface tension of TTAB: lines are best-fitted curves with $K = 1716 \text{ L/mol}$ and $\Gamma_m = 3.76 \times 10^{-6} \text{ mol/m}^2$

6.3.1.3 Summary

In contrast to previous modeling results in the literature, the new model clearly demonstrated that diffusion-controlled mechanism is adequate for $C_n\text{TAB}$. The modeling results exposed the uncertainty in determining adsorption constants from equilibrium data solely.

As the chain length of $C_n\text{TAB}$ gets longer, the adsorption rate is lower. This phenomenon can be evaluated by comparing the set of fitting parameters K and Γ_m . There was a correlation between these fitting parameters with chain length: K increases from 1716 L/mol ($C_{14}\text{TAB}$) to 68577 L/mol ($C_{18}\text{TAB}$); Γ_m also increased with the length of the tail (from $3.76 \times 10^{-6} \text{ mol/m}^2$ of TTAB to $2.638 \times 10^{-5} \text{ mol/m}^2$ of OTAB).

6.3.2 Alcohol : branching nonanol.

The dynamic surface tension of alcohols was measured by the PAT1.

The equilibrium data of alcohols which are well described in chapter 4 were fitted by the new equation, Eq. 6-1. Table 6-6 shows the fitting parameters for equilibrium surface tension of different investigated alcohols.

Table 6-6 Fitting parameters for equilibrium surface tension of nonanol series.

<i>Alcohols</i>	<i>Adjustable parameters</i>	<i>Best-fitted value</i>	<i>95% Confidence interval</i>	<i>δ (mN/m)</i>
2-nonanol	χ (M ⁻¹)	391.2	402.63 – 379.79	0.59
	γ_0 (mN/m)	71.99	71.75 - 71.26	
3-nonanol	χ (M ⁻¹)	284.57	286.73 – 282.4	0.13
	γ_0 (mN/m)	71.53	71.48 - 71.58	
5-nonanol	χ (M ⁻¹)	202.75	207.29 – 198.2	0.24
	γ_0 (mN/m)	71.48	71.33 - 71.62	

This χ (new adsorption constant) can also be used for comparing the equilibrium adsorption activity. It is clear that as the hydroxyl group moves inside the chain, the value of this parameter decreases from 391.2 of 2-nonanol to 284.57 of 3-nonanol and 202.75 of 5-nonanol.

6.3.2.1 Dynamic adsorption of nonanol series

Two concentrations for model fitting and that set of fitting parameters (K and Γ_m) was applied for estimating other concentrations. The dynamic fitting parameters of newly developed models for nonanol series were shown in Table 6-7. The fitting and standard deviation from the new model demonstrated that diffusion-controlled is adequate for branching alcohols investigated and kinetic step is not required.

The predicted surface tension was fitted against experimental data at two different concentrations of each investigated chemicals by adjusting K and Γ_m as shown in Table 6-7. All the standard deviation for two curves fitting of nonanol series are lower than 1mM meant that the new model fitting is excellent.

To validate the new model, these fitting sets of nonanol series (Table 6-7) were applied to predict dynamic surface tension of other concentrations.

Table 6-7 Fitting parameters of new models for nonanol series

<i>Chemicals</i>	<i>Two chosen fitting concentrations</i>	<i>K (L/mol)</i>	<i>Γ_m (mol/m²)</i>	<i>Standard deviation</i>
2-nonanol	0.4 and 0.7 mM	2017	6.34×10^{-6}	0.305
3-nonanol	0.4 and 0.7 mM	1000	6×10^{-6}	0.406
5-nonanol	0.3 and 0.7mM	990	5.6×10^{-6}	0.47

6.3.2.2 Prediction efficiency of the new model for nonanols

(a) 2-nonanol

The set of fitting parameters ($K = 2017$ and $\Gamma_m = 5.34 \times 10^{-6}$) was used to predict dynamic surface tension of 2mM, 6 mM and 8mM. Without further fitting, the model predicted the dynamic surface tension very well (with a standard variation for three concentrations lower than 1mM/m). Figure 6-6 shows the dynamic adsorption results of 2-nonanols, with dotted lines are model prediction, solid lines are model fitting. The standard deviations of each concentration of 2-nonanol are described in Appendix 4.

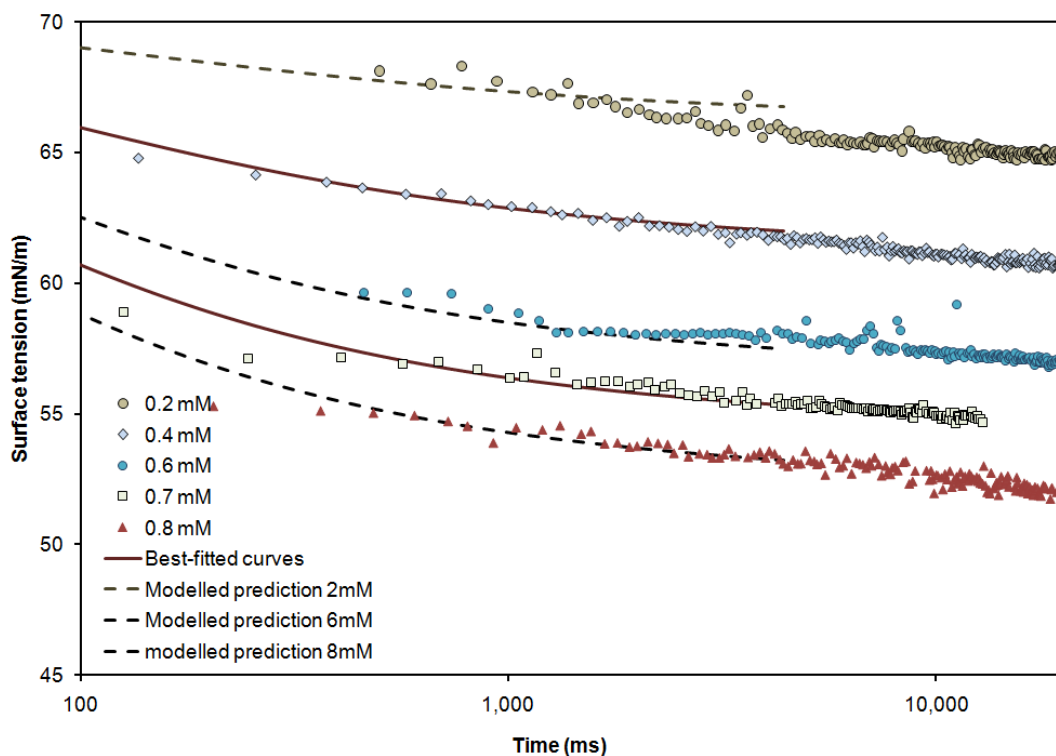


Figure 6-6 Dynamic surface tension of 2-nonanol: lines are best-fitted curves with $K = 2017 \text{ L/mol}$ and $\Gamma_m = 6.34 \times 10^{-6} \text{ mol/m}^2$.

(b) 3-nonanol

The set of K of 1000 L/mol and Γ_m of $6 \times 10^{-6} \text{ mol/m}^2$, obtained by applying this new equation for two concentrations of 0.4 mM and 0.7 mM at the same time, is used to predict dynamic surface tension of 0.2 mM , 0.3 mM , 0.6 mM and 0.8 mM . All the standard deviations for those predictions were lower than 1 mN/m (Appendix 5). Figure 6-7 shows the fitting result of different concentration of 3-nonanol.

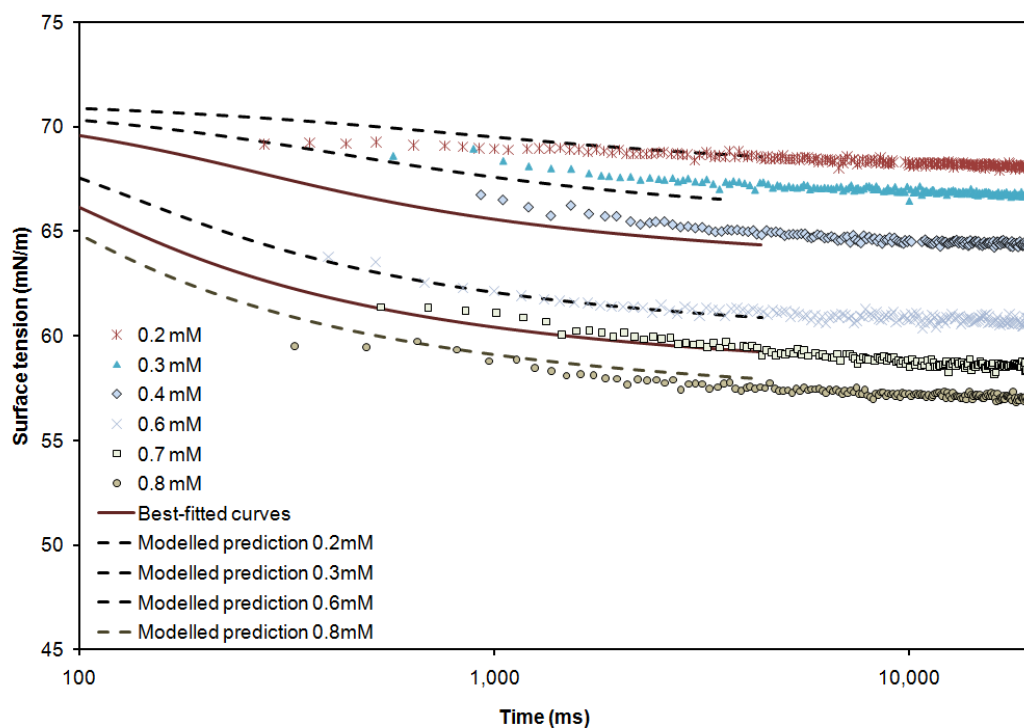


Figure 6-7: Dynamic surface tension of 3-nonanol: lines are best-fitted curves with $K= 1000$ L/mol and $\Gamma_m= 6.00\times 10^{-6}$ mol/m²

(c) Dynamic of 5-nonanol

The set of K (990 L/mol) and Γ_m (5.6×10^{-6}) was used to predict the dynamic surface tension of 0.4mM, 0.5mM, 0.8mM. The values of standard deviation for each concentration are shown in Appendix 6 (all are very low which mean excellent prediction). The dynamic adsorption of different concentration of 5-nonanols is displayed in Figure 6-8.

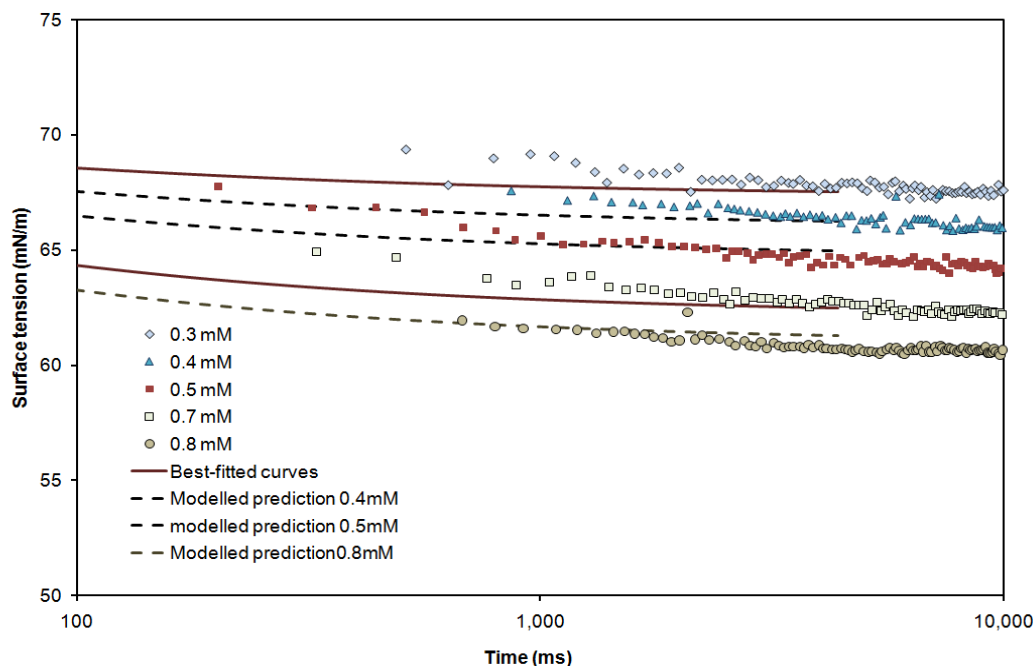


Figure 6-8 Dynamic surface tension of 5-nonanol: lines are best-fitted curves with $K = 990 \text{ L/mol}$ and $\Gamma_m = 5.6 \times 10^{-6} \text{ mol/m}^2$

6.3.2.3 Comparing influence of chain structure of nonanol:

Newly developed model

It can be seen that the values of the maximum adsorption density Γ_m of all investigated branched nonanol were in typical range of 1×10^{-6} to $10 \times 10^{-6} \text{ mol/m}^2$ (Chang and Franses 1995; Chang and Franses 1995; Pan, Green et al. 1998; Phan, Nguyen et al. 2005). As mentioned above, the advantage of this new method is its capability to predict all concentrations with the same set of model parameters gained from two experimental concentrations. So we can compare two different chemicals based on the new model fitting parameters can be compared. With the second fitting approach applied to study octanol isomers (Phan 2010), there was no correlation of fitting parameters and structures relationship.

We can observe that as the OH group move inside the carbon chain, the lower value of Γ_m was observed and the lower values of K while the adsorption rate is faster. Dynamic adsorption of all branching nonanols investigated are diffusion control which is the same with 1-nonanol (Fainerman and Miller 1996; Lee, Liou et al. 2002), octanol series (1-octanol, 2-octanol, 3-octanol) (Phan 2010).

Diffusion time scale (Ferri and Stebe 2000)

Ferri and Stebe introduced the idea of diffusion time scale which is very useful for comparing the surfactant.

The time scales of three investigated alcohols were calculated from the equilibrium isotherms (reported in chapter 4) and a diffusion coefficient as equation

The adsorption depth

$$h = \frac{\Gamma}{c} \quad (6-3)$$

with Γ is the maximum packing on the interface, identified from the equilibrium isotherm; c is the bulk concentration of surfactant in solution

The diffusion time scale:

$$\tau_D = \frac{h^2}{D} \quad (6-4)$$

with D is the diffusion coefficient

The τ_D of different n-nonanol is shown in Table 6-8.

Table 6-8 Diffusion time scale (ms) of n-nonanol

<i>Type of alcohol</i>	<i>Concentration</i>	<i>Adsorption depth, meter (h)</i>	<i>Diffusion time scale, ms (τ_D)</i>
2-nonanol	2×10^{-4}	9.5×10^{-6}	165.92
	4×10^{-4}	9.1×10^{-6}	153.32
	6×10^{-4}	8.8×10^{-6}	142.56
	7×10^{-4}	8.6×10^{-6}	137.68
	8×10^{-4}	8.5×10^{-6}	132.81
3-nonanol	2×10^{-4}	7.58×10^{-6}	106.60
	3×10^{-4}	7.44×10^{-6}	102.63
	4×10^{-4}	7.30×10^{-6}	98.95

	6×10^{-4}	7.04×10^{-6}	92.06
	7×10^{-4}	6.91×10^{-6}	88.72
	8×10^{-4}	6.80×10^{-6}	85.72
5-nonanol	3×10^{-4}	5.40×10^{-6}	54.15
	4×10^{-4}	5.30×10^{-6}	52.17
	5×10^{-4}	5.21×10^{-6}	50.33
	7×10^{-4}	5.03×10^{-6}	46.93
	8×10^{-4}	4.94×10^{-6}	45.36

As proven in several publications (Ferri and Stebe 1999; Ferri and Stebe 2000), τ_D is a meaningful parameter to compare the surface active properties of different surfactants. For the investigated nonanol, these times are faster than the first data point which can be determined by our instrument. As alcohols are weak absorbers, the dynamic adsorption of these alcohols is rapid thus the depth depletion by adsorption is small. However, we can see that as the functional group moves inside the tail length, the higher capacity in reducing the surface tension (τ_D is smaller). The more bulkiness in the lengths of two tails in molecule, the longer time is required for nonanols diffusing to interface and reaching the equilibrium state.

6.4 CHAPTER CONCLUSION

A new and simple equation (Phan 2010) models the equilibrium surface tension, which directly relates the surface tension to bulk concentration. The equation has only one parameter instead of multiple parameters as in Szyszkowski equation and other equations in the literature. The higher reliability of this new equation than conventional equation was proved by analyzing equilibrium surface tension of CTAB at air/water interface. This method used 1 parameter and always provided unique fitting solution for the adsorption experimental data. The application of the equation is still under further investigation.

Subsequently, the new equation was incorporated into the dynamic model to predict dynamic adsorption at different concentrations. The model was fitted to dynamic surface tension at two different concentrations simultaneously. Two sets of chemicals (nonanol isomers and CnTAB) were investigated to identify the fitting quality and prediction capacity of this new model.

The diffusion-controlled model fitted the experimental data well, with small standard deviation ($<1\text{mN/m}$) and physically feasible value of Γ_m . The model consistently predicted the surface tension for all investigated data.

Most critically, both new equation and dynamic model do not require Gibbs adsorption isotherm and thus can be applied regardless of molecular arrangements at the adsorption zone. The new model is simpler and more effective than current methods for predicting the dynamic adsorption of soluble surfactants at air/water interface. Further investigation with other surfactant systems is carried out to determine the applicability and limitation of the new model.

CHAPTER 7

INFLUENCE OF MOLECULAR STRUCTURES TO EQUILIBRIUM ADSORPTION OF MIXTURE OF SURFACTANTS

7.1 INTRODUCTION

Synergistic properties of surfactant mixtures have been intensively studied to understand the performance of surfactant systems both in theoretical and engineering aspects in a number of areas beyond flotation (Holland 1992; Gohsuke, Shigemi et al. 2008). Generally, the aggregated structures of mixture surfactants have attracted more attention than the adsorption performance due to the great contrast between mixed and individual micelles (Zana R. 1995). However, the surfactant adsorption at the interface occurs at concentrations well below the critical micelle concentration (CMC). The interfacial adsorption is essential for changing the contact angle between an air bubble and a solid surface (Vogler 1992) and the rate of wetting solid surfaces, or foaming in enhancing oil recovery or fire extinguisher (Nguyen 1988; Zdziennicka and Janczuk 2008). Mixtures of surfactants are often used in these applications.

In spite of the importance of adsorption behaviour of mixtures in practical application, in literature, studying the influence of molecular structure to adsorption behaviour of mixtures is almost blank. In addition, all experimental mixture systems as aforementioned in literature contain straight alcohols only.

In this chapter, two common theoretical models described in chapter 2 were employed to analyze the adsorption behaviour of all binary mixtures. Both applied models used molecular interaction parameters to evaluate properties of mixture. The value of this parameter is different with different mixture systems as shown in Table 7-1.

The adsorption behaviour of surfactant mixtures were investigated by using Wihelmy plate method as described in section 3.2.1.1.

7.2 MIXTURE OF NON-IONIC SURFACTANTS: ALCOHOLS

In flotation process, frothers are added to ensure the stability of the bubbles to prevent them from losing the attached solid particles. The phenomenon results from the migration of the frothers to air/water interface (adsorption) to minimize the contact between their hydrophobic groups and water. The significant effect of the adsorption phenomenon is the lowering of the interfacial tension. In flotation practice of a number of companies, the predominant frothers are the low molecular weight C5 to C8 alcohols (Aston, Lane et al. 1989). Alcoholic frother mixtures sometimes are more effective or economic than a single frother for some specific mineral flotation (Crozier and Klimpel 1989). The available studies on mixed adsorption of alcoholic frothers was conducted for straight chain alcohols only, such as 1-octanol/1-heptanol, 1-octanol/1-hexanol (Fainerman 1983).

Among the industrial aliphatic alcohol frothers, MIBC (methyl isobutyl carbinol) is the most common one used due to its powerful frothability and excellent solubility (Strydom, Spitzer et al. 1983; Crozier and Klimpel 1989). Most of research on binary mixtures containing MIBC, such as MIBC with DIBSS (sodium di-isobutyl sulfosuccinate) (Strydom, Spitzer et al. 1983); Tritron X-100 and MIBC (Ozma 2006), focused on application aspects such as solid recovery in flotation or froth stability while neglecting the fundamental adsorption. It is believed that the interaction between molecules of mixture forming monolayer depends on their structure: the length of the hydrocarbon tail and the size of the hydrophobic head (Penfold, Staples et al. 2003; Szymczyk, Zdziennicka et al. 2005). As MIBC is a secondary alcohol, the molecular arrangement of MIBC and other alcohols might be different with the composition of straight chain alcohol. This part focuses on the adsorption behaviour of MIBC/1-heptanol and MIBC/1-octanol mixtures by using surface tension technique.

Table 7-1: Interaction parameter between molecules of different mixture of surfactants.

Mixture	Interaction parameter	Reference
1-octanol/1-heptanol	-0.5	(Fainerman 1983)
1-octanol/1-hexanol	-0.8	(Fainerman 1983)
SDS/C ₁₄ E ₈	1.4	(Fainerman, Aksenenko et al. 2010)
SDS/propanol	0.61	(Janczuk, Zdziennicka et al. 2004)
SDS/C ₁₂ E ₈	-3.2 ^(*)	(Siddiqui and Frances 1996)
C12E5/Triton X-100	-3 ^(*)	(Siddiqui and Frances 1996)
SDS/ethanol	0	(Kovtun, Khilko et al. 2010)
SDS/n-propanol	0.5	(Kovtun, Khilko et al. 2010)

^(*) these parameters were obtained using Siddiqui and Frances model.

7.2.1 Adsorption of single surfactant systems

Adsorption isotherm of MIBC, 1-octanol and 1-heptanol at water/air interface (**Figure 7-1**) with fitting parameters as described Table 7-2.

It can be seen that the standard deviations were exceptionally small compared to the acceptable threshold of 1 mN/m (Prosser and Frances 2001). Since the best-fitted value of A of 1-octanol is non-zero so its adsorption isotherm can be modelled by Frumkin equation. Whereas MIBC and 1-heptanol, with the best-fitted value of A are zero, they can be modelled by Langmuir isotherm. The influence of molecular structure to the surface tension could be evaluated by the isotherms constants (section 4.2.1.3). The maximum surface concentration (Γ) decreased with decreasing number of carbon in alcohol chain. The second fitting parameters K is having the same trend with the parameter Γ as described.

Table 7-2 Adsorption isotherm parameter of MIBC, 1-heptanol, 1-octanol

Alcohol	Γ (mol/m^2)	K (M^{-1})	A	δ_γ (mN/m)
MIBC*	13×10^{-6}	49	0	0.41
1-heptanol	19×10^{-6}	116	0	0.55
	22×10^{-6}	87	0.6	0.7
1-octanol*	23×10^{-6}	174	1.25	0.13

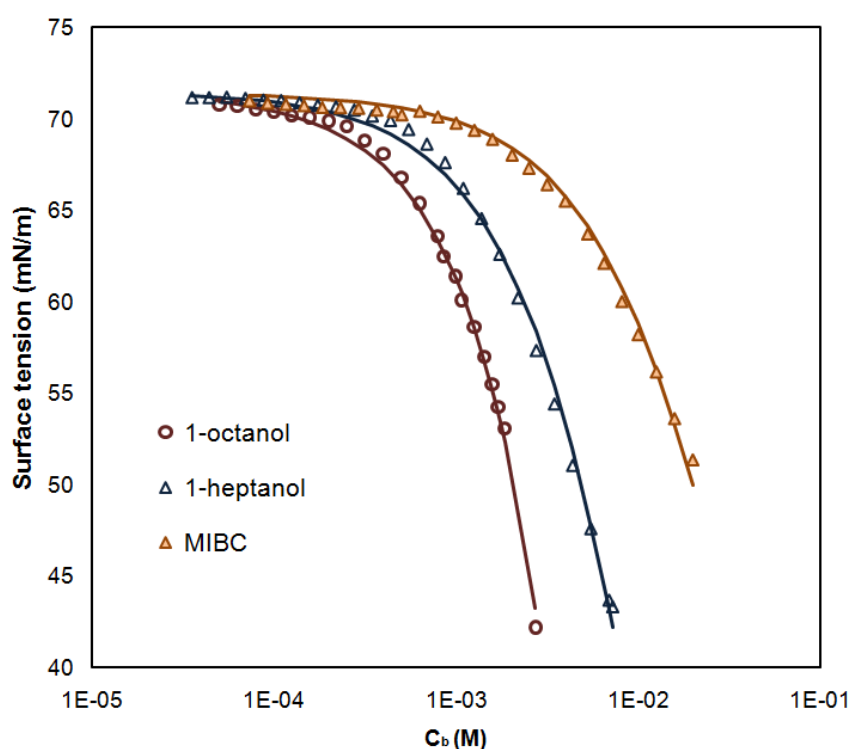


Figure 7-1 Surface tension as function of bulk concentrations for MIBC, 1-heptanol and 1-octanol (points: experimental data, lines: best-fitted curves)

As 1-octanol was described by Frumkin isotherm, we used Fainerman’s model only for investigating the absorption behaviour of mixtures. The binary model required parameters of single isotherm $\Gamma_{m,i}$ and K_i, A_i ($i=1,2$) as shown in described Table 7-2. With these parameters predetermined, model has only one adjustable parameter: A_{12} . Equations **Eq. 2-5** and **Eq. 2-6** were solved simultaneously using the Jacobian method (Beers 2006) to find θ_1 and θ_2 . Subsequently, θ_1 and θ_2 were used to calculate

surface tension Eq. 2-8. MS Excel Solver was utilized to fit the modelled surface against experimental data by adjusting A_{12}

7.2.2 MIBC/1-heptanol

The surface tension was measured for different sets of concentrations, which contained unchanged MIBC concentration (5.3×10^{-4} mol/L to 8.8×10^{-3} mol/L) but with gradually increased concentration of 1-heptanol (5×10^{-6} mol/L to 7.9×10^{-3} mol/L). The surface tension of the mixture decreased with addition of the second component (1-heptanol) to MIBC solution (see Figure 7-2).

It can be seen that modeling results are satisfactory, with reasonable standard deviations (0.85 mN/m). The value of interaction constant A_{12} is -0.516.

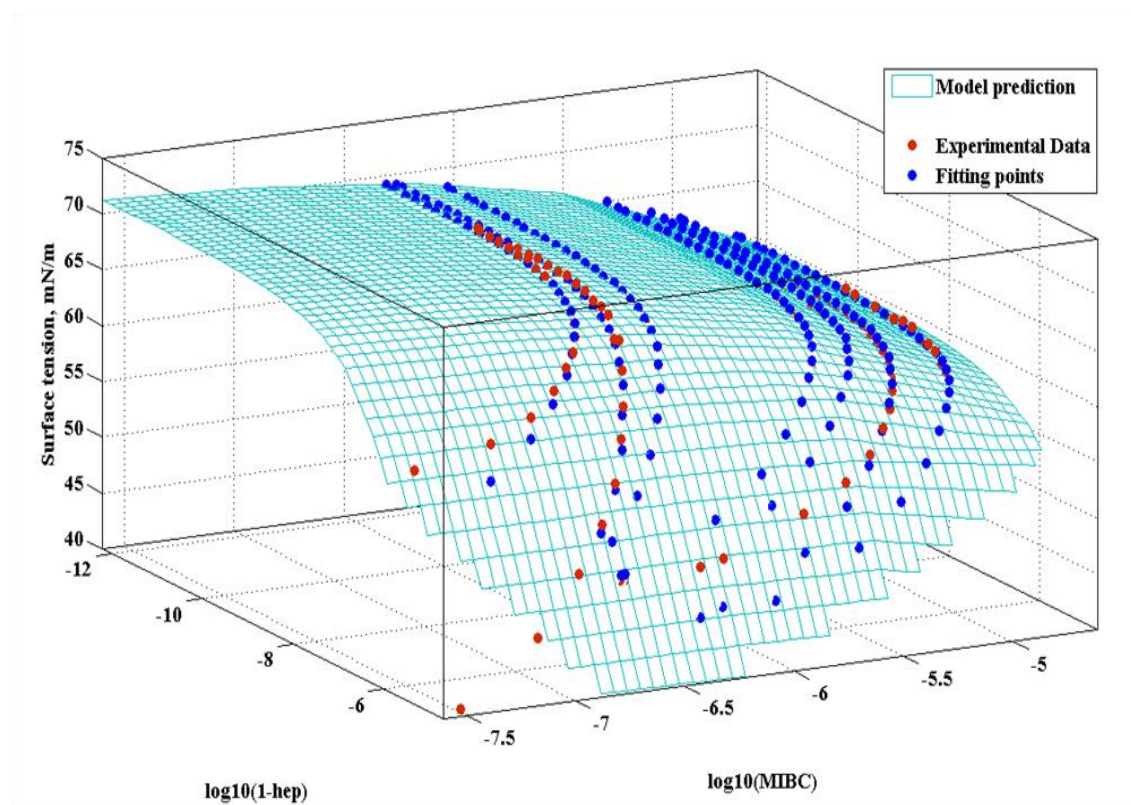


Figure 7-2: Surface tension of MIBC/1-heptanol mixture: fitted by Fainerman's model, ($A_{12} = -0.516$, $\delta_y = 0.85$ mN/m)

7.2.3 MIBC/1-octanol

The surface tension was measured for different sets of concentrations, which contained unchanged MIBC concentration (4.9×10^{-4} mol/L to 7.1×10^{-3} mol/L) but with gradually increased concentration of 1-octanol (2×10^{-7} mol/L to 5.6×10^{-4} mol/L).

Contrasting to a monotonic decrease with increasing 1-octanol as observed with mixture of 1-hexanol/ 1-octanol (Fainerman 1983) or MIBC/1-heptanol (this study), the surface tension of the mixture gradually increased to a peak before decreasing with further increasing 1-octanol concentration.

The same fitting procedure was applied for the mixture of MIBC/1-octanol. The standard deviation for 1-octanol/MIBC mixture is quite large, 1.36 mN/m, with a positive value of interaction parameter ($A_{12}=1.477$). Most importantly, the model did not predict the observed peaks of experimental data (Figure 7-3).

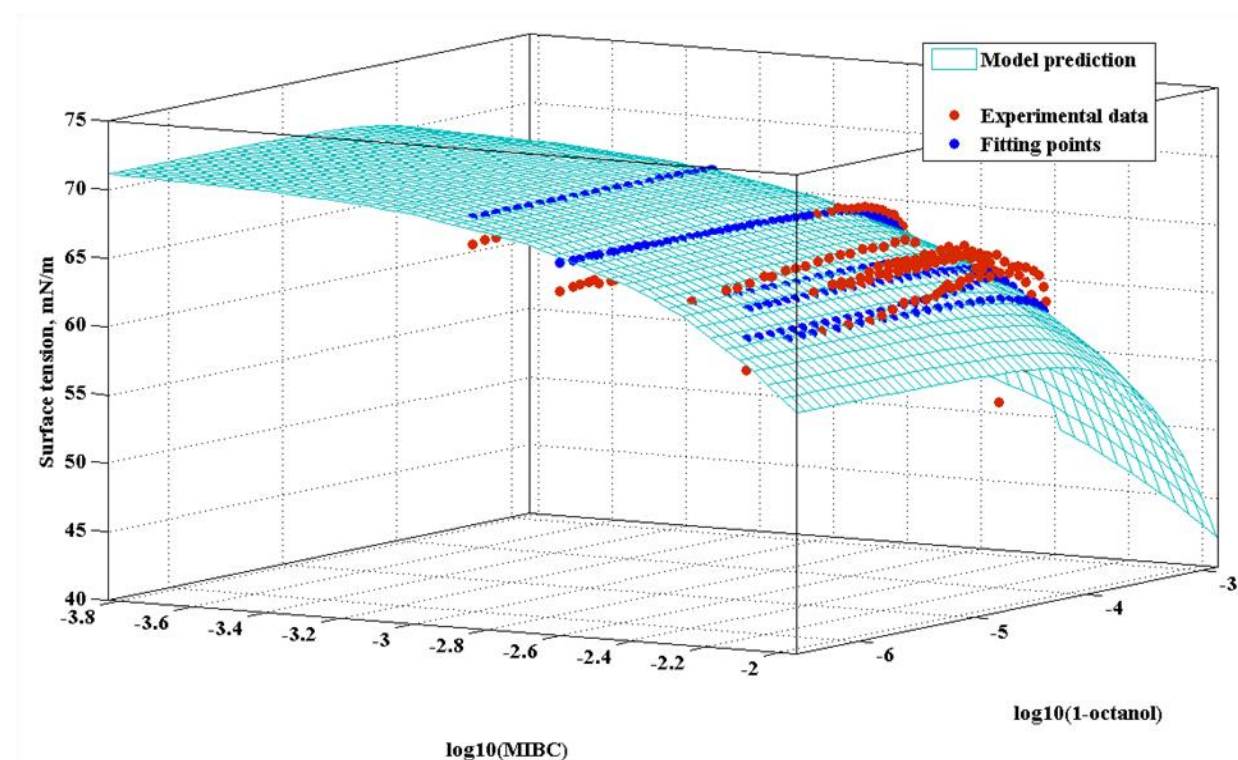


Figure 7-3: Surface tension of MIBC/1-octanol mixture: fitted by Fainerman’s model ($A_{12} = 1.477$, $\delta y = 1.36$ mN/m)

7.2.4 Discussion

According to theoretical model (Fainerman, Miller et al. 2002), the interaction of surfactant molecules at surface is characterized by A_{12} . For negative value of A_{12} , there is a repulsive force between two different molecules of mixture (Fainerman 1983). In this study, the interaction parameter between adsorbed molecules of MIBC/1-heptanol was found to be similar with that of 1-octanol/1-heptanol and 1-octanol/1-hexanol (Fainerman 1983), as shown in Table 7-1. The repulsion force

between 1-heptanol/1-octanol is nearly the same as the interaction between MIBC/ 1-heptanol molecules at the surface layer.

On the other hand, MIBC/1-octanol mixture was not explained well by the model, with a positive interaction parameter. More importantly, the model could not describe the synergistic peaks, the modelling result was not appropriate for this mixture.

The observed synergism could have resulted for two possible reasons. The first reason could be due to the difference in packing at the surface of the odd and the even (7 and 8 carbons) numbered carbon in the alkyl chain (Esumi K. and M. 1997; Warszynski and Jachimska 2002; Zdziennicka 2010). Accordingly, 1-heptanol (odd number of carbon atoms) is packing looser compared to 1-octanol, which lead to the special arrangement of MIBC and 1-octanol at the surface. Second reason is raised from the effect of the branched or straight structure of alcohols (Le, Phan et al. 2010). Nevertheless, both 1-octanol/1-hexanol (Fainerman 1983) and MIBC/1-heptanol mixtures did not show any synergistic effect and were described well by this model.

Consequently, it can be concluded that the unique combination between branched structure of MIBC and hydrophobicity of 1-octanol is the underpinning cause of synergism in MIBC/1-octanol. The synergism indicates a complex arrangement in the mixed adsorbed layers. The overall influence of MIBC structure on mixed adsorbed layer needs further investigations by other methods like neutron reflection.

7.2.5 Summary

The adsorption of MIBC with two straight chain alcohols: 1-heptanol and 1-octanol was investigated through measuring surface tension by Wilhelmy plate. The mixture of MIBC/1-heptanol was interpreted with high accuracy (standard deviation is 0.85 mN/m) by the available model (Fainerman and Miller 2001). However, the mixture with 1-octanol demonstrated positive azeotropy. The model failed to describe the experimental data for this latter mixture. The bulky structure of MIBC (branched structure and relative position of hydrophobic group along carbon chain) could be the reason for the synergistic effect. New theoretical model should be developed to take into account the synergistic interaction of these molecules at the air/water surface.

In addition to surface tensiometry, further investigations (such as molecular dynamics) on the depth of adsorption zones and the arrangement(s) of adsorbed molecules are required to explore the phenomena. New insights into adsorption of branched surfactants mixtures could lead to better surfactant mixtures for industrial processes such as coal flotation, in which branched surfactants have proved superior (Aston, Lane et al. 1989).

7.3 MIXTURE OF CATIONIC/NONIONIC SURFACTANTS

Different types of reagents are used to meet different roles in froth flotation processes. For example, anionic surfactants such as xanthates and dithiophosphates are added as collectors in sulfide flotation, which adsorb at the mineral-water interface, rendering the mineral surface hydrophobic. Non-ionizing surfactants such as alcohols and polyglycols are added as frothers to control the bubble coalescence and the frothing behaviour of the flotation system. In such mixed reagent systems, it is important to consider the interaction between the different types of surfactants (Schulman and Leja 1954; Leja 1982). Indeed, synergistic interactions between flotation collectors and between flotation collectors and frothers have long been recognized in flotation research and plant practice (Crozier and Klimpel 1989). A number of mechanisms have been proposed to explain the enhancement of flotation performance by reagent mixtures. These proposed explanations focussed on the effects related to adsorption of the mixed reagents on the particle and bubble surfaces, interactions between the reagents, either in the bulk or at the interfaces. The reagent mixtures can also change the key surface properties of air bubbles, foam films and Plateau borders, such as Gibbs-Marangoni elasticity, surface viscosities and mobility, which are known to significantly affect bubble coalescence and froth drainage and stability (Leja 1982; Nguyen and Schulze 2004).

It is customarily assumed that collectors and frothers in their mixtures co-adsorb at the air-water interface and synergistically reduce the surface tension more significantly than the individual component surfactants. The addition of alcohols improved the stability of the cationic solution in froth flotation (Bergeron 1997). Mixture of CTAB and alcohols is widely used in theoretical research (Zdziennicka, Jańczuk et al. 2004; Zdziennicka and Janczuk 2008). We found that though MIBC and 1-hexanol are in the same series of n-hexanol, but due to different structure of carbon chain, their individual adsorption behaviours are different (section 4.2). In

addition, most of alcohols used in research on theoretical aspect of binary mixture are straight chain carbon only. It was decided to compare the adsorption behaviour of mixture of MIBC and CTAB; 1-hexanol and CTAB at concentrations lower than CMC.

7.3.1 Adsorption of single surfactants systems

Adsorption isotherm of 1-hexanol, MIBC and CTAB at water/air interface (Figure 7-4) with fitting parameters as displayed in Table 7-3.

Table 7-3. Fitting parameters for single surfactant: CTAB, 1-hexanol, MIBC

Surfactant	Γ_m (mol/m ²)	K (M ⁻¹)	A	Standard deviation δ_γ (mN/m)
CTAB	5.34×10^{-6}	2596	0	0.18
MIBC	1.5×10^{-5}	40.99	0	0.42
1-hexanol	2.0×10^{-5}	39.6	0.0209	0.135

Except for 1-hexanol whose value of A is different from 0, the isotherm of 1-hexanol is modelled by Frumkin model. While the best-fitted values of A is zero for both surfactants CTAB and MIBC, they can be modelled by Langmuir isotherm individually (the standard deviations were exceptionally small compared to the acceptable threshold of 1 mN/m(Prosser and Frances 2001). Consequently, CTAB can be modeled as a non-ionic surfactant with $n=1$, $\Gamma_m = 1.1 \times 10^{-5}$ mol/m².

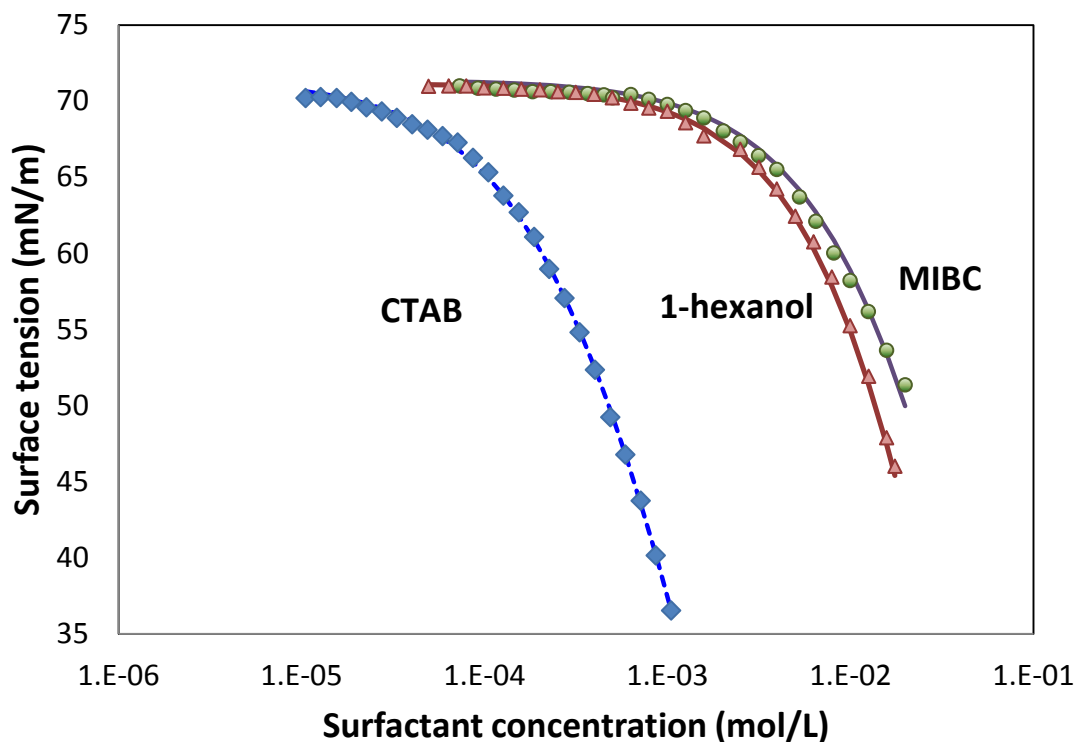


Figure 7-4 Adsorption isotherm of individual surfactants: CTAB, MIBC, 1-hexanol

7.3.2 MIBC/CTAB

7.3.2.1 General observation of mixed adsorption

The surface tension was measured for different sets of concentrations, containing unchanged MIBC concentration (0.02 mol/L to 0.003 mol/L) with gradually increasing concentration of CTAB (3×10^{-7} mol/L to 9×10^{-4} mol/L).

At constant concentration of MIBC, surface tension was expected to decrease monotonically with increasing CTAB concentration as observed with mixture of 1-heptanol/ 1-octanol (Fainerman 1983), C12E5/Triton X-100 and C12E8/SDS (Siddiqui and Franses 1996). In this study, however, the surface tension of the mixture gradually increased to a peak with the increasing CTAB concentration. The peaked surface tensions were ~ 3 mN/m higher than that of pure MIBC solution. After the peak, the surface tension of mixture decreases with further increasing CTAB concentration. This type of positive synergism has not been reported in earlier literature.

7.3.2.2 Fitting procedure for mixture and results

Both Fainerman and Siqquidi required parameters of single isotherm $\Gamma_{m,i}$ and K_i as shown in Table 7-3. As these parameters are predetermined, each model has only one adjustable parameter: A_{12} (Fainerman's model) and β (Siqquidi's model).

With Fainerman's model, **Eq. 2-5** and **Eq. 2-6** were solved simultaneously using the Jacobian method to find θ_1 and θ_2 . Subsequently, θ_1 and θ_2 were used to calculate surface tension **Eq. 2-8**. MS Excel Solver was utilized to fit the modeled surface against experimental data by adjusting A_{12} (Figure 7-5).

Similarly, θ_1 and θ_2 in Siqquidi's model were determined by solving **Eq. 2-9** and **Eq. 2-10** simultaneously. Subsequently, the surface tension, determined by **Eq. 2-14**, is fitted against experimental data using Solver by adjusting β . The results are demonstrated in Figure 7-6.

It can be seen that both modeling results are unsatisfactory, with large standard deviations. Most significantly, neither model can describe the positive peaks demonstrated experimentally.

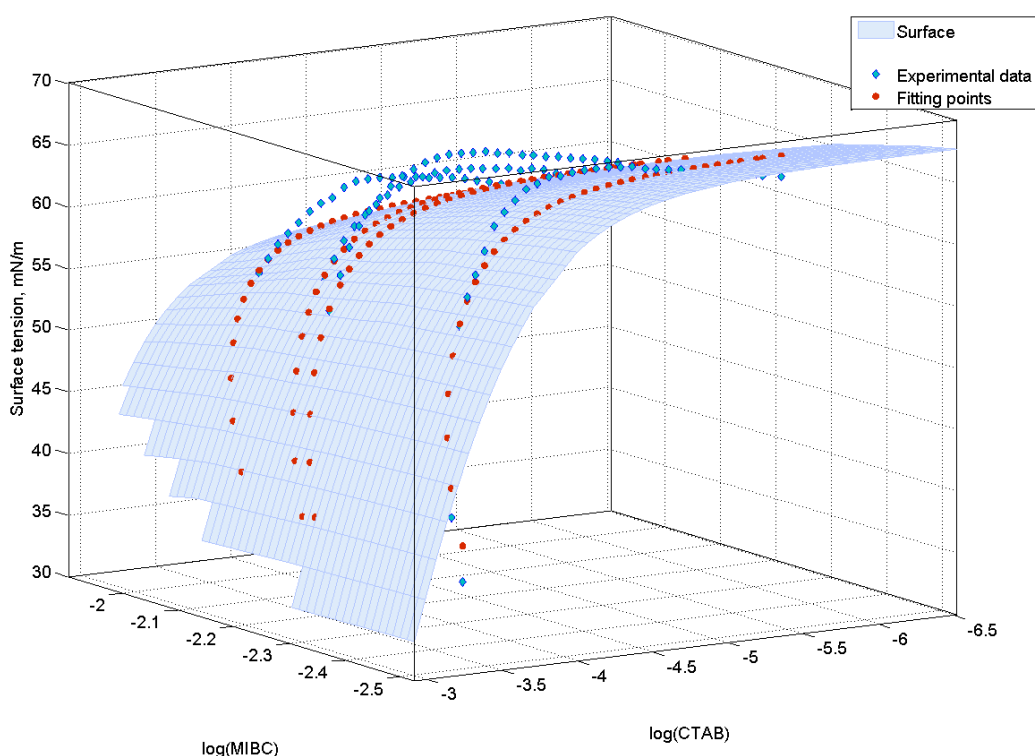


Figure 7-5 Fainerman model, best fitted value of $A_{12} = -0.96$, $\delta_y = 1.77 \text{ mN/m}$

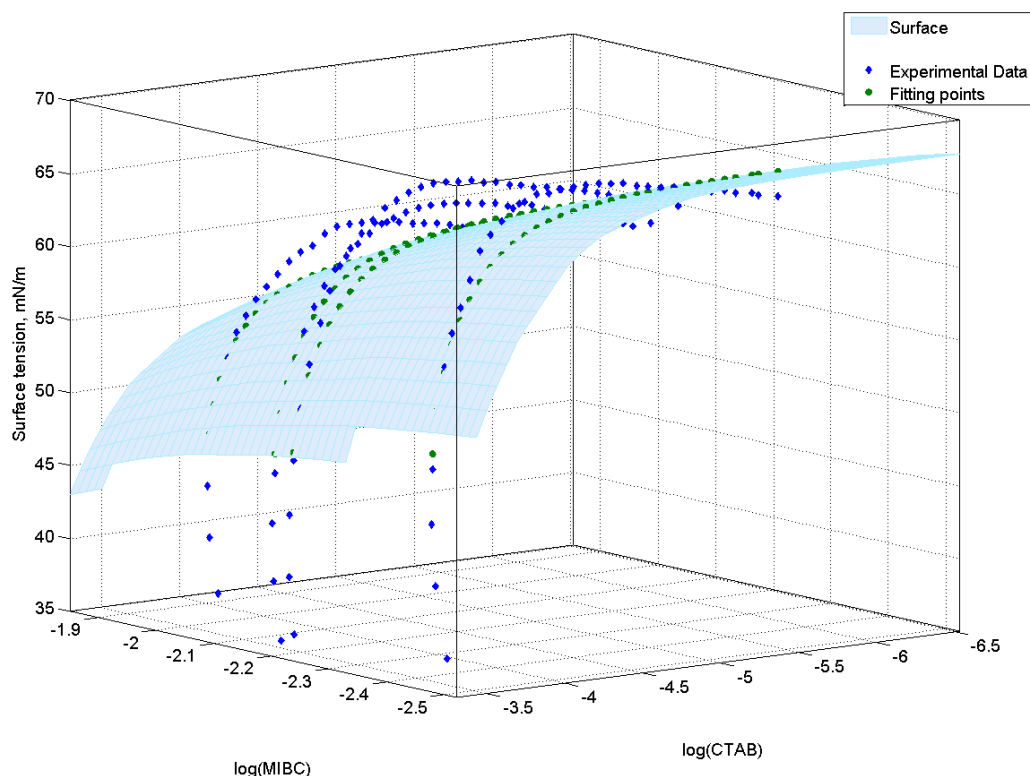


Figure 7-6 Siddiqui model, best fitted value of $\beta=0.51$, $\delta_y = 2.2\text{mN/m}$

7.3.2.3 Determination of synergistic points

Since both models above failed to describe the synergistic behaviour, especially the positive azeotropy, two-variable polynomials were attempted. A high order polynomial was able to correlate the experimental data very well with a standard deviation of 0.52 mN/m and goodness of fit, $R^2 = 0.9997$. The results are plotted in Figure 7-7.

To describe the experimental data with high accuracy, the polynomial requires a high (5^{th}) order regarding CTAB concentration:

$$\gamma(x,y) = p_{00} + p_{10}x + p_{01}y + p_{20}x^2 + p_{11}xy + p_{02}y^2 + p_{21}x^2y + p_{12}xy^2 + p_{03}y^3 + p_{22}x^2y^2 + p_{13}xy^3 + p_{04}y^4 + p_{23}x^2y^3 + p_{14}xy^4 + p_{05}y^5$$

With $x = \ln(c_1)$, $y = \ln(c_2)$, c_1 , c_2 are concentrations of MIBC and CTAB, respectively. The value of the coefficients of this polynomial was tabulated in Table 7-4.

Consequently, the synergistic points are determined by searching for maximum surface tension at fixed MIBC concentrations. These points are plotted in Figure 7-8. The bulk concentration ratio (MIBC/CTAB) along this line is greater than 100 times.

Chapter 7 Molecular structures and equilibrium adsorption of surfactant mixture

Subsequently, the adsorbed concentration Figure 7-9 is estimated individual assuming non-interference between two surfactants, i.e. applying the values in Table 7-1. Hence, the ratio between Γ_1 and Γ_2 varies from 2 to 5. At the highest CTAB concentration of synergistic composition $\Gamma_{2max} = 6.95 \times 10^{-7} \text{ mol/m}^2$, the ratio equals 3.6.

Table 7-4 Coefficient values of polynomial function fitted for mixture

Coefficients	Value
P00	8414
P10	2598
P01	2772
P20	206.5
P11	766.9
P02	340.2
P21	57.76
P12	75.60
P03	20.20
P22	5.1088
P13	2.8646
P04	0.62391
P23	0.14739
P14	0.029176
P05	0.009174

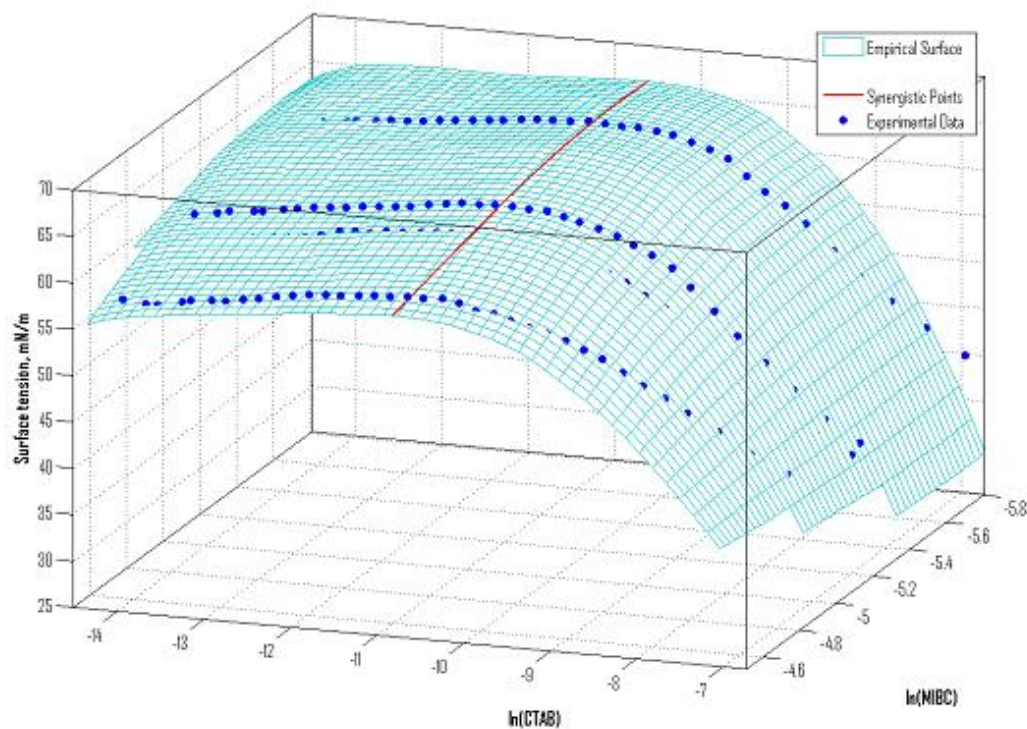


Figure 7-7 Best-fitted surface created by the empirical polynomial

7.3.2.4 Discussion

Our experimental results demonstrated a positive synergism instead of a negative one as often reported in the literature (Zdziennicka and Janczuk 2008; Zdziennicka and Janczuk 2010). The conventional definition of adsorption synergism (Siddiqui and Frances 1996) is "the total surface density was larger than the pure component surface density". To further demonstrate the synergistic effect, surface tension (obtained from empirical polynomial) was plotted against CTAB percentage at fixed total concentrations (see Figure 7-9). Again, a positive peak was demonstrated around 1% CTAB concentration. Following classical Gibbs adsorption theory (i.e. adsorbed molecules form a monolayer), higher surface density qualitatively equals to lower surface tension and vice versa. In that sense, a maximum surface tension has shown in Figure 7-7 and Figure 7-8 means a minimum total adsorbed concentration, which is very unlikely. Since the two theoretical models above are based on Gibbs adsorption theory, they predictably failed to describe this positive synergism.

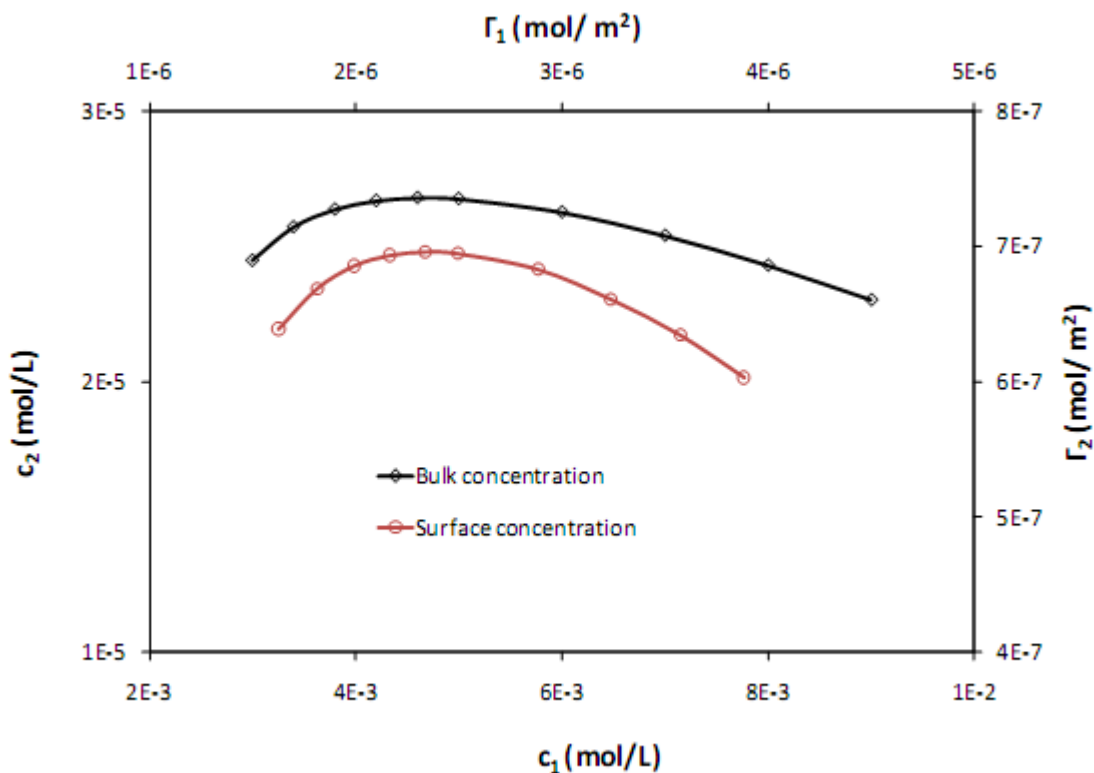


Figure 7-8 The synergistic points of MIBC/CTAB (c_1 and Γ_1 are MIBC bulk and surface concentration, c_2 and Γ_2 are CTAB bulk and surface concentration, respectively).

It should be noted that the change in surface potential, which was developed for anionic surfactant (Karakashev, Nguyen et al. 2008; Manev, Sazdanova et al. 2008), is not included in the above binary models. However, surface potential charges should have small influence on surface tension (Karraker and Radke 2002). For example, surface charge due to adsorption of CTAB (Nakahara, Shibata et al. 2011) and MIBC (Phan, Nakahara et al. 2011) were found to be less than 250 mV. Similar zeta-potential of MIBC was found to be less than 200mV. Such changes in potential may decrease surface tension ~ 0.3 mN/m, and cannot explain the scale of synergism found in this study.

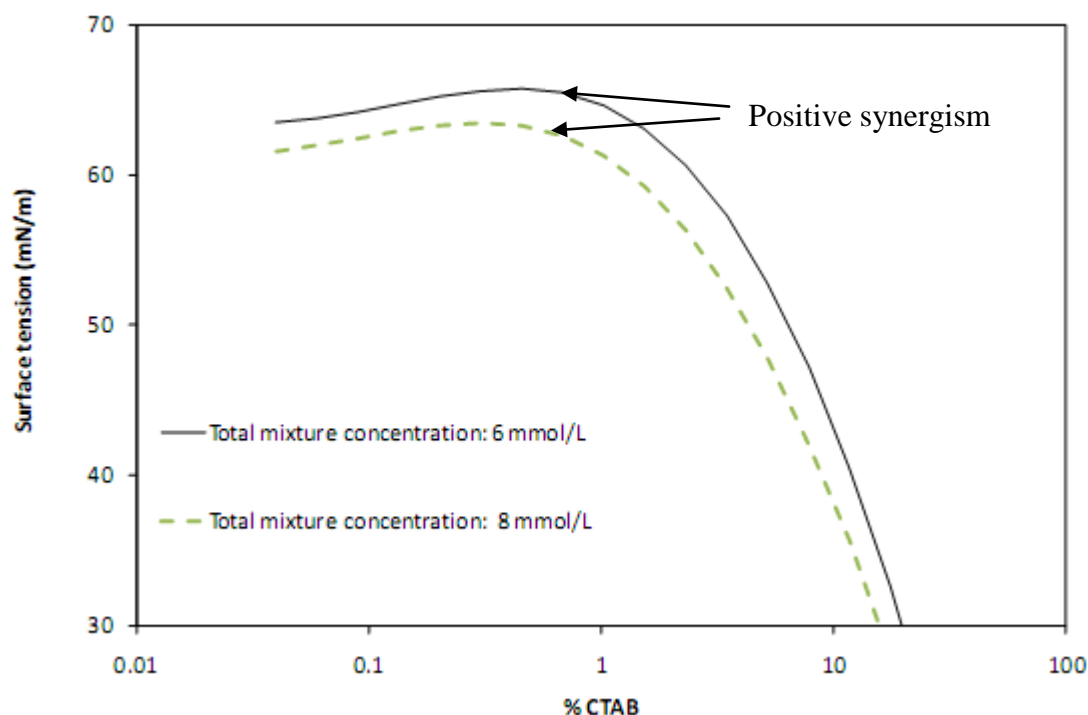


Figure 7-9 Surface tension versus percentage of CTAB at constant total concentration of mixture

In the literature, mixed adsorption between CTAB and propanol has also been investigated by Zdziennicka and Janczuk (Zdziennicka and Janczuk 2008). They found that at low CTAB concentration, the surface tension of the mixture appeared to be dominated by propanol concentration. With CTAB concentration closer to CMC, the surface tension of mixture is dominated strongly by CTAB (lower than those of pure propanol). Similar phenomena was also observed with SDS/ethanol and SDS/propanol mixtures (Kovtun, Khilko et al. 2010). Therefore, it is conceivable that binary alcohol/CTAB mixture can form two molecular arrangements at adsorbed zone: one dominated by alcohol, the other dominated by CTAB. The arrangements depend on the composite concentration. For propanol/CTAB mixture, the shift between two mechanisms was quite smooth and difficult to clarify. In contrast, the shift was demonstrated distinguishingly by a positive synergistic line for MIBC/CTAB mixture. From **Figure 7-8**, it can be estimated that change in structure occurs when ratio between adsorbed MIBC and CTAB molecules is around 3.5.

7.3.2.5 Summary

The adsorption of CTAB and MIBC was investigated through measuring surface tension by Wilhelmy plate. This studied mixture show that there was a positive

azeotropy instead of negative one as often reported in the literature. Two mixture models of Fainerman (Fainerman, Miller et al. 2002) and Siddiqui (Siddiqui and Franses 1996) were fitted against experimental data. Neither model can describe the positive synergism. Subsequently, a polynomial equation was applied to determine the synergistic points, at which the bulk ratio is greater than 100 times. On the other hand, concentration ratio at the adsorption layer at would correspond to 2 to 5 times, assuming non-interaction between adsorbed molecules.

The positive synergism could be explained by the existence of two distinct molecular arrangements at absorption zone: one dominated by alcohol, the other dominated by CTAB. The bulky structure of MIBC (branched structure and relative position of hydrophobic group along carbon chain) may be the reason for the sharp distinguishing line between the two mechanisms.

In addition to surface tensiometry, further investigations (such as molecular dynamics) on the depth of adsorption zones and the arrangement(s) of adsorbed molecules to explore the phenomena. New insights into adsorption of branched surfactants mixtures could lead to better surfactant mixtures for industrial processes such as mineral flotation, in which branched surfactants have been proved superior.

7.3.3 1-hexanol/CTAB

As mentioned above, to compare the possibility of influence of chain structure to adsorption behaviour of mixture, we investigated mixture of CTAB and 1-hexanol which is the isomer of MIBC but having a straight chain carbon. The experiment procedure and was the same as the earlier investigated mixture systems. As adsorption isotherm of 1-hexanol is qualitative by Frumkin equation (Table 7-3), the generalized model of Fairnerman was used for evaluating the static adsorption behaviours of mixture CTAB/1-hexanol

7.3.3.1 Result and discussion

The surface tension was measured for different sets of concentrations, which contained unchanged 1-hexanol concentration (8.14×10^{-4} mol/L to 7.28×10^{-3} mol/L) but with gradually increased concentration of CTAB (8.37×10^{-7} mol/L to 0.89×10^{-3} mol/L). The surface tension of the mixture decreased with addition of the second component (CTAB) to 1-hexanol solution (see Figure 7-10)

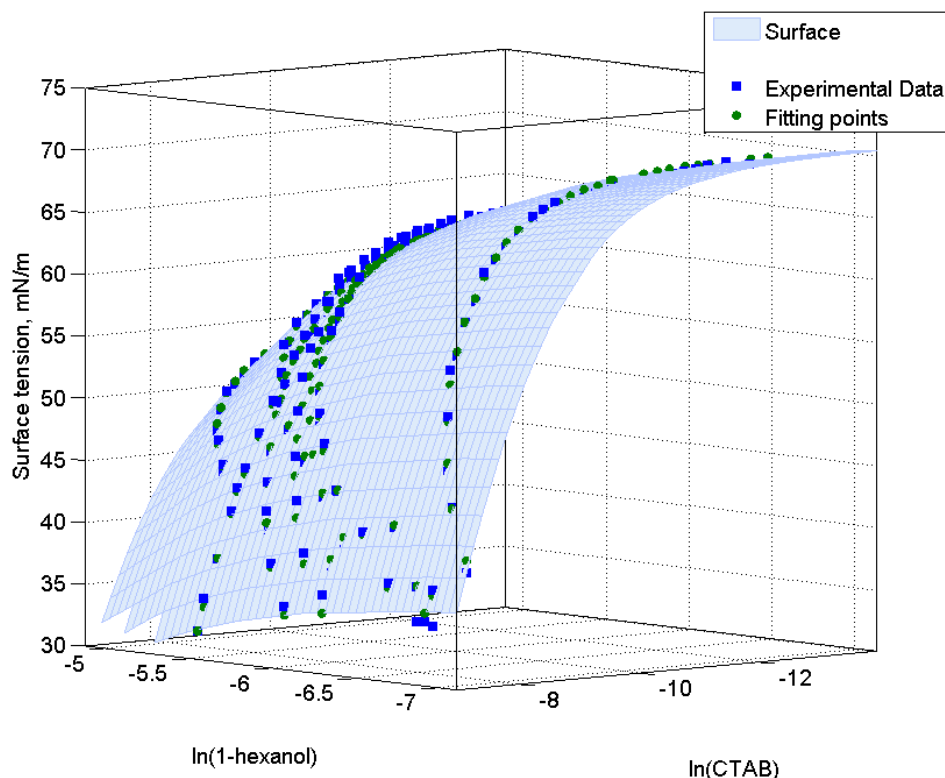


Figure 7-10 Fainerman's models, best fitted value of $A_{12}=0.34$, $\delta_y=0.77\text{mN/m}$

The adsorption behaviour of mixture 1-hexanol/CTAB was well described by Fainerman's model with the standard deviation of the fitting mole and deviation was 0.77 mN/m . The interaction parameter for this mixture was 0.34 . This model gave good prediction of mixture of CTAB and short chain carbon methanol, ethanol and propanol (Zdziennicka and Janczuk 2008; Zdziennicka and Janczuk 2010)

7.3.3.2 Summary

The surface tension of mixture of 1-hexanol/CTAB and MIBC/CTAB at room temperature was conducted by Wilhelmy plate method. It is the first time the influence of straight chain and bulky chain structure to synergism of mixture was conducted. For 1-hexanol/CTAB mixture, the general model of Fainerman was applied due to equilibrium adsorption isotherm of 1-hexanol was interpreted by Frumkin equation, while MIBC/CTAB was analyzed by two models: one from Fainerman and another from Siddiqui. The mixture of CTAB/1-hexanol was predicted very well by Fainerman's model with the decrease of surface tension of solution as another surfactant added, while CTAB/MIBC could not described by both models applied as the surface tension increased to a peak with the increasing concentration of second surfactant added. After the peak, the surface tension of

mixture decreases with further increasing concentration of added surfactant. This phenomenon was not reported in the literature.

This result showed that for the same number of carbon chain of the chemical, the straight chain will follow the general trend model while the branching structure of MIBC created a different phenomenon. The arrangement of these chemicals with CTAB at water/ air interface was different.

Though the results in this research are not sufficient enough to understand this phenomenon but the experimental data confirm the special effect of chain structure on synergism of mixture. To get a clearer solution on the arrangement of straight chain and branched chain alcohol in the mixture with CTAB, different methods which can provide more accurate estimation of the surface excess at the interface, such as neutron reflection should be conducted.

7.4 CHAPTER CONCLUSION

Equilibrium adsorption of mixture MIBC with other surfactants (alcohol, cationic) was investigated by using Wilhemy plate method. Two most applied models of Fainerman and Siddiqui were applied as the quantitative tool for understanding these interfacial behaviours. The results showed that there was a positive synergism in case of mixtures MIBC/1-octanol and MIBC/CTAB. The two general models could not be used to analyze these cases. Moreover, 1-hexanol, was mixed with CTAB to compare the difference in equilibrium adsorption between the straight chain and the branching chain in the binary mixture with CTAB. The results showed that equilibrium adsorption of 1-hexanol/CTAB mixture could be well described by general models. This finding could strengthen the explanation of positive synergism which has not been reported in literature before. However, to provide more accurate solution for this special phenomenon, other methods such as neutron reflection, or molecular stimulation should be applied.

CHAPTER 8

CONCLUSIONS AND FUTURE RESEARCH DIRECTIONS

8.1 THESIS SUMMARY

This thesis has provided a systematically comparative picture on the surface reducing capacity with different chain length, branching structures of two popular groups of surfactants: alcohols which are frothers in mining industry; alkylmethylammonium bromide which also used in iron ore separation. Equilibrium surface tension data was analyzed by two famous models, Frumkin and Langmuir isotherms. These isotherms provided the quantitative parameters for comparative purposes. The founding results strengthen the conclusion of other works that longer chain length of the surfactant molecules would lead to higher surface activity of those surfactants. The branching structure of the tail of the surfactant make it more complicated in arrangement in the surface which results in lower capacity of surface activity. The higher the difference in the length of the branching compositions of the tail, the better arrangement at the interface resulting in better surface tension reduction. These sets of data were used further as the basis for calculating another property of interfaces: Gibbs surface elasticity. This parameter is important in studying the foaming properties of these surfactants.

In addition, a simple equation (Phan 2010) can be used instead of using the famous isotherms in analyzing the equilibrium surface tension. This new equation can be incorporated into dynamic model in analyzing dynamic adsorption activities of surfactants. The advantages of this equation application are: (1) more reliable fitting equilibrium surface tension than the conventional equation; (2) high consistency in fitting dynamic adsorption activity with the same set of two parameters for all concentrations; (3) high prediction efficiency with very low standard deviation; (4) comparative dynamic activity capacity of different surfactants by comparing the set of fitting parameters. To prove these advantages of this new fitting procedure, two sets of chemicals were investigated: (1) The dynamic adsorption of nonanol isomers (2-nonanol, 3-nonanol, 5-nonanol) was measured by pendant bubble method; (2) dynamic adsorption of C_n TAB ($n=14, 16, 18$) were measured by maximum bubble

method. The first set of chemicals evaluated the influence of branching structure of the tail to dynamic adsorption while the second set of chemicals considered the influence of the chain length. We found that as the functional group move forward inside the chain, the adsorption rate is faster. As C_n TAB getting longer tail, it took more time for that surfactant to reach the interface.

Another new finding of this thesis is the positive synergism in surface activity in some mixture systems with the presence of MIBC, a branching structure (MIBC/1-octanol; MIBC/CTAB). Two general models applied widely in the field could not be used for analyzing these positive synergism cases. The possible reasons for the positive synergism could be the existences of two distinguish molecular arrangements at the absorption zone or the branch structure of MIBC. An additional experiment conducted with 1-hexanol/CTAB, did not have the positive synergism, strengthening the assumption of the existence of special synergism due to bulky structure of MIBC.

8.2 FUTURE RESEARCH DIRECTIONS

Measuring the surface tension is the most simple and widely commercialization method in studying surfactants. It can quickly provide a picture on the impact of molecule structure on interfacial activity. However, sometimes directly measuring surface tension could not provide clear evidence due to a small difference of surface tension not detected due to the limited accuracy of the instruments, or being affected by ambient several factors: temperature, moisture content, pH, and purity, surface potential. Moreover, the Gibbs equation applied to calculate surface excess from the surface tension measurement was based on the assumption of dividing surface. This assumption does not include the surfactant molecules arranged in several layers instead of just one layer as assumed. The arrangement of interfacial zone is a complex system which has not been explained fully. This study focuses on the macro-properties only. It is recommended to combine the surface tensiometry with direct probing method such as neutron reflectometry (Lee E.M., Thomas R. K. et al. 1989; Lee, Liou et al. 2002) to fully explain the adsorption process.

To strengthen the finding of this work on the impact of branching molecule to interfacial properties, neutron reflection is the most potential method. As this method can provide important information of surfaces composition through gaining neutron

refractive index profile in a certain layer of the solution to the interface, the shortcomings of directly measuring surface tension can be overcome.

Another interfacial property that should be involved is surface potential which can identify the difference in interfacial activity in some cases where surface tension showed no difference. It will be very useful for comparing the equilibrium of two isomers having very close equilibrium properties.

For further application studies, the influence of structure of molecules to foaming stability and formation can be investigated through foam property measurements. The equilibrium and dynamic adsorption results obtained from this thesis can be integrated with foam experiment data to evaluate the practical application aspects of these chemicals. In addition, the foaming properties of mixtures can also be evaluated at different mixture ratios. Finally, the flotation experiments with different operation conditions, different particle sizes, and different composition of surfactants can be further investigated.

8.3 CONCLUSION REMARKS

Firstly, this work utilized widely adopted models in the field as the quantitative tool for systematically evaluating the branching as well as chain length structure of two sets of chemicals (anionic and cationic surfactants) to equilibrium adsorption. Secondly, one new fitting approach was proposed for fitting dynamic adsorption. This new approach proved simple in application and more consistent in results analyzed. Furthermore, this new approach is also more efficient for qualitative comparative dynamic properties of different surfactant structures and provided more accurate prediction for other concentrations using data of only two concentrations. Finally, the positive synergism in mixture of surfactants was a new finding not reported in literature. The possible explanation for this new phenomenon as the special arrangement of branching structure of chemicals at interface was strongly supported by several cases. All these findings of this thesis are a few pieces of puzzle to contribute to the large picture of fundamental study on structure-interfacial properties.

REFERENCES

REFERENCES

- A.W. Adamson and A. G. Gast (1997). Physical Chemistry of Surfactants. New York, A Wiley-Interscience Publication.
- Addison, C. C. (1945). "The properties of freshly formed surfaces. Part IV. The influence of the chain length and structure on the static and the dynamic surface tensions of aqueous alcoholic solutions." Journal of Chemical Society: 98-106.
- Aksenenko, E. V., A. V. Makievski, et al. (1998). "Dynamic surface tension of aqueous alkyl dimethyl phosphine oxide solutions:: Effect of the alkyl chain length." Colloids and surfaces. A, Physicochemical and engineering aspects **143**(2-3): 311-321.
- Antonietti, M. (2001). "Surfactants for novel templating applications." Current Opinion in Colloid & Interface Science **6**: 244-248.
- Aston, J. R., J. E. Lane, et al. (1989). "The solution and interfacial chemistry of nonionic surfactants used in coal flotation." Mineral processing and extractive metallurgy review **5**(1): 229-256.
- Battal, T., G. C. Shearman, et al. (2003). "Determination of dynamic surface excess of a homologous series of cationic surfactants by ellipsometry." Langmuir **19**: 1244-1248.
- Beers, K. J. (2006). Numerical Methods for Chemical Engineering. Applications in MATLAB, Massachusetts Institute of Technology.
- Beneventi, D., B. Carre, et al. (2001). "Role of surfactant structure on surface and foaming properties." Colloids and surfaces. A, Physicochemical and engineering aspects **189**(1-3): 65.
- Bergeron, V. (1997). "Disjoining Pressures and Film Stability of Alkyltrimethylammonium Bromide Foam Films." Langmuir **13**(13): 3474-3482.
- Bleys, G. and P. Joos (1985). "Adsorption kinetics of bolaform surfactants at the air/water interface." Journal of physical chemistry **89**(6): 1027.
- Bleys, G. and P. Joos (1985). "Adsorption kinetics of bolaform surfactants at the air/water interface." The Journal of Physical Chemistry **89**(6): 1027-1032.
- Borwankar, R. P. and D. T. Wasan (1983). "The kinetics of adsorption of surface active agents at gas-liquid surfaces." Chemical Engineering Science **38**(10): 1637-1649.
- Bradley J.E., Lee E.M., et al. (1988). "Adsorption at liquid surface studied by means of Specular Reflection of Neutrons." Langmuir **4**: 821-826.
- Buzzacchi, M., P. Schmiedel, et al. (2006). "Dynamic surface tension of surfactant systems and its relation to foam formation and liquid film drainage on solid surfaces." Colloids and Surfaces A: Physicochemical and Engineering Aspects **273**(1-3): 47-54.
- Chang, C. H. and E. I. Franses (1992). "Modified Langmuir-Hinshelwood kinetics for dynamic adsorption of surfactants at the air/water interface." Colloids and Surfaces **69**: 189-201.

REFERENCES

- Chang, C. H. and E. I. Franses (1995). "Adsorption dynamics of surfactants at air/water interface: a critical review of mathematical models, data and mechanisms." Colloids and Surfaces A: Physicochemical and Engineering Aspects **100**: 1-45.
- Chang, C. H. and E. I. Franses (1995). "Adsorption dynamics of surfactants at the air/water interface: a critical review of mathematical models, data, and mechanisms." Colloids and Surfaces A: Physicochemical and Engineering Aspects **100**: 1-45.
- Chang, C. H. and E. I. Franses (1995). "Adsorption dynamics of surfactants at the air/water interface: a critical review of mathematical models, data, and mechanisms." Colloids and Surfaces A **100**: 1-45.
- Chotipong, A., J. F. Scamehorn, et al. (2007). "Removal of solvent-based ink from printed surface of high-density polyethylene bottles by alkyltrimethylammonium bromides: Effects of pH, temperature, and salinity." Colloids and Surfaces A: Physicochemical and Engineering Aspects **297**: 163–171.
- Christenson, H. K. and V. V. Yaminsky (1995). "Solute Effects on Bubble Coalescence." Journal of Physical Chemistry **99**(25): 10420-10420.
- Comley, B. A., P. J. Harris, et al. (2002). "Frother characterisation using dynamic surface tension measurements." International Journal of Mineral Processing **64**(2-3): 81-100.
- Crozier, R. D. and R. R. Klimpel (1989). "Frothers: plant practice." Mineral processing and extractive metallurgy review **5**(1): 257-279.
- D'Errico, G., O. Ortona, et al. (2001). "Transport Properties of Aqueous Solutions of Alkyltrimethylammonium Bromide Surfactants at 25 C degree." Journal of Colloid and Interface Science **239**: 264-271.
- Danov, K. D., V. L. Kolev, et al. (2000). "Adsorption Kinetics of Ionic Surfactants after a Large Initial Perturbation. Effect of Surface Elasticity." Langmuir **16**(6): 2942-2956.
- Dukhin, S. S., K. G., et al., Eds. (1995). Dynamics of adsorption at liquid interfaces : theory, experiment, application Studies in interface science. Amsterdam ; New York Elsevier
- Eastoe, J. and J. Dalton (2000). "Dynamic surface tension and adsorption mechanisms of surfactants at the air-water interface." Advances in Colloid and Interface Science **85**(2-3): 103-144.
- Eastoe, J., J. S. Dalton, et al. (1997). "Dynamic surface tensions of nonionic surfactant solutions." Journal of Colloid and Interface Science **188**(2): 423-430.
- Esumi K. and U. M. (1997). Structure-performance relationships in surfactants. New York, Marcel Dekker.
- Fainerman, V. (1983). "Mixed adsorption monolayers of alcohols on solution-air interface." Colloid journal of the USSR **45**(3): 435-442.

REFERENCES

- Fainerman, V., R. Miller, et al. (2002). "Simple model for prediction of surface tension of mixed surfactant solutions." Advances in Colloid and Interface Science **96**: 339-359.
- Fainerman, V. B., E. V. Aksenenko, et al. (2010). "Adsorption layer characteristics of mixed Sodium Dodecyl Sulfate/CnEOm solutions: 1. Dynamic and Equilibrium Surface tension." Langmuir **26**(1): 284-292.
- Fainerman, V. B., E. V. Aksenenko, et al. (2010). "Adsorption Layer Characteristics of Mixed Oxyethylated Surfactant Solutions." Journal of Physical Chemistry B **114**: 4503-4508.
- Fainerman, V. B. and R. Miller (1996). "Adsorption kinetics of short-chain alcohols at the water/air interface: diffusion controlled adsorption under the conditions of a nonequilibrium surface layer." Journal of Colloid and Interface Science **178**: 168-175.
- Fainerman, V. B. and R. Miller (2001). "Simple method to estimate surface tension of mixed surfactant solutions." The journal of physical chemistry. B **105**(46): 11432-11438.
- Fainerman, V. B., R. Miller, et al. (2000). "Adsorption behavior of Oxyethylated alcohols at the solution/air interface." Langmuir **16**: 4196-4201.
- Fainerman, V. B., R. Miller, et al. (2002). "Simple model for prediction of surface tension of mixed surfactant solutions." Advances in Colloid and Interface Science **96**(1-3): 339-359.
- Ferri, J. K. and K. J. Stebe (1999). "A structure-property study of the dynamic surface tension of three acetylenic diol surfactants." Colloid & Surfaces. A. Physicochemical and Engineering Aspects **156**: 567-577.
- Ferri, J. K. and K. J. Stebe (2000). "Which surfactants reduce surface tension faster? A scaling argument for diffusion-controlled adsorption." Advances in Colloid and Interface Science **85**(1): 61-97.
- Furó, I. (2005). "NMR spectroscopy of micelles and related systems." Journal of Molecular Liquids **117**(1-3): 117-137.
- Geeraerts, G., P. Joos, et al. (1993). "Dynamic surface tensions and dynamic surface potentials." Colloids and Surfaces A: Physicochemical and Engineering Aspects **75**: 243-256.
- Georgieva, D., A. Cagna, et al. (2009). "Link between surface elasticity and foam stability." Soft matter **5**: 2063-2071.
- Ghaicha, L., R. M. Leblanc, et al. (1992). "Ellipsometric study of surfactants comprising linear and branched hydrocarbon chains at the air-water interface." Journal of Physical Chemistry **96**(26): 10948-10953.
- Gilányi, T., I. Varga, et al. (2008). "Adsorption of alkyl trimethylammonium bromides at the air/water interface." Journal of Colloid and Interface Science **317**(2): 395-401.
- Gliniski, J., G. Chavepeyer, et al. (1998). "Surface properties of diluted aqueous solutions of normal short-chain alcohols." Journal of Chemical Physics **109**(12): 5050-5053.

REFERENCES

- Gohsuke, S., N. Shigemi, et al. (2008). "A review of recent studies on aqueous binary mixed surfactant systems." Journal of Oleo Science **57**(2): 61-92.
- Goloub, T. and R. J. Pugh (2005). "The role of the surfactant head group in the emulsification process: Single surfactant systems." Journal of colloid and interface science **257**(2): 337-343.
- Grieves, R. B., D. Bhattacharyya, et al. (1976). "Surfactant-colligend particle size effects on ion flotation: Influences of mixing time, temperature, and surfactant chain length " Colloid & Polymer Science **254**(5): 507-515.
- Hao, L. and D. G. Leaist (1996). "Binary mutual diffusion coefficients of aqueous alcohols. Methanol to 1-heptanol." Journal of Chemical and Engineering Data **41**(2): 210-213.
- Harris, G. H. and R. Jia (2005). "An improved class of flotation frothers." International Journal of Mineral Processing **58**: 35-43.
- Holland, P. M. and D. N. Rubingh (1992). "Mixed Surfactant Systems: An Overview." ACS SYMPOSIUM SERIES VOL 501.
- Holland, P. M. R., D. N. (1992). "Mixed Surfactant Systems: An Overview." ACS SYMPOSIUM SERIES VOL 501.
- J., P. and T. R. K. (1990). "The application of the specular reflection of neutrons to the study of surfaces and interfaces." Journal of Physics: Condensed Matter **2**: 1369-1412.
- Jachimska, B., K. Lunkenheimer, et al. (1995). "Effect of Position of the Functional Group on the Equilibrium and Dynamic Surface Properties of Butyl Alcohols." Journal of Colloid and Interface Science **176**(1): 31-38.
- Janczuk, B., A. Zdziennicka, et al. (2004). "Adsorption of sodium dodecyl sulphate and propanol mixtures at aqueous solution-air interface." Colloids and Surfaces A: Physicochemical and Engineering Aspects **244**: 1-7.
- Joos, P. and G. Serrien (1989). "Adsorption kinetics of lower alkanols at the air/water interface: Effect of structure makers and structure breakers." Journal of colloid and interface science **127**(1): 97-103.
- Karakashev, S., A. Nguyen, et al. (2008). Equilibrium Adsorption of Surfactants at the Gas-Liquid Interface. Interfacial Processes and Molecular Aggregation of Surfactants. R. Narayanan, Springer Berlin / Heidelberg. **218**: 25-55.
- Karraker, K. A. and C. J. Radke (2002). "Disjoining pressures, zeta potentials and surface tensions of aqueous non-ionic surfactant/electrolyte solutions: theory and comparison to experiment." Advances in Colloid and Interface Science **96**(1-3): 231-264.
- Klimpel, R. R. (1991). "Some industrial implications of changing frother chemical structure." International Journal of Mineral Processing **33**(1-4): 369.
- Kolev, V. L., K. D. Danov, et al. (2002). "Comparison of the van der Waals and Frumkin Adsorption Isotherms for Sodium Dodecyl Sulfate at Various Salt Concentrations." Langmuir **18**(23): 9106-9109.
- Kovtun, A. I., S. L. Khilko, et al. (2010). "Effect of lower alcohols on adsorption characteristics of sodium dodecyl sulfate solutions at liquid-gas interfaces." Colloid journal of the Russian Academy of Sciences **72**(3): 389-395.

REFERENCES

- Kralchevsky, P. A., K. D. Danov, et al. (2003). "Effect of nonionic admixtures on the adsorption of ionic surfactants at fluid interfaces. 1. Sodium dodecyl sulfate and dodecanol." Langmuir **19**: 5004-5018.
- Kwan, C. C. and M. J. Rosen (1980). "Relationship of structure to properties in surfactants. 9. Syntheses and properties of 1,2- and 1,3-alkanediols." Journal of Physical Chemistry **84**(5): 547-551.
- Lavi, P. and A. Marmur (2000). "Adsorption Isotherms for Concentrated Aqueous-Organic Solutions (CAOS)." Journal of Colloid and Interface Science **230**(1): 107-113.
- Le, T. N., M. C. Phan, et al. (2010). " Influence of molecular structure on the adsorption of surfactant on water/air interface. ." Asian-Pacific Journal of Chemical Engineering. **Article first published online: 29 DEC 2010**.
- Leaist, D. (2002). "Realing multicomponent mutual diffusion and intradiffusion for associating solutes. Application to couples diffusion in water-in-oil microemulsions." Physical Chemistry Chemical Physics **4**: 4732-4739.
- Leaist, D. G. and L. Hao (1994). "Simultaneous Measurement of Mutual Diffusion and Intradiffusion by Taylor Dispersion." Journal of Physical Chemistry **98**(17): 4703-4706.
- Lee E.M., Thomas R. K., et al. (1989). "Structure of Aqueous Decyltrimethylammonium Bromide Solutions at the Air/Water Interface Studied by the Specular Reflection of Neutrons " Journal of Physical Chemistry **93**: 381-388.
- Lee, Y.-C., S.-Y. Lin, et al. (2001). "Role of Equation of State on Studying Surfactant Adsorption Kinetics." Langmuir **17**(20): 6196-6202.
- Lee, Y. C., Y. B. Liou, et al. (2002). "Adsorption Kinetics of Nonanol at the Air Water Interface: Considering Molecular Interaction or Aggregation within Surface Layer." Langmuir **18**: 2686-2692.
- Leja, J. (1982). Surface Chemistry of Froth Flotation. New York, NY, Plenum Press.
- Lin, S.-Y., W. J. Wang, et al. (1997). "Adsorption Kinetics of 1-Octanol at the Air-Water Interface." Langmuir **13**(23): 6211-6218.
- Lin, S. Y., K. McKeigue, et al. (1991). "Diffusion-Limited Interpretation of the Induction Period in the Relaxation in Surface Tension Due to the Adsorption of Straight Chain, Small Polar Group Surfactants: Theory and Experiment " Langmuir **7**(6): 1055-1066
- Lindman, B., M. C. Puyal, et al. (1984). "Micelle formation of anionic and cationic surfactants from Fourier transform proton and lithium-7 nuclear magnetic resonance and tracer self-diffusion studies." The Journal of physical chemistry **88**: 5048-5057.
- Malysa, K. and K. Lunkenheimer (2008). "Foams under dynamic conditions." Current Opinion in Colloid & Interface Science **13**(3): 150-162.
- Manev, E. D., S. V. Sazdanova, et al. (2008). "Adsorption of ionic surfactants." Colloids and Surfaces A: Physicochemical and Engineering Aspects **319**(1-3): 29-33.

REFERENCES

- Markin, V. S. and A. G. Volkov (2002). "Quantitative Theory of Surface Tension and Surface Potential of Aqueous Solutions of Electrolytes." Journal of Physical Chemistry **106**: 11810-11817.
- Miller, R. (1981). "On the solution of diffusion controlled adsorption kinetics for any adsorption isotherms." Colloid and Polymer Science **259**: 375-381.
- Miller, R., V. B. Fainerman, et al. (2002). "Comparison of Two Methods to Estimate the Standard Free Energy of Adsorption." Journal of Surfactants and Detergents **5**(3): 281-286.
- Miller, R. and G. Kretzschmar (1980). "Numerical solution for a mixed model of diffusion kinetics-controlled adsorption." Colloid and Polymer Science **258**: 85-87.
- Monroy, F., J. G. Kahn, et al. (1998). "Dilational viscoelasticity of surfactant monolayers." Colloids and Surfaces A: Physicochemical and Engineering Aspects **143**(2-3): 251-260.
- Mulqueen, M. and D. Blankshtein (1999). "Prediction of equilibrium surface tension and surface adsorption of aqueous surfactant mixtures containing ionic surfactants." Langmuir **15**(26): 8832-8848.
- Mysels, K. J. (1982). "Diffusion-Controlled Adsorption Kinetics. General Solution and Some Applications." Journal of Physical Chemistry **86**: 4648-4651.
- Nakahara, H., O. Shibata, et al. (2011). "Examination of Surface Adsorption of Cetyltrimethylammonium Bromide and Sodium Dodecyl Sulfate." Journal of Physical Chemistry B **115**(29): 9077-9086.
- Neys, B. and P. Joos (1998). "Equilibrium surface tensions and surface potentials of some fatty acids." Colloids and Surfaces A: Physicochemical and Engineering Aspects **143**: 467-475.
- Nguyen, A. V. and H. J. Schulze (2004). Colloidal science of flotation. New York, Marcel Dekker.
- Nguyen, C. M., Scamehorn J. F. (1988). "Thermodynamics of mixed monolayer formation at the air--water interface." Journal of Colloid and Interface Science **123**(1): 238.
- Nikas, Y. J. (1992). "Surface tensions of aqueous nonionic surfactant mixtures." Langmuir **8**(11): 2680.
- Ozmaç, M., Aktas Z. (2006). "Coal froth flotation: Effects of reagent adsorption on the froth structure." Energy & fuels **20**(3): 1123-1130.
- Pan, R., J. Green, et al. (1998). "Theory and Experiment on the Measurement of Kinetic Rate Constants for Surfactant Exchange at an Air /Water Interface." Journal of colloid and interface science **205**: 213-230.
- Penfold, J., E. Staples, et al. (2003). "The structure of mixed nonionic surfactant monolayers at the air-water interface: the effects of different alkyl chain lengths." Journal of Colloid and Interface Science **262**(1): 235-242.
- Phan, C. (2010). "Dynamic adsorption of octanols at air/water interface." The Canadian journal of chemical engineering **9999**: 1-5.

REFERENCES

- Phan, C. M. (2010). Adsorption Kinetics of Secondary Alcohols at Air/Water Interface. 10th International Conference on Fundamentals of Adsorption (FOA10). Awaji, Hyogo, Japan.
- Phan, C. M., H. Nakahara, et al. (2011). "Surface Potential of Methyl Isobutyl Carbinol Adsorption Layer at the Air/Water Interface." The Journal of Physical Chemistry B **116**(3): 980-986.
- Phan, C. M., A. V. Nguyen, et al. (2005). "Dynamic adsorption of sodium dodecylbenzene sulphonate and dowfroth 250 onto the air–water interface." Minerals Engineering **18**(6): 599-603.
- Piotto, M., V. Saudek, et al. (1992). "Gradient-tailored excitation for single-quantum NMR spectroscopy of aqueous solutions " Journal of Biomolecular NMR **2**(6): 661-665.
- Poling, B. E., J. M. Prausnitz, et al., Eds. (2001). The properties of gases and liquids, McGraw-Hill.
- Posner, A., J. Anderson, et al. (1952). "The surface tension and surface potential of aqueous solutions of normal aliphatic alcohols." Journal of Colloid Interface Science **7**: 623-644.
- Pradines, V., V. B. Fainerman, et al. (2010). "Adsorption of alkyl trimethylammonium bromides at the water/air and water/hexane interfaces." Colloids and Surfaces A: Physicochemical and Engineering Aspects **371**(1–3): 22–28
- Prosser, A. J. and E. I. Frances (2001). "Adsorption and surface tension of ionic surfactants at the air-water interface: review and evaluation of equilibrium models." Colloids and surfaces. A, Physicochemical and engineering aspects **178**(1-3): 1-40.
- Pugh, R. J. (2000). "Non-ionic polyethylene oxide frothers in graphite flotation." Minerals Engineering **13**(2): 151-162.
- Rekvig, L., M. Kranenburg, et al. (2003). "Effect of surfactant structure on interfacial properties." Europhysics Letters **63**(6): 902-907.
- Ribeiro, A. C. F., V. Lobo, M.M., et al. (2004). "Transport properties of alkyltrimethylammonium bromide surfactants in aqueous solutions." Colloid & Polymer Science **283**: 277-283.
- Rosen, M. J. (1972). "The relationship of structure to properties in surfactants." Journal of the American Oil Chemists' Society **49**: 293-297.
- Rosen, M. J. (1974). "Relationship of Structure to Properties in Surfactants: II. Efficiency in Surface or Interfacial Tension Reduction " Journal of the American Oil Chemists' Society **51**(10): 461-465.
- Rosen, M. J. (1976). "The relationship of structure to properties in surfactants. IV. Effectiveness in surface or interfacial tension reduction." Journal of Colloid and Interface Science **56**(2): 320-327.
- Rosen, M. J. (1978). Chapter 5. Surfactants and Interfacial Phenomena, Wiley-Interscience, New York.

REFERENCES

- Rosen, M. J. (1989). Surfactants and Interfacial Phenomena. New York, A Wiley-Interscience
- Rosen, M. J., A. W. Cohen, et al. (1982). "Relationship of Structure to Properties in Surfactants. 10. Surface and Thermodynamic Properties of 2-Dodecyloxypoly(ethenoxyethanol)s, $C_{12}H_{25}(OC_2H_4)_x OH$, in Aqueous Solution " Journal of Physical Chemistry **86**: 541-545
- Rosen, M. J., M. Dahanayake, et al. (1982). "Relationship of structure to properties in surfactants. 11. surface and thermodynamic properties of N-dodecylpyridinium bromide and chloride." Colloids and Surfaces **5**(2): 159-172
- Rosen, M. J. and C. C. Kwan (1979). "Relationship of Structure to Properties in Surfactants. 8. Synthesis and Properties of Sodium 3-Alkyltetrahydropyranyl 4-Sulfates " The Journal of Physical Chemistry **83**(21): 2727-2732.
- Rosen, M. J. and Y. H. Xi (1990). "Dynamic surface tension of aqueous surfactant solution." Journal of Colloid and Interface Science **139**(2): 397-407.
- Rosen, M. J. and Q. Zhou (2001). "Surfactant-surfactant Interactions in mixed monolayer and mixed micelle formation." Langmuir **17**: 3532-3537.
- Rosen, M. J., Z. H. Zhu, et al. (1992). "Relationship of structure to properties of surfactants. 16. Linear decyldiphenylether sulfonates " Journal of the American Oil Chemists' Society **69** (1): 30-33.
- Rybinski, W. V. and M. J. Schwuger (1986). "Adsorption of surfactant mixtures in froth flotation." Langmuir **2**(5): 639-643
- Scamehorn, J. F. (1986). Phenomena in Mixed Surfactant Systems. Chapter1: An overview of phenomena involving surfactant mixtures. Washington, DC, American Chemical Society.
- Schramm, L. L. (2000). Surfactants: Fundamentals and Applications in the Petroleum Industry, Cambridge University Press.
- Schramm, L. L. and W. H. F. Green (1992). "An absolute differential maximum bubble pressure surface tensiometer employing displaced capillaries." Colloid and Polymer Science **270**(7): 694-706.
- Schramm, L. L. and W. H. F. Green (1995). "The influence of marangoni surface elasticity on gas mobility reductions by foams in porous media." Colloids and Surfaces A: Physicochemical and Engineering Aspects **94**(2): 13-28.
- Schramm, L. L., E. N. Stasiukb, et al. (2003). " Surfactants and their applications." Annual Report Progress of Chemistry., Section C. **99**: 3-48.
- Schulman, J. H. and J. Leja (1954). "Molecular interactions at the solid-liquid interface with special reference to flotation and solid-particle stabilized emulsions." Kolloid-Z. **136**: 107-119, discussion 119-120.
- Siddiqui, F. A. and E. I. Frances (1996). "Surface tension and adsorption synergism for solutions of binary surfactants." Industrial & engineering chemistry research **35**(9): 3223-3232.
- Siddiqui, F. A. and E. I. Frances (1996). "Equilibrium adsorption and tension of binary surfactant mixtures at the air/water interface." Langmuir **12**(2): 354-362.

REFERENCES

- Simister, E. A., R. K. Thomas, et al. (1992). "Comparison of neutron reflection and surface tension measurements of the surface excess of tetradecyltrimethylammonium bromide layers at the air/water interface." Journal of Physical Chemistry **96**(3): 1383-1388.
- Söderman, O., P. Stilbs, et al. (2004). "NMR studies of surfactants." Concepts in Magnetic Resonance Part A **23A**(2): 121–135.
- Sokolowski, A. and B. Burczyk (1983). "Chemical Structure and Surface Activity. VIII. Statistical Evaluation of the Influence of Alkyl Monoethers of Polyoxyethylene Glycols Structure on Their Adsorption at the Aqueous Solution-Air Interface " Journal of Colloid and Interface Science **94**(2): 369-379.
- Strydom, P. J., D. P. Spitzer, et al. (1983). "Fine coal flotation with alcohol: Dialkyl sulfosuccinate frothing systems." Colloids and surfaces **8**(2): 175-185.
- Stubenrauch, C., V. B. Fainerman, et al. (2005). "Adsorption behavior and dilational rheology of the cationic alkyl trimethylammonium bromides at the water/air interface." The journal of physical chemistry. B **109**(4): 1505-1509.
- Stubenrauch, C. and K. Khristo (2005). "Foams and foam films stabilized by CnTAB: Influence of the chain length and of impurities." Journal of Colloid and Interface Science **286**(2): 710-718.
- Sulthana, S. B., P. V. C. Rao, et al. (2000). "Solution Properties of Nonionic Surfactants and Their Mixtures: Polyoxyethylene (10) Alkyl Ether [CnE10] and MEGA-10." Langmuir **16**(3): 980-987.
- Szymczyk, K. and B. Jańczuk (2007). "The properties of a binary mixture of nonionic surfactants in water at the water/air interface." Langmuir **23**(9): 4972-4981.
- Szymczyk, K., A. Zdziennicka, et al. (2005). "The properties of mixtures of two cationic surfactants in water at water/air interface." Colloids and surfaces. A, Physicochemical and engineering aspects **264**(1-3): 147-156.
- Tadros, T. F. (2005). Applied Surfactants: Principles and Applications. The Federal Republic of Germany, WILEY-VCH Verlag GmbH & Co., KGaA, Weinheim.
- Tan, S. N., D. Fornasiero, et al. (2005). "The role of surfactant structure on foam behaviour." Colloids and surfaces. A, Physicochemical and engineering aspects **263**(1-3): 233-238.
- Tan, S. N., D. Fornasiero, et al. (2006). "The interfacial conformation of polypropylene glycols and their foam properties." Minerals engineering **19**(6-8): 703-712.
- Tan, S. N., R. J. Pugh, et al. (2005). "Foaming of polypropylene glycols and glycol/MIBC mixtures." Minerals engineering **18**(2): 179-188.
- Thomas, R. K. (2004). "Neutron reflection from liquid interfaces " Annual Review of Physical Chemistry **55**: 391-426.
- Tsonopoulos, C., J. Newman, et al. (1971). "Rapid aging and dynamic surface tension of dilute aqueous solutions." Chemical Engineering Science **26**: 817-827.

REFERENCES

- Tsonopoulos, C., J. Newman, et al. (1971). "Rapid aging and dynamic surface tension of dilute aqueous solutions." Chemical Engineering Science, **26**: 817-827.
- Ueno M., Takasawa Y., et al. (1981). "Effect of alkyl chain length on surface and micellar properties of octaethyleneglycol-n alkyl ethers." Colloid and Polymer Science **259**: 761-766.
- Varadaraj, R., J. Bock, et al. (1991). "Fundamental Interfacial Properties of Alkyl-Branched Sulfate and Ethoxy Sulfate Surfactants Derived from Guerbet Alcohols. 2. Dynamic Surface Tension " Journal of Physical Chemistry **95**(4): 1677-1679
- Varadaraj, R., J. Bock, et al. (1991). "Fundamental Interfacial Properties of Alkyl-Branched Sulfate and Ethoxy Sulfate Surfactants Derived from Guerbet Alcohols. 1. Surface and Instantaneous Interfacial Tensions." Journal of Physical Chemistry **95**(4): 1671-1676.
- Varadaraj, R., J. Bock, et al. (1991). "Effect of Hydrocarbon Branching on Interfacial Properties of Monodisperse Ethoxylated Alcohols Surfactants." Journal of Colloid and Interface Science **147**(2): 387-394.
- Vogler, E. A. (1992). "Practical use of concentration-dependent contact angles as a measure of solid-liquid adsorption. 1.Theoretical aspects." Langmuir **8**(8): 2005-2012.
- Wade, W. H., J. C. Morgan, et al. (1978). "Interfacial Tension and Phase Behavior of Surfactant Systems." Society of Petroleum Engineers Journal: 242-252.
- Wang, L. and R. H. Yoon (2008). "Effects of surface forces and film elasticity on foam stability." International Journal of Mineral Processing **85**(4): 101-110.
- Wang, L. K., E. M. Fahey, et al., Eds. (2005). Dissolved Air Flotation. Handbook of Environmental Engineering, Springer.
- Wantke, K., K. Małysa, et al. (1994). "A relation between dynamic foam stability and surface elasticity." Colloids and Surfaces A: Physicochemical and Engineering Aspects **82**(2): 183-191.
- Ward, A. F. H. and L. Tordai (1946). "Time-dependence of boundary tensions of solutions. I. The role of diffusion in time effects." The Journal of Chemical Physics **14**(7): 453-461.
- Warszynski, P. and B. Jachimska (2002). "Conformation of hydrophobic chains at liquid/gas interface and their implications on surfactant adsorption." Physicochemical Problems of Mineral Processing **36**: 39-49.
- Wormuth, K. R. and S. Zushma (1991). "Phase behavior of branched surfactants in oil and water." Langmuir **7**(10): 2048-2053.
- Yalkowsky, S. H. and Y. He (2003). Handbook of aqueous solubility data, CRC.
- Zana R. (1995). "Aqueous surfactant-alcohol systems: A review " Advances in Colloid and Interface Science **57**(30): 1-64.
- Zdziennicka, A. (2010). "Surface behavior of Triton X-165 and short chain alcohols mixtures." Langmuir **26**(3): 1860-1869.

REFERENCES

- Zdziennicka, A., B. Janćzuk, et al. (2004). "Adsorption of mixtures of sodium dodecyl sulphate and propanol at water-air and polytetrafluoroethylene-water interfaces." Colloids and surfaces. A, Physicochemical and engineering aspects **249**(1-3): 73-77.
- Zdziennicka, A. and B. Janćzuk (2010). "Effect of anionic surfactant and short-chain alcohol mixtures on adsorption at quartz/water and water/air interfaces and the wettability of quartz." Journal of Colloid and Interface Science **354**(1): 396-404.
- Zdziennicka, A. and B. Janczuk (2008). "Adsorption of cetyltrimethylammonium bromide and propanol mixtures with regard to wettability of polytetrafluoroethylene. I. Adsorption at aqueous solution-air interface." Journal of Colloid and Interface Science **317**(1): 44-53.
- Zdziennicka, A. and B. Janczuk (2010). "Behavior of cationic surfactants and short chain alcohols in mixed surface layers at water-air and polymer-water interfaces with regard to polymer wettability. I. Adsorption at water-air interface." Journal of Colloid and Interface Science **349**: 374-383.

Every reasonable effort has been made to acknowledge the owners of copyright material. I would be pleased to hear from any copyright owner who has been omitted or incorrectly acknowledged.

APPENDICES

Appendix 1: Standard deviation of different concentration of OTAB with fitting parameter $K = 68577$ L/mol) and $\Gamma_m = 2.638 \times 10^{-5}$ mol/m²

OTAB concentration	Standard deviation
0.06mM	0.86
0.08mM	0.405
0.1mM	0.659

Appendix 2: Standard deviation of different concentration of CTAB with fitting parameter $K = 1998$ L/mol) and $\Gamma_m = 6.323 \times 10^{-6}$ mol/m²

CTAB concentration	Standard deviation
0.4mM	0.772
0.5mM	0.211
0.6mM	0.6768
0.7mM	0.178
0.8mM	0.246

APPENDICES

Appendix 3: Standard deviation of different concentration of TTAB with fitting parameter $K = 1716 \text{ L/mol}$ and $\Gamma_m = 3.76 \times 10^{-6} \text{ mol/m}^2$

TTAB concentration	Standard deviation
0.4mM	0.399
0.6mM	0.887
0.8mM	0.403
1.1mM	0.475
1.5mM	0.895

Appendix 4: Standard deviation of different concentration of 2-nonanol with fitting parameter $K = 2017 \text{ L/mol}$ and $\Gamma_m = 6.32 \times 10^{-6} \text{ mol/m}^2$

2-nonanol concentration	Standard deviation
0.2 mM	0.88
0.4mM	0.315
0.6mM	0.378
0.7mM	0.33
0.8mM	0.61

APPENDICES

Appendix 5: Standard deviation of different concentration of 3-nonanol with fitting parameter $K = 1000 \text{ L/mol}$ and $\Gamma_m = 6 \times 10^{-6} \text{ mol/m}^2$

3-nonanol concentration	Standard deviation
0.2 mM	0.7
0.3mM	0.42
0.4mM	0.71
0.7mM	0.949
0.8mM	0.819

Appendix 6: Standard deviation of different concentration of 5-nonanol with fitting parameter $K = 990 \text{ L/mol}$ and $\Gamma_m = 5.6 \times 10^{-6} \text{ mol/m}^2$

5-nonanol concentration	Standard deviation
0.3 mM	0.589
0.4mM	0.569
0.5mM	1
0.7mM	0.492
0.8mM	0.763